

Type Ia supernova progenitors: a contemporary view of a long-standing puzzle

Ashley Jade Ruiter · Ivo Rolf Seitenzahl

Received: April 2024 / Accepted: 2024

Abstract Type Ia supernovae (SNe Ia) are runaway thermonuclear explosions in white dwarfs that result in the disruption of the white dwarf star, and possibly its nearby stellar companion. SNe Ia occur over an immense range of stellar population age and host galaxy environments, and play a critical role in the nucleosynthesis of intermediate-mass and iron-group elements, primarily the production of nickel, iron, cobalt, chromium, and manganese. Though the nature of their progenitors is still not well-understood, SNe Ia are unique among stellar explosions in that the majority of them exhibit a systematic lightcurve relation: more luminous supernovae dim more slowly over time than less luminous supernovae in optical light (intrinsically brighter SNe Ia have broader

A.J. Ruiter
School of Science
University of New South Wales
Australian Defence Force Academy
Canberra, ACT, Australia
and
OzGrav: The Australian Research Council
Centre of Excellence for Gravitational
Wave Discovery, Hawthorn VIC 3122, Australia
and
ASTRO-3D: The Australian Research Council
Centre of Excellence for All-Sky Astrophysics
in 3 Dimensions
and
Heidelberger Institut für Theoretische Studien
Schloss-Wolfsbrunnenweg 35
Heidelberg, 69118, Germany
E-mail: ashley.ruiter@gmail.com

I.R. Seitenzahl
Heidelberger Institut für Theoretische Studien
Schloss-Wolfsbrunnenweg 35
Heidelberg, 69118, Germany

lightcurves). This feature, unique to SNe Ia, is rather remarkable and allows their peak luminosities to be determined with fairly high accuracy out to cosmological distances via measurement of their lightcurve decline. Further, studying SNe Ia gives us important insights into binary star evolution physics, since it is widely agreed that the progenitors of SNe Ia are binary (possibly multiple) star systems. In this review, we give a current update on the different proposed Type Ia supernova progenitors, including descriptions of possible binary star configurations, and their explosion mechanisms, from a theoretical perspective. We additionally give a brief overview of the historical (focusing on the more recent) observational work that has helped the astronomical community to understand the nature of the most important distance indicators in cosmology.

Keywords Supernovae · Binary stars · White dwarfs · Nucleosynthesis · Chemical evolution

Contents

1	Introduction	3
1.1	Importance to astrophysics	3
1.2	Progenitor scenario: star types	7
1.2.1	White dwarf with non-white dwarf: SD scenarios in brief	7
1.2.2	White dwarf with white dwarf: DD scenarios in brief	10
1.2.3	Early history – observed SNe Ia	13
1.2.4	Type Ia supernovae: the last 100 years	14
2	The 21st century: direct observations that constrain the explosion	18
2.1	Spectra and lightcurves that constrain the explosion mechanism	20
2.1.1	Early interaction (early excess)	21
2.1.2	Photospheric velocities	23
2.1.3	The importance of spectra in the nebular phase	26
2.1.4	H α , circumstellar medium, and high-velocity features	26
2.2	Polarimetry	27
2.3	Direct imaging	28
2.3.1	Companion searches	28
2.3.2	Lensed supernovae	29
3	Indirect constraints of the explosion	30
3.1	Host environment	30
3.2	Chemical evolution	32
3.2.1	Milky Way	33
3.2.2	Dwarf galaxies	33
3.2.3	Intra-cluster medium	35
3.3	Radioactive nickel and ejecta masses from lightcurves and spectra	36
3.4	Supernova abundance tomography	38
3.5	Potential surviving companions	39
3.6	Supernova-remnant archaeology	40
3.7	Rates and delay time distributions	41
4	Near-Chandrasekhar mass SN Ia explosion models	46
4.1	The central ignition problem	46
4.2	Nuclear burning in Chandrasekhar mass white dwarfs	47
4.2.1	Recent comparison of observational iron-group element masses and isotope ratios with explosion model predictions (Chandrasekhar vs. sub-Chandrasekhar)	49
4.3	Progenitor scenarios of near-Chandrasekhar mass explosions	51

4.3.1	Merging white dwarfs leading to near-Chandrasekhar mass WD ignition	51
4.3.2	The core-degenerate scenario	52
4.3.3	Single-degenerate near-Chandrasekhar mass scenario	53
4.4	Explosion mechanisms	54
4.4.1	Pure deflagrations (failed detonations)	54
4.4.2	Deflagration-to-detonation transition models	56
4.4.3	Gravitationally confined detonation models	57
4.4.4	Pulsational reverse detonation models	59
4.4.5	Alternative models	59
5	Sub-Chandrasekhar mass SN Ia explosion models	60
5.1	Historical context	60
5.2	Non-dynamical mass transfer	61
5.2.1	Double-detonation models in binaries undergoing non-dynamical mass transfer	62
5.3	Dynamically-driven	66
5.3.1	Mergers of white dwarfs	68
5.4	WD+WD collisions	70
6	Final remarks	71
	References	73

1 Introduction

1.1 Importance to astrophysics

Type Ia (or thermonuclear) supernovae are extremely energetic stellar transients that quickly evolve to outshine 100,000,000 stars before rapidly fading in brightness. Though now understood to be a heterogeneous population, it is agreed that a Type Ia supernova (SN Ia) stems from a runaway nuclear reaction in a degenerate (and assumed to be rich in carbon and oxygen) white dwarf star when that star has achieved physical conditions that enable explosive nuclear burning to take place (Thielemann et al. 1986; Khokhlov 1991a).

Type Ia supernovae occur only under special circumstances involving interacting stars with initial masses below $\sim 10 M_{\odot}$, and under completely different physical conditions than core-collapse supernovae. Core-collapse SNe involve the collapse of a stellar core to a compact object, which can only occur in stars with a massive stellar core (e.g. stars whose total mass on the Zero-Age Main Sequence was on the order of $\sim 8 - 10 M_{\odot}$ or heavier, assuming they do not produce [pulsational] pair-instability supernovae (Rahman et al. 2022)). The explosion mechanism in core-collapse supernovae, of which there are a growing number of observationally-classified sub-types (Gal-Yam 2017) is an ongoing debate (Fryer et al. 2012; Müller et al. 2017). Type Ia supernova explosions on the other hand are fueled by a nuclear energy source – on the order of 10^{51} erg with typical bolometric luminosities reaching 10^{43} erg/s (Maguire 2017). SNe Ia involve the explosion of a carbon-oxygen¹ white dwarf that has obtained sufficiently high density to initiate sub-sonic and/or super-sonic burning, likely brought on via matter accretion from a close stellar companion. We discuss in more detail the various explosion mechanisms for Chandrasekhar

¹ but see also Kirsebom et al. (2019).

mass (approximately $1.4 M_{\odot}$) and sub-Chandrasekhar mass explosion models in Sects. 4 and 5, respectively, after first giving a more holistic overview of the field. For a modern overview of stellar evolution, we encourage the reader to look up ‘Understanding Stellar Evolution’ by [Lamers and Levesque \(2017\)](#).

In particular, SNe Ia are famous for the characteristic that it is possible to ‘standardize’ a large number of their lightcurves (i.e. stretch or compress them to fit a template), which then allows us to use them as our most important distance indicators on the astrophysical distance ladder ([Rust 1974](#); [Pskovskii 1977](#); [Phillips 1993](#); [Hamuy et al. 1996](#); [Phillips and Burns 2017](#)). While observed properties of some massive-star (core-collapse) supernovae such as Type II-P ([Hamuy and Pinto 2002](#); [Poznanski et al. 2009](#); [Maguire et al. 2010](#)) and superluminous supernovae (SLSNe, [Inserra and Smartt 2014](#)) have allowed some core-collapse supernovae to be regarded as useful cosmological distance indicators, the typically larger luminosities of SNe Ia, as well as their birthrates ([Li et al. 2011c](#); [Prajs et al. 2017](#)), have rendered SNe Ia as fundamental cosmological tools over the decades. The technique of SN Ia standardization has grown in complexity over the decades, and requires lightcurve fitting to models in a variety of band passes and spectra. For an excellent review on the ‘rise’ of SNe Ia as trusted standardizable candles in cosmology, we refer the reader to [Kirshner \(2010\)](#).

It is observational data of SNe Ia that enabled the Supernova Cosmology Project and High- z Supernova Search teams to determine that the rate of expansion of the Universe is actually accelerating (Nobel Prize in Physics, 2011). This fundamental discovery firmly rejuvenated the importance of a cosmological constant – the seedling idea having been postulated by [Einstein \(1917\)](#) as a universal constant permeating the Universe (then denoted by λ in the Einstein Field Equations), though its effects are negligible over small (\sim galactic) scales. Since this profound discovery, there has been significant research dedicated toward understanding the concept of ‘dark energy’ (for a review, see [Frieman et al. 2008](#)).

In addition to their importance in the advancement of cosmological studies, and thus our understanding of our Universe’s previous and future evolution, SNe Ia are also the most important source of iron-group elements (e.g. V, Cr, Mn, Co, Fe, Ni) in the Universe. Though core-collapse supernovae (types II, Ic, Ib and their sub-types) exceed SNe Ia by number among young stellar populations, per event a typical SN Ia produces around $0.5 M_{\odot}$ of iron (e.g. [Stritzinger et al. 2006a](#); [Mazzali et al. 2007](#); [Scalzo et al. 2014](#); [Bora et al. 2022](#)), and therefore about 12 times more iron than a typical Type II core-collapse SN ([Rodríguez et al. 2021](#)). Stripped envelope core-collapse SNe (e.g. SNe Iib, SNe Ib/c) produce more iron than their Type II SN cousins, but event-by-event, the mean over-production of iron by SNe Ia relative to core-collapse SNe that also include stripped envelope events is still a factor of about 9 ([Rodríguez et al. 2023](#)). This results in about just over half of the iron at the current epoch originating from SNe Ia (see e.g. Fig. 3 of [Maoz and Graur 2017](#)). Iron is the most critical element for spectroscopic measurements of metallicity in stellar populations because iron is used as a tracker of chemical enrichment

in studies of galaxy evolution, especially for our own Milky Way (Sharma et al. 2022). In addition to elements near the iron-peak (which also includes notable production of Cu and Zn), SNe Ia also produce a significant amount of intermediate-mass elements, especially the even atomic number elements Si, S, Ar, Ca, and the transitional element Ti, which sits at the border between intermediate-mass elements (IMEs) and iron-group elements (IGEs).

‘Catching’ a supernova in the act of exploding, or even capturing data in those first hours or days after explosion where crucial physics can be constrained, is not easy. It can take days for the new SN to be recognized by the community as an astrophysical transient. This was especially true prior to the age of synoptic sky surveys (e.g. SkyMapper, Scalzo et al. 2017). Amateur astronomers have also had a substantial contribution toward the discovery of new SNe (Gal-Yam et al. 2013).

Around 15-20 days after explosion, the SN Ia will reach its maximum value in bolometric luminosity, and it is around this time when the SN Ia can be classified further (see below). The SN Ia optical lightcurve is powered by the radioactive decay of ^{56}Ni (see Sect. 2.1)². The time evolution of Type Ia supernova lightcurves around maximum light is shaped by the interplay of the ongoing yet decreasing energy input (due to the exponentially decaying activity from the radioactive decay law) and the diffusion/propagation of the photons through the SN ejecta towards the stellar photosphere. It is this delaying effect of the diffusion through the initially opaque ejecta that leads to a maximum in the lightcurve (as opposed to a purely exponentially decaying function) in the first place (Arnett 1982, see Sect. 3.3).

In simple terms, more radioactive ^{56}Ni in the centre of the supernova tends to yield more luminous events, and more mass surrounding it leads to greater diffusion times and broader lightcurves with a reduced luminosity at maximum. Whether a SN Ia’s lightcurve evolves more quickly than average (having a narrow lightcurve) or more slowly than average (broader lightcurve) already allows us to speculate that these two types of events are intrinsically different – especially when accounting for the fact that the faster events tend to be found among regions with less active star formation.

Taking together SN Ia lightcurve behaviour in combination with a notable variation in spectral properties near maximum light, and occasionally other physical properties too, it has become possible to delineate most SNe Ia into various “sub-classes” (Taubenberger 2017): the sub-luminous, fast-declining SNe Ia – the most well-known of which are the 1991bg-likes (Leibundgut et al. 1993); the ‘super-luminous’ SN Ia such as the broad-lightcurve 1991T-likes (Phillips et al. 1992) or the so-called ‘Super-Chandrasekhar’ events (Silverman et al. 2011, see also Sects. 3.3 and 4.3); Ca-rich (or ‘gap transient’) faint events that are more often associated with old quiescent stellar populations, sometimes relatively far from their host galaxies (Kasliwal et al. 2012; De et al. 2020); the ‘Type Iax’ supernovae (see Sect. 2.3.1) comprises a large, rather

² ^{56}Ni (with a half-life of 6.075 days) decays to the radioactive isotope ^{56}Co (with a half-life of 77.236 days), which then eventually decays to the stable isotope ^{56}Fe .

diverse group, of which the most infamous is the 2002cx-like sub-population (Li et al. 2003) – a type of ‘peculiar’ supernova. Finally, the “normal” SNe Ia (Branch et al. 1993) refer to those Type Ia supernovae whose lightcurves are well-behaved in the sense that it is possible to fit them to a template that is useful for cosmological studies.

This is by no means an exhaustive list of sub-classes. We also note that these sub-class labels are tied directly to observational features, namely peak luminosity and lightcurve ‘speed’, with no initial link to theoretical predictions, though over the years certain explosion scenarios have emerged as arguably more favourable over others for certain sub-classes (e.g. a ‘failed’ explosion of a Chandrasekhar mass white dwarf for the case of SN Iax event SN 2020udy, Maguire et al. 2023, see also Sect. 4.4.1). We refer the reader to Sect. 2 of Gal-Yam (2017) for a discussion on various SN Ia sub-classes with reference to specific spectral properties (see also Ruiter 2020, for a brief overview of the different sub-classes).

There is widespread agreement that different progenitor scenarios result in the synthesis of chemical elements in different proportions (e.g. Röpke et al. 2012). Therefore, not knowing the nature of SN Ia progenitors, or what fraction the different sub-classes of progenitors contribute among different stellar environments, makes for quite a challenging puzzle for galactic chemical evolution studies, which rely on yields from the explosive nucleosynthesis in SNe Ia as critical simulation input. Append the fact that different SN Ia progenitors have a variety of feedback-timescales, or ‘delay time distributions’³ (see Sect. 3.7), and we have a truly challenging problem if we are to understand the process of chemical enrichment in galaxies in detail.

Even though SNe Ia have famously served as extremely useful cosmological tools, this review focuses on the role SNe Ia play in astrophysics from a perspective of understanding stellar and binary evolution of low- and intermediate-mass stars, while highlighting the critical role that SNe Ia play in nucleosynthesis, and thus chemical evolution (see Sect. 3.2).

In this section, we give a brief overview of what we know about SNe Ia in terms of their progenitor configuration, with an emphasis on historically significant pioneering theoretical works. In Sects. 2 and 3, we provide an overview of observational works that have made substantial contributions to understanding the nature of SN Ia progenitors through direct and indirect methods, respectively. In Sects. 4 and 5, we shift our focus to theoretical work pertaining to the study of Chandrasekhar mass and sub-Chandrasekhar mass explosion models, respectively, that were published this century (for a review on earlier works, see Hillebrandt and Niemeyer 2000).

³ The Delay Time Distribution (DTD) is the distribution of times over which SNe Ia explode following a (hypothetical) burst of star formation assuming all stars were born at time $t = 0$.

1.2 Progenitor scenario: star types

Historically, SNe Ia were seen as residing in one of two silos: single degenerate (SD) or double degenerate (DD). Both categories involve a white dwarf that ultimately makes up the bulk of the exploding mass that had reached ignition conditions (i.e. critical density/temperature), but the star that is donating this crucial extra mass (the ‘donor’) could be either a regular star still undergoing nuclear burning in its core or in a shell(s), or it could be a degenerate (e.g. another white dwarf) star.

Such a categorization (SD or DD), though elegant in some ways, ignores the implied explosion mechanism – which is thought to be predominantly governed by the exploding white dwarf mass – and thus the nucleosynthetic implications of the progenitor become washed out. This silo categorization also leaves little room for ‘grey’ areas in terms of how one defines degeneracy, as some donor stars might exist in the realm of ‘semi-degenerate’ (see [Nelemans et al. 2001](#); [Iben and Tutukov 1991](#)).

Delineating the progenitor types by exploding white dwarf mass rather than donor star type gives a simpler, more physically-motivated line of reasoning in discussing SN Ia origin, since it is widely believed that Chandrasekhar mass white dwarfs undergo a thermonuclear explosion through a different mechanism than white dwarfs that explode well below the Chandrasekhar mass limit ([Hillebrandt et al. 2013](#), Sect. 4). It turns out that both ‘silos’ of progenitors (SD and DD) can each harbour both Chandrasekhar mass and sub-Chandrasekhar mass SNe Ia. Additionally, DD SNe Ia can occur at nearly any stellar age, or delay time, from ~ 50 Myr post-star formation, and the situation is similar for SD progenitors, especially when including progenitors with helium-burning donors ([Yungelson and Livio 2000](#); [Wang et al. 2009a](#); [Ruiter et al. 2011](#); [Claeys et al. 2014](#)). For a schematic picture of several progenitor evolutionary channels, we refer to reader to Fig. 2 from [Liu et al. \(2023\)](#).

1.2.1 White dwarf with non-white dwarf: SD scenarios in brief

The canonical view of the SD scenario ([Whelan and Iben 1973](#)) consists of a white dwarf rich in carbon and oxygen that approaches the Chandrasekhar mass limit via stable⁴ mass transfer from a non-degenerate star (but see Sect. 4 regarding the ‘core-degenerate’ scenario). The donor is usually assumed to be a main sequence star or a red giant, but could be another type (see below). Binary systems with a massive white dwarf accreting from a non-degenerate companion are indeed observed in nature, which has given some credence to this proposed scenario compared to others.⁵

⁴ In this context, ‘stable’ Roche-lobe overflow (RLOF) means mass is transferred to the accretor on either a nuclear or thermal timescale, but is not necessarily conservative.

⁵ The dearth of observed white dwarf binaries having short orbital periods has been one (poor) argument against the plausibility of double degenerate binaries contributing to the SN Ia population; see Sect. 1.2.2.

For the case of a Chandrasekhar mass explosion that results in a Type Ia supernova, the favoured explosion scenario involves a sub-sonic deflagration followed by a super-sonic detonation that explodes the white dwarf star. In a nutshell, the central density of the carbon-oxygen-rich white dwarf becomes high enough for carbon-burning to begin. After some time on the order of 1000 years (e.g. [Piro and Chang 2008](#)) of quiescent, convective carbon-burning referred to as the ‘simmering phase’ ([Piro and Bildsten 2008](#)), explosive carbon-burning is ignited as a flame (e.g. [Garcia-Senz and Woosley 1995](#); [Kuhlen et al. 2006](#)), which, in most if not all cases, completely disrupts the white dwarf star. In some cases, a carbon detonation may not be successfully achieved in a Chandrasekhar mass white dwarf, resulting in a ‘failed detonation’, often termed a ‘failed deflagration’, since the sub-sonic deflagration did not successfully transform into a super-sonic detonation. These weaker explosions are currently the favoured mechanism in explaining some peculiar supernovae that exhibit SN Ia-like features but with lower luminosities and lower ejecta velocities ([Jha 2017](#)) referred to as SN Iax (see Sect. 2.3.1 for a bit more discussion on this sub-class). We refer to Sect. 4 for details on modelling approaches for Chandrasekhar mass explosions. In fact, the failed deflagration explosions are not only the favoured model to explain the fainter SN Iax supernovae, but it is also suspected that the donating star in these cases was not a red giant or main sequence companion, but a star that had previously lost its hydrogen envelope through binary interactions but was still burning helium – imagine an AGB star without its envelope. The helium-burning star channel in the context of Chandrasekhar mass SNe Ia has been found to be a promising formation scenario to explain SNe Iax events ([Maguire et al. 2023](#)), given their affinity for being found among young stellar environments, e.g. at short delay times ([Ruiter et al. 2009](#); [Wang et al. 2009a](#); [Takaro et al. 2020](#)). Single degenerate SNe Ia could also occur in sub-Chandrasekhar mass white dwarfs through the ‘classical’ double-detonation scenario in which a star that is rich in helium donates matter to a white dwarf through RLOF at relatively low accretion rates ([Woosley and Weaver 1994b](#); [Yungelson and Livio 2000](#)). The star donating helium rich matter could be a white dwarf (see Sect. 1.2.2) or a star that is still undergoing significant nuclear burning, or could be partially degenerate. The star would have lost its hydrogen-rich envelope in previous binary interactions, as wind mass loss rates in low- and intermediate-mass stars are generally not high enough to cause any significant loss of the hydrogen-rich envelope ([Iben and Renzini 1983](#)). A hydrogen-stripped, helium-burning star is rather compact in size compared to a red giant. Therefore, when such a helium-burning donor fills its Roche lobe, the separation from the accreting white dwarf would be much smaller compared to the separation in the red giant donor case (see [Eggleton 1983](#), for equations characterizing the Roche lobe radius). When accretion from the helium-rich star begins, it may proceed on a thermal timescale and thus initially have a high rate of mass transfer ($\sim 10^{-5} M_{\odot}/\text{yr}$), but later decrease to a lower value as the binary system’s orbital separation increases over time. We note that the mass transfer may not necessarily be conservative ([Piersanti et al. 2014](#)). For such binaries containing

rather compact stars where it may be assumed that mass transfer is driven by gravitational wave radiation, one can estimate the mass transfer rate as

$$\dot{M} = \left(\frac{5}{6} + \frac{\beta}{2} - \frac{M_2}{M_1} \right)^{-1} \frac{M_2}{\tau_g}, \quad (1)$$

where M_1 and M_2 are the accretor and donor masses respectively, τ_g is the timescale of orbital decay as a consequence of gravitational wave emission, and β is a dimensionless factor related to the masses of both stars (see [Savonije et al. 1986](#), Sect. 2; see also [Paczynski 1971](#) for a general description of common assumptions that are made when modelling mass transfer in close binaries). When accretion rates are rather low ($< 2 \times 10^{-8} M_\odot \text{ yr}^{-1}$), helium-burning is not able to take place and rather a shell of helium-rich material accumulates on the white dwarf, which can eventually detonate ([Taam 1980](#); [Iben and Tutukov 1987](#); [Livne and Arnett 1995](#); [Fink et al. 2007](#)). This initial detonation in the helium-rich shell drives shock-waves through the white dwarf surface layers and core, which converge off-centre on the opposite side of the ignition region. The convergent shocks result in compression and drive up the temperature and density of the white dwarf in a region off-set from the star's (carbon-oxygen-rich) centre, resulting in a subsequent, second detonation (thus there is a 'double-detonation'; [Livne 1990](#); [Livne and Glasner 1991](#); [Fink et al. 2010](#); [Woosley et al. 2011](#))⁶. It is this second detonation which unbinds the (sub-Chandrasekhar mass) white dwarf star. It was pointed out by [Perets et al. \(2010\)](#) that the low-luminosity, calcium-rich transient SN2005, labelled initially as a Type Ib supernova, was a prime example of a helium detonation explosion⁷. Given SN 2005E's low ejecta mass, large amounts of intermediate mass elements and low amounts of Fe-peak elements observed in the spectra, in addition to its apparent old stellar population age, SN 2005E remains a promising example of an explosion that involved a helium detonation of some kind (see also [Dessart and Hillier 2015](#)). In Sect. 5, we discuss in more detail models of sub-Chandrasekhar mass explosions.

Both of these 'sub-categories' of single degenerates – Chandrasekhar mass explosion and sub-Chandrasekhar double-detonation – require different criteria in terms of chemical composition (donor and accretor) and rate of accretion to end up as a Chandrasekhar mass explosion, a sub-Chandrasekhar mass explosion, or a nova eruption, with not all studies in total agreement regarding the physical conditions necessary to result in the various outcomes ([Hashimoto et al. 1983](#); [Starrfield et al. 1985](#); [Isern et al. 1991](#); [Priainik and Kovetz 1995](#); [Nomoto et al. 2007](#); [Shen and Bildsten 2009](#); [José et al. 2020](#)). Different assumptions of how accretion proceeds regarding retention efficiency of the accreted material ([Bours et al. 2013](#); [Toonen et al. 2013](#); [Ruiter et al. 2014](#); [Piersanti et al. 2014](#)) and how this varies with composition, and from

⁶ Double-detonation SNe Ia explosions can stem from non-degenerate, helium burning donor stars as discussed here, but they can also plausibly stem from semi- or fully-degenerate helium-rich white dwarf donors.

⁷ The reader is referred to [Frohmaier et al. \(2018\)](#) or [De et al. \(2020\)](#) for a recent overview of a search for these transients with the Zwicky Transient Facility.

which location in the binary system the angular momentum is removed from the orbit, are just some factors that should be included in assessing the relative numbers of plausible progenitor scenarios in binary population synthesis (BPS) studies (see [Han et al. 2020](#); [Riley et al. 2022](#), for a comprehensive example of binary star evolution modelling in population synthesis). These physical considerations of course matter not only during the final RLOF phase preceding the SN Ia explosion, but also during any mass loss/transfer episodes that occur over the course of binary evolution.

1.2.2 White dwarf with white dwarf: DD scenarios in brief

The double degenerate scenario involves the merger of two white dwarfs that typically are assumed to merge as a consequence of orbital angular momentum loss brought about by gravitational radiation emission ([Peters 1964](#); [Paczynski 1967](#); [Iben and Tutukov 1984](#); [Webbink 1984](#)). The time between the last mass-exchange (i.e. a common envelope or a stable RLOF phase) and the merger has a large range; it can be anywhere from just a few years to many Gyrs after the two white dwarfs are formed. The time delay t between formation of a binary system on the Zero-Age Main Sequence and the time when the resulting two white dwarfs merge can be estimated if we assume that the main mechanism for loss of orbital angular momentum is gravitational wave emission (see [Ruiter et al. 2009](#), Sect. 3) and is found to be fairly well-represented by a power-law t^{-s} with $s \sim 1$ ([Maoz and Mannucci 2012](#); [Castrillo et al. 2021](#)). An observationally-derived delay time distribution (DTD) from Type Ia supernovae in elliptical galaxies was measured by [Totani et al. \(2008\)](#) and the resulting DTD was found to align very well with the one predicted to arise from white dwarf mergers (see Sect. 3.7 for further discussion on the SN Ia DTD).

One must realise though that there are large uncertainties associated with deriving an observational DTD because in most cases, one must make important assumptions about the star formation history of the stellar population (e.g. [Maoz et al. 2010](#), but see also [Maoz et al. 2011](#); [Strolger et al. 2020](#) for alternative approaches). Mass exchange interactions within binaries can significantly alter the nuclear burning lifetimes of the stars, which also affects the delay time. The [Totani et al. \(2008\)](#) observations sparked a rejuvenated interest in the double degenerate scenario of SNe Ia, launching a stream of new theoretical work in this area. In the case of degenerate donors, it could be a helium white dwarf or possibly a ‘hybrid’ He-CO white dwarf. Both types of helium-rich WDs are only made through binary star interactions ([Iben and Tutukov 1985](#))⁸. We discuss such models in some more detail in Sect. 5.3.

[Badenes and Maoz \(2012\)](#) used radial velocity measurements to estimate the merger rate of double white dwarfs in the Galaxy. Their (lower velocity resolution) sample was limited to systems with small separations between

⁸ We note that the term ‘hybrid’ is also used to refer to white dwarfs that are of carbon-oxygen-neon composition. We do not discuss those heavier white dwarfs here but refer the reader to [Denissenkov et al. \(2013\)](#).

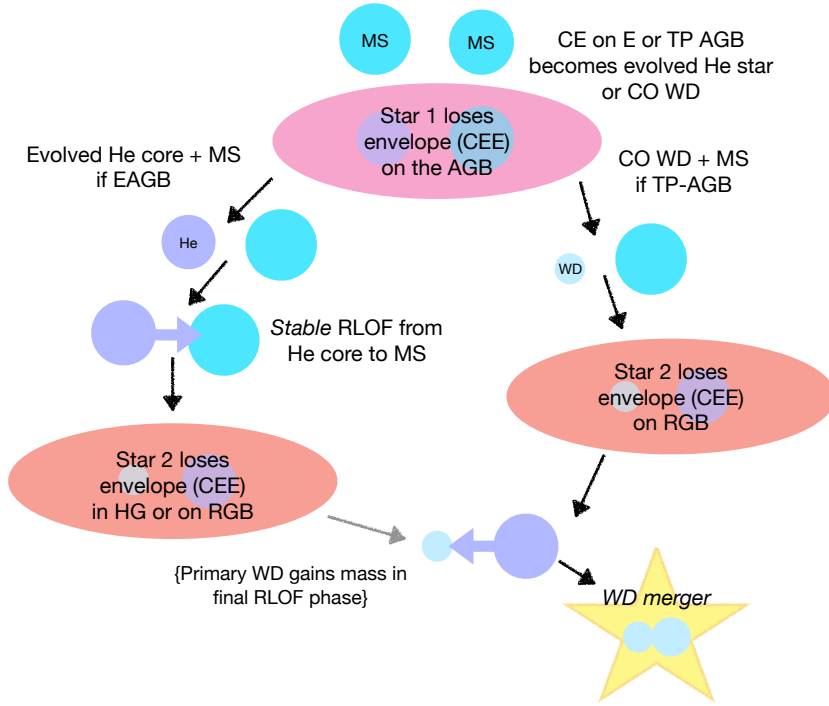


Fig. 1 Schematic cartoon showing two channels of white dwarf mergers that can plausibly lead to SNe Ia from the STARTRACK (Belczynski et al. 2008) binary population synthesis code. The two channels shown are those more likely to occur when the first mass transfer episode is unstable (i.e. a common envelope), which often results in a second CE later on in the evolution. We note however that double white dwarf merger progenitors can also easily form through undergoing just one CE event. *Left channel:* When the first CE occurs on the early-AGB (EAGB), the binary will often undergo a stable mass transfer event before the second CE takes place when the initially more massive star is a slightly-evolved, H-stripped, He-burning star. Then, another CE event occurs when the secondary is either in the Hertzsprung Gap or on the RGB. *Right channel:* When the first CE occurs later in the AGB’s evolution, when it is thermally-pulsating (TPAGB), the emerging core is a white dwarf, and the next mass transfer episode to take place is unstable. *Both channels:* In both channels, there is a stable mass transfer episode predicted to occur later in the evolution of the binary (after both CEs in this case) whereby the slightly-evolved, hydrogen-stripped, helium-burning star donates mass to the first-formed white dwarf. Such a phase is crucial for building up the mass of the primary white dwarf to be on the order of $\sim 1 M_{\odot}$ (Ruiter et al. 2013), but further detailed studies should be carried out to determine the thermal response of the stars to assess whether this phase indeed leads to continued, stable accretion and eventual formation of two white dwarfs, or whether a ‘premature’ merger is likely to occur during this phase. The grey arrow indicates the phase is encountered less frequently.

0.001–0.05 AU. They found that the total Galactic DWD merger rate – including WD mergers whose total mass would be below the Chandrasekhar mass limit – was consistent with the estimated specific rate of SNe Ia in the Galaxy from Li et al. (2011b), their Fig. 4, in other words 0.1 SNum, or $\sim 1 \times 10^{-13}$ SNe Ia $\text{yr}^{-1} M_{\odot}^{-1}$). Expanding the sample, Maoz et al. (2018) were able to

probe binaries with separations out to 4 AU to set more stringent limits on the Galactic merger rate of white dwarfs. They found the double WD merger rate to be even larger than their previous estimate: 6 times higher than the expected Galactic SN Ia rate. In other words, if most SNe Ia do arise from white dwarf mergers, ~ 15 per cent of Galactic double WD mergers will eventually produce a SN Ia (see Sect. 3.7 for more discussion on SN Ia rates). For a recent study on detection of close white dwarf binaries and their properties, we refer the reader to [Shahaf et al. \(2024\)](#).

To date, very few double white dwarf binaries have been directly detected ([Napiwotzki et al. 2020](#), 39 systems in Table 2). However, such low detection rates are expected within a limited volume given their faint nature. This is not a concern for the double white dwarfs as a leading progenitor scenario for SNe Ia, since current technology does not even enable us to easily detect large numbers of double white dwarfs. Unlike the ‘textbook’ SN Ia progenitors that involve a white dwarf stably accreting from a non-degenerate star – occasionally exhibiting thermonuclear outbursts – detached double white dwarf binary systems are electromagnetically ‘quiet’ (see [Rebassa-Mansergas et al. 2019](#), who analysed the probability of detecting plausible double degenerate progenitors with current facilities). It is expected that with the launch of the first space-based gravitational wave observatory, anticipated to be the Laser Interferometer Space Antenna (LISA, see Living Review by [Amaro-Seoane et al. 2023](#)), we will finally be able to detect the presence of $\sim 60,000$ double white dwarf binaries in the Galaxy ([Korol et al. 2018, 2022](#)), some of which we can expect to be likely progenitors of SNe Ia. Though it is quite unlikely that LISA will ‘see’ directly the merger of a double white dwarf over the lifetime of the mission,⁹ detection of many thousands of white dwarf binary pairs that will merge many Myr from now will give us the opportunity to understand pre-merger white dwarf system parameters in an unprecedented way. This will be useful not only for solving the progenitor problem ([Maoz and Mannucci 2012](#)), but will give insights into the formation of other, non-explosive transient sources also presumed to be formed via white dwarf mergers, such as hydrogen-deficient carbon (HdC) stars (R Coronae Borealis, ‘dustLess’ HdC stars, and extreme helium stars, [Tisserand et al. 2022](#)). In Fig. 1, we show a schematic picture of just two plausible formation channels leading to the formation of a merging double CO WD binary.

In terms of the explosion mechanism, double degenerate systems possessing the right physical properties are now thought to readily lead to explosions in sub-Chandrasekhar mass white dwarfs, likely through a double-detonation (see Sect. 5). Even so, the more traditional idea of a white dwarf merger leading to the disruption of a larger, less-massive white dwarf that forms an accretion

⁹ LISA will be sensitive to double white dwarfs within a certain frequency band that corresponds to orbital periods on the order of a few hours or less, thus the very wide (and more numerous) systems will not be observable. Further, LISA will only be able to detect close double white dwarf binaries in our own Galaxy and nearby, which limits the total detection volume, but see [Yoshida \(2021\)](#) regarding observations of post-WD-merger remnants in the decihertz band.

torus around the more massive primary, which subsequently accretes mass until the Chandrasekhar limit is approached, still remains a possibility (see a detailed hydrodynamical study by [Neopane et al. 2022](#)). In this case, the explosion mechanism would proceed similarly to what occurs in the single degenerate Chandrasekhar mass explosion (see Sect. 4).

1.2.3 Early history – observed SNe Ia

In the 19th century a supernova occurred in the nearby spiral galaxy Andromeda: SN 1885A ([de Vaucouleurs and Corwin 1985](#)), also called S Andromedae, thought to have been a SN Ia based on historical records. Observations were not made easier by the fact that the supernova appeared relatively close to M31’s nucleus. Going back further and closer to home, the Galactic remnant SN 1181 AD has gained much recent attention. This supernova event has been identified to have properties that render it a poor match to ‘normal’ SNe Ia that are used for cosmological studies, but is a reasonable candidate to link to another SN Ia sub-class. It has been speculated by [Schaefer \(2023\)](#) that this was a SN Iax event that could have been triggered from the merger of a CO WD and an ONe WD (see also [Fesen et al. 2023](#)).

The earliest known supernova thought to have been of Type Ia observed by and recorded by humans dates back as early as 185 BC (SN 185, well documented by Chinese court astronomers, see also [Broersen et al. \(2014\)](#)), followed by the more well-known SN Ia events SN 1006, SN 1572 (Tycho) and SN 1604 (Kepler) ([Hamacher 2014](#), table 1). However, we know based on supernova remnant observations that there have indeed been Type Ia supernovae exploding over the last ~ 2 millennia, but only a handful have present-day lasting records. For example, SN remnants SNR 0509-67.5, 0519-69.0, and N103B in the Large Magellanic Cloud (LMC) are estimated to have ages of 400 ± 120 , 600 ± 200 , and ≈ 860 years, respectively, from observations of their light echoes ([Rest et al. 2005](#)). These events were likely observable from communities in the Southern Hemisphere, and ongoing collaborations with Indigenous elders are examining possible records of these events in oral tradition (cf. [Hamacher et al. 2022](#)). The lack of any record of the supernova that gave rise to SNR 0509-67.5 seems particularly puzzling since supernova remnant evolution models that take the position of the reverse shocked ejecta emitting in $[\text{Fe XIV}]5303 \text{ \AA}$ into account place the explosion into the early 18th century ([Seitenzahl et al. 2019](#); [Arunachalam et al. 2022](#)).¹⁰ Perhaps the most plausible explanation is that the supernova simply exploded in the (southern hemisphere) winter, when the LMC was below the observable horizon for most localities frequented by humans at the time. A summary of historical supernovae is out of the scope of this review, but the interested reader is encouraged to see [Pagnotta et al. \(2020\)](#).

¹⁰ Reverse shocked ejecta in SNR 0509-67.5 were detected in MUSE data as forbidden highly-ionized ‘coronal’ lines, so named because the same optical lines are seen in the solar corona ([Seitenzahl et al. 2019](#)).

1.2.4 Type Ia supernovae: the last 100 years

Edwin Hubble is famous for having made observations of far-away galaxies and is credited with the discovery of the expanding Universe (Hubble 1929), though it should be noted that the same redshift-distance relation was discovered by Georges Lemaître even earlier (Lemaître 1927). Though the presence of something we now refer to as dark energy was predicted by Einstein’s field equations, the notion that the rate of expansion of our Universe is increasing with time would not be confirmed until near the turn of the 20th century. Hubble used Cepheid variable stars to demonstrate the Universe is expanding. It was possible to use Cepheids as ‘standard candles’ owing to their well-known pulsation period–luminosity relationship, first uncovered by Henrietta Leavitt (Leavitt and Pickering 1912). As instrumentation capability and technology grew, it became possible to detect other, more luminous and thus distant ‘standard candles’: Type Ia supernovae (more accurately referred to as ‘standardizable candles’ since lightcurve-fitting must first be applied; see Sect. 3.1).

Burbidge et al. (1957), famously known as B²FH, and independently Cameron (1957) first outlined rather comprehensively the plausible mechanisms for synthesis of the elements. B²FH showed that elements from Li to U were created in stars, not synthesized in the Big Bang. The fact that the B²FH paper offered testable predictions – namely through chemical evolution of galaxies – makes it a profound discovery paper. More than two decades earlier, it was reported by Lundmark (1932) through careful consideration of historical records available at that time that there indeed appeared to be two different classes of explosion sites capable of polluting the interstellar medium based on their peak luminosity – common novae (today known simply as novae), and supernovae (see also Baade and Zwicky 1934a,b; Lundmark 1935; Baade 1938; Minkowski 1939). It was noticed even around that time that these supernova explosions occur more frequently (per unit stellar mass) in galaxies that host primarily young stellar populations (Zwicky 1942).

The concept that core-collapse supernovae likely arise from massive stars and Type Ia supernovae might originate from degenerate cores of evolved stars was pointed out by Hoyle and Fowler (1960):

“...there appear to be two distinct conditions that can lead to a major stellar explosion: (1) A catastrophic implosion of the core. This condition is necessary when the nuclear fuels are non-degenerate. We shall find this to be the case in massive stars ($M > 30 M_{\odot}$). (2) Degenerate nuclear fuels are inherently unstable. Explosion can take place during normal evolution – i.e., without a catastrophic implosion being necessary. We shall find this to be the case in stars with mass somewhat greater than M_{\odot} . The existence of two distinct conditions for explosion suggests an association with the two types of supernovae identified by observers.”

The idea that the dominant abundance of ^{56}Fe among the stable iron-group¹¹ isotopes in the solar system is linked to its radiogenic origin from the doubly-magic ^{56}Ni likely goes back to German nuclear physicist Otto Haxel (for a historical review see Clayton 1999). In his PhD thesis, Pankey (1962) made the important connection between the amount of ^{56}Ni synthesized and the peak luminosity:

“It is also obvious that any large scale formation of iron by this method, in the explosion of a super nova, would lead to a subsequent decay of activity that would be linear for approximately 100 days, and then would follow the exponential beta decay of Co-56 to Fe-56”.

With a new value (but at the time uncertain) for the binding energy of ^{56}Ni available, Clifford and Tayler (1965) showed, by numerically solving the equations of nuclear statistical equilibrium, that for nuclear matter of nearly equal numbers of protons and neutrons, under many conditions ^{56}Ni will indeed be the preferred nucleus synthesized. Truran et al. (1967) then showed with time-dependent nuclear reaction network calculations that supernova shock waves in material composed of self-conjugate intermediate mass nuclei, such as ^{12}C , ^{16}O , or ^{32}S , leads to copious amounts of ^{56}Ni produced and relative isotopic ratios of the stable iron-peak elements that can explain those found in the solar system.

Colgate and McKee (1969) further investigated explosion models with subsequent radioactive decay, concluding that radioactive decay of ^{56}Ni may indeed play a significant role in providing the bulk of optical luminosity in supernova lightcurves (see Fig. 2). Seitenzahl et al. (2009c) extended the theory of the source terms of radioactively powered supernova lightcurves by including the ^{57}Ni and ^{55}Co decay chains, which owing to their longer half-lives dominate the heating at late times (observational evidence of this prediction can be found in Graur et al. 2016; Tucker et al. 2022).

The influential papers of Hansen and Wheeler (1969) and Arnett (1969) first proposed detonations in massive white dwarfs powered by the explosive thermonuclear fusion of $^{12}\text{C} + ^{12}\text{C}$ as a model for SNe Ia. While the $1.37 M_{\odot}$ carbon-detonation model of Arnett (1969) and the $1.42 M_{\odot}$ model of Hansen and Wheeler (1969) were soon after rejected as viable models for SNe Ia, the key ideas that SNe Ia are powered by detonations in massive WDs, fusing lighter carbon (and e.g. oxygen) nuclei into more tightly bound nuclei, including large amounts of radioactive ^{56}Ni , has survived the test of time. The general idea that lower- and intermediate-mass stars may be the main contributors to such thermonuclear explosions was gaining ground, as supported by Paczyński (1970): “Stars of 3, 5 and 7 M_{\odot} ignited carbon in the centre at the density of 3×10^9 g/cc. This will probably lead to the type of thermonuclear supernova explosion suggested by Arnett.”

Later on, it would be agreed that the specific Arnett (1969) direct-detonation model of an accreting near-Chandrasekhar mass WD fails because the di-

¹¹ For some general guidance regarding what we refer to as iron-group elements, we refer the reader to Woosley et al. (1973), Figs. 2 and 6.

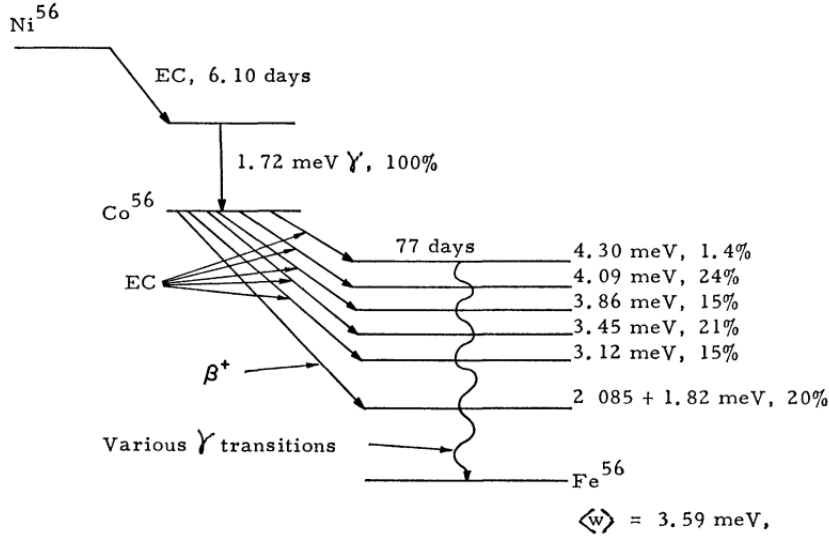


Fig. 2 Decay scheme of $^{56}\text{Ni} \rightarrow ^{56}\text{Co} \rightarrow ^{56}\text{Fe}$, which is long-known to supply the most power to the optical lightcurve of thermonuclear supernovae. Image reproduced with permission from Colgate and McKee (1969), copyright by AAS.

rect initiation of a central detonation – where the white dwarf eludes a pre-expansion phase – is unlikely (e.g. Niemeyer and Woosley 1997); the thermonuclear flame should rather ignite as a sub-sonic deflagration slightly off-centre (e.g. Nonaka et al. 2012). Moreover, and more importantly, the incineration of a near-Chandrasekhar mass WD by a super-sonically advancing detonation leads to very high explosion energies and the production of predominantly iron-group elements (mostly radioactive ^{56}Ni) – and only small amounts of intermediate mass elements such as silicon or sulfur are produced, which is in conflict with observations (Arnett et al. 1971).

But even in the 1970s, it was still not clear what the progenitors of various types of supernovae (thermonuclear or core-collapse) in general were, though the dichotomy was becoming increasingly apparent in that core-collapse supernovae were being found among more massive, younger stellar populations while ‘type I’ supernovae originate in lower mass stars (Oke and Searle 1974; Tinsley 1977). It was already suggested by Finzi and Wolf (1967) that such ‘Type I’ supernovae could arise from electron captures resulting in the implosion of heavy white dwarfs near the Chandrasekhar mass limit. Arnett (1979) postulated that Type I supernovae may arise from the core-collapse of an evolved star that underwent mass-loss of its H-rich envelope, the pre-SN progenitor being a helium-rich star in the mass range $1.5 - 4 M_{\odot}$. In terms of progenitor configuration, Whelan and Iben (1973) discussed the likelihood of type I supernovae originating from near-Chandrasekhar mass white dwarfs accreting from a low-mass, highly-evolved giant companion. This picture would

become the favoured scenario configuration for SN Ia progenitors for the next ~ 4 decades (see also [Hansen and Wheeler 1969](#)).

After the pioneering work of [Arnett \(1969\)](#), hydrodynamical studies on detonation and deflagration physics started in the 1970s ([Bruenn 1971](#); [Buchler et al. 1974](#); [Ivanova et al. 1974](#); [Nomoto et al. 1976](#)) (see also the early work of [Nomoto and Sugimoto 1977](#), in the context of rejuvenation of helium cores). Progress on theoretical work on explosive nuclear burning in degenerate matter and nucleosynthesis calculations paved the way for more plausible connections with problems in stellar astrophysics. The 1980s brought the development of more sophisticated burning models for both Chandrasekhar mass and sub-Chandrasekhar mass white dwarfs: ([Taam 1980](#); [Nomoto 1982a](#); [Hashimoto et al. 1983](#); [Starrfield et al. 1985](#); [Nomoto et al. 1984b,a](#); [Nomoto and Iben 1985](#); [Branch et al. 1985](#); [Thielemann et al. 1986](#); [Müller and Arnett 1986](#); [Woosley et al. 1986](#); [Hernanz et al. 1988](#)).

The most successful and famous model of the early explosion models is the eminent W7 model of [Nomoto et al. \(1984a\)](#), a 1D explosion model of a $1.38 M_{\odot}$ CO WD where the nuclear burning occurs behind a parameterized fast deflagration flame. While initial variants of the W7 model nucleosynthesis ([Thielemann et al. 1986](#); [Iwamoto et al. 1999](#)) overproduced certain stable iron-group isotopes (e.g. ^{54}Fe , ^{58}Ni), implementation of the revised electron capture rates on pf-shell nuclei ([Langanke and Martinez-Pinedo 2000](#)) removed much of this problem ([Brachwitz et al. 2000](#)). Such 1D models like W7, although un-physical in the sense that the buoyancy and hydrodynamical instabilities (especially the Rayleigh-Taylor instability) that accelerate the flame are suppressed, resulted in an explosion profile that in many ways matched characteristics such as spectra and lightcurves (e.g. [Höflich and Khokhlov 1996](#)) and nucleosynthesis ([Khokhlov 1991c](#)) of “normal” ([Branch et al. 1993](#)) SNe Ia. More realistic simulations of deflagrations in near-Chandrasekhar mass white dwarfs that modelled the thermonuclear flame propagation and hydrodynamical evolution, including the growth of hydrodynamical instabilities in 3D, however failed to create sufficient amounts of fast intermediate mass elements (such as S, Si) and explosions strong enough to resemble “normal” SNe Ia, (see e.g. [Niemeyer et al. 1996](#); [Niemeyer and Woosley 1997](#); [Reinecke et al. 1999](#)).

The situation was thus that for near-Chandrasekhar mass explosion models, on the one hand an initial period of sub-sonic burning was required to expand parts of the star to lower density to avoid the pitfalls of the [Arnett \(1969\)](#) pure detonation model. On the other hand, after some period of expansion the burning had to accelerate again to a supersonic combustion front to produce sufficient amounts of intermediate mass elements and sufficiently energetic explosions. A particular variant of this “delayed detonation” is the pulsational delayed detonation model, where a detonation is triggered via an interplay of the turbulent combustion at the flame front and the strong pulsation of the white dwarf (the explosion was not strong enough to disrupt the star fully, [Ivanova et al. 1974](#); [Khokhlov 1991c](#)).

Another, more widely accepted and elegant solution to this problem invokes the transition of the subsonic turbulent deflagration to a supersonic detonation (deflagration-to-detonation-transition – DDT), a physical phenomenon that is also observed in terrestrial combustion (see e.g. Zel’dovich et al. 1980). Khokhlov (1991a) first proposed DDTs as a solution to obtaining explosions in near-Chandrasekhar mass white dwarfs that produced ^{56}Ni and intermediate mass elements in the right proportions to explain normal SNe Ia. The literature on how to model the physics of unconfined DDTs in the context of turbulent combustion in SNe Ia is vast and often rather technical, and we therefore refer the interested reader to the review by Röpke (2017) as a first point of entry.

The apparent success of the (un-physical) 1D near-Chandrasekhar mass models in reproducing observable characteristics, such as spectra and lightcurves, and the at the time perceived high-degree of homogeneity among observed SNe Ia led to a strong acceptance in the community of near-Chandrasekhar mass explosion models as the natural explanation for SNe Ia. Explosion models with lower mass primary WDs were certainly discussed and investigated, but the influential work by Woosley and Weaver (1994a) investigated double-detonation models with rather low mass primaries and quite massive helium shells ($\sim 0.2 M_{\odot}$). The detonation in the massive helium which produced nucleosynthesis yields contradicting the solar system values and the low core mass resulted in sub-luminous events (see Sect. 5). Sub-Chandrasekhar mass primaries thus fell out of favour for an extended period of time in comparison with their near-Chandrasekhar mass “competitors”. For a comprehensive review on the state of the art of Type Ia supernova models up until the year 2000 see Hillebrandt and Niemeyer (2000).

The ground-breaking discovery that Type Ia supernovae could be used as cosmological distance indicators sparked a whole new global effort to try to better-understand the nature of their progenitors, thus launched a rich era of observational supernova research. Toward the end of the 1990s, SNe Ia were being discovered at rather large distances with the Hubble Space Telescope. The discovery of the accelerating Universe by these teams led to the Nobel Prize in Physics (2011) being awarded jointly to Saul Perlmutter (50%) and Adam Riess (25%) and Brian Schmidt (25%) “for the discovery of the accelerating expansion of the Universe through observations of distant supernovae”¹² (Riess et al. 1998; Schmidt et al. 1998; Perlmutter et al. 1999).

In the next sections, we discuss in some more detail the observations and theoretical models that have guided our understanding of SNe Ia over the course of this century so far.

2 The 21st century: direct observations that constrain the explosion

It is almost haunting how in all of their cosmological prowess, the lack of understanding of what make SNe Ia has not been a major obstacle in our ability

¹² <https://www.nobelprize.org/prizes/physics/2011/press-release/>

to use them as effective cosmological tools. However, this lack of understanding profoundly affects our knowledge about the yield/origin of the elements, particularly those in and near the iron-group (Ti, V, Cr, Mn, Fe, Co, & Ni). There have been a number of direct SN Ia observations where spectra and lightcurve information have contributed to a deeper understanding of the physics behind these explosions, and in some cases the nature of the progenitor system. We refer the reader to the relatively recent review papers by [Jha et al. \(2019\)](#) and [Maoz et al. \(2014\)](#) for an overview of observational properties of Type Ia supernovae. The SN Ia observables are of course affected by the physics of the explosion mechanism, which is affected by stellar structure (namely WD mass but also ignition and other factors) as well as, to some degree though indirectly, the nature of the donor star. So far, relatively nearby SNe Ia have been used to calibrate or ‘standardize’ SNe Ia and the (empirical) relationship between intrinsic brightness and lightcurve width is mapped and applied to more distant supernovae, assuming that high-redshift supernovae ‘behave’ the same way as those that are closer to us.

Though more luminous SN Ia have historically been observed among younger stellar populations ([Branch et al. 1996](#); [Umeda et al. 1999](#)), recent photometric data (IR and optical) confirm previous cosmological studies that, after applying cosmological standardization fits to the data, the brighter SNe Ia are those occurring among more massive host galaxies ([Ivanov et al. 2000](#); [Hamuy et al. 2000](#); [Uddin et al. 2020](#)). We discuss more about SNe Ia in the context of their hosts in Sect. 3.1.

The large range in maximum luminosity within the observed SN Ia population has been known for a few decades ([Phillips 1993](#); [Filippenko 1997](#); [Phillips et al. 1999](#)). 1991T-like supernovae, characterized as being very luminous, can be $\sim 3\times$ more luminous at peak in B-band than the fainter, faster-declining 1991bg-like supernovae ([Spyromilio et al. 1992](#)). This is nicely illustrated in Fig. 3, adapted from [Taubenberger \(2017\)](#), which shows B-band and I-band lightcurves and spectra of 1991T-like supernovae alongside those of 1991bg-like supernovae. While normal SNe Ia make up the majority of SNe Ia, there is a substantial fraction, on the order of $\sim 15 - 35\%$, that do not fit into this category ([Möller et al. 2016](#); [Graur et al. 2017](#)).

Indeed, a large fraction of non-normals are more likely to be missed observationally owing to the fact that most peculiar SN Ia events are sub-luminous compared to normal SNe Ia. SN2011fe and SN2003du are shown for comparison with black lines in all panels. We note as well that through photometric studies, [Yang et al. \(2022\)](#) found the sub-class of 1991T/1999aa-like supernovae to also be very useful distance indicators. Going in the other direction, [Graur \(2024\)](#) found that a nearby sample of sub-luminous 1991bg-like SNe function as very promising standardizable candles when taking into account correlations between their peak absolute magnitudes and the ‘colour-stretch’ parameter s_{BV} .

With the more recent benefit of deep transient surveys, the true diversity among SNe Ia has become even more apparent than is illustrated here (see [Taubenberger 2017](#), especially their Fig. 1). Fainter, more exotic sources

thought to be thermonuclear in nature are being found in surveys and can more readily be followed-up spectroscopically. Spectroscopy is indeed what is needed to learn more about the detailed physics of the explosion as it gives us an opportunity to test the explosion + nucleosynthesis + radiative transfer predictions from detailed models.

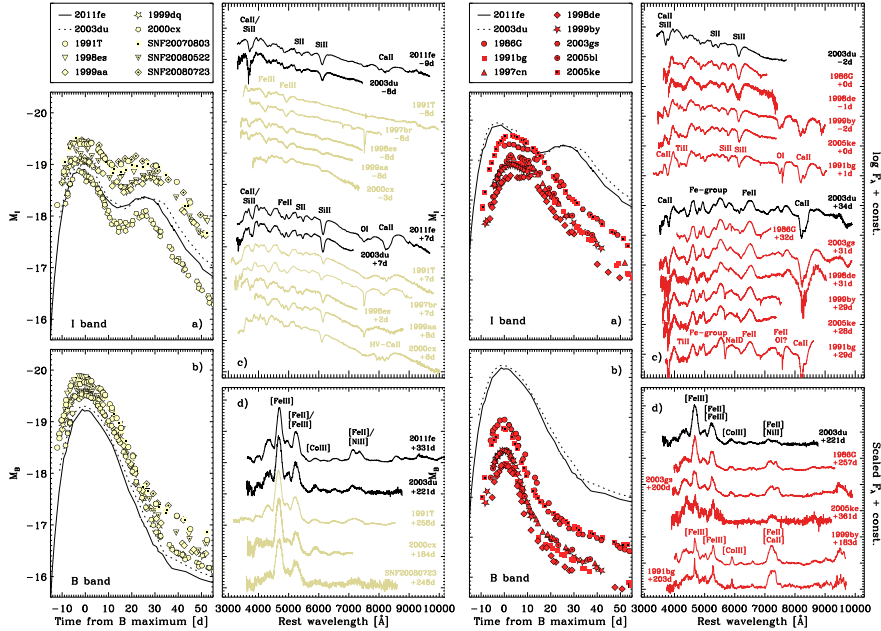


Fig. 3 Lightcurves and spectra of canonically-luminous SNe Ia (shown in yellow; left) and canonically sub-luminous SNe Ia (shown in red; right). In both (yellow and red) examples: lightcurves are in B-band (lower left) and I-band (upper left), while photospheric (top right) and nebular (bottom right) spectra are shown for comparison. In all figure panels, the lightcurve or spectrum of a normal SN Ia (2011fe and 2003du in this case) is plotted for comparison. Images reproduced with permission from [Taubenberger \(2017\)](#), copyright by Springer.

2.1 Spectra and lightcurves that constrain the explosion mechanism

Lightcurves of SNe Ia directly probe how much radioactive material (^{56}Ni) is synthesized in the explosion, which is often used as a proxy for how much mass was in the exploding white dwarf ([Leibundgut 2000](#)). Spectra are the most useful observational asset and act a decoder for the explosion, because from spectra we can learn about the nucleosynthetic composition of the explosive process and, possibly to some extent, the nature of the stars involved in the explosion. For example, for pure deflagration models that fail to unbind

the star, less carbon-oxygen fuel is consumed compared to delayed-detonation models, so we would expect a large amount of unburned carbon and oxygen to be present even deep within the ejecta structure, and this may give rise to certain observables even at late times (Blondin et al. 2012). Ejecta line velocities give us information about the energy of the explosion, while measured velocities from material in the vicinity of the supernova can also potentially help to reveal the progenitor evolutionary channel, because such material is indicative of circumstellar non-accreted material originating from the donor (e.g. blueshifted, time-varying Na I D absorption features, Patat et al. 2007; Sternberg et al. 2011).

We anticipate the ability to put tighter constraints of the explosion mechanism(s) of SNe Ia to greatly improve as the number and quality of state-of-the-art spectral observations increases. We note that while there are many works that focus on directly constraining SN Ia explosions at high energies (UV, X-rays; Wang et al. 2012; Immler et al. 2006; Margutti et al. 2014), and low energies (radio; Chomiuk et al. 2016), our overview here is by no means complete and focuses on the optical regime, as this is where the bulk of the results thus far have fallen, especially in terms of modelling predictable observables (spectra and lightcurves). Thus far, setting any robust constraints on explosion models by comparing synthetic spectra and lightcurves from different models to real SNe Ia (e.g. Röpke et al. 2012, for SN2011fe) has been partly limited due to the dearth of nearby events, in addition to an overall lack of 3D explosion models (Pakmor et al. 2024). Some recent work has already been published using infrared nebular spectra with JWST where a number of lines from species near the iron-peak were measured (Kwok et al. 2023). However, one should remain cautious in the interpretation of observational data when making comparisons with models. Since a supernova explosion is inherently 3D – particularly important when considering Chandrasekhar mass explosions or double degenerate mergers in which both white dwarfs explode (Pakmor et al. 2022) – it is not currently possible to accurately infer progenitor structure by comparing 1D explosion models to nebular spectra alone. Therefore, it is necessary to compute and carry out full analyses, both of the explosion and radiative transfer simulations, in 3 dimensions to make any significant progress as a scientific community in understanding SN Ia progenitor structure from observed nebular spectra.

2.1.1 Early interaction (early excess)

Obtaining very early-time spectra of SNe Ia can be quite a challenge. However, early-time spectra can reveal crucial information about the explosion mechanism. Interaction between the companion and the supernova ejecta at early times is predicted to result in excess emission in the blue and in the UV bands (Kasen 2010), though such signatures may be difficult to observe for certain viewing angles.

A strong reverse shock is expected to form when the supernova ejecta smacks into the companion, thus causing surrounding material to heat up.

As such, thermal radiation can be seen as an excess in the blue region of the lightcurve. Such an excess is expected to appear rather early, and may quickly fade a few days after explosion (Cao et al. 2015). Observational evidence of early shock interaction has not been ubiquitous. This is not surprising given the short timescales over which the early excess signature appears, though pushing for shorter cadence intervals (than the more typical 3-day cadence) in synoptic surveys could help to rectify this (Magee et al. 2022). Hayden et al. (2010) analyzed lightcurves of 108 supernovae from the SDSS-II Supernova Survey in search for signatures of early interaction, but no such candidates were found in the data. Now, a number of years later and owing to statistical analysis of improved early observations (e.g. Magee et al. 2022), it is becoming apparent that a significant fraction (about one in five) of SNe Ia shows an early excess bump in the lightcurve, with the sub-class of 91T/99aa SNe showing the greatest (about one in two) prevalence (Deckers et al. 2022). Some well-studied individual examples that cover a range of sub-types and interpretations include iPTF14atg (Cao et al. 2015), SN2017cbv (Hosseinzadeh et al. 2017), SN2020hvf (Jiang et al. 2021), SN2021zny (Dimitriadis et al. 2023), SN2023bee (Hosseinzadeh et al. 2023; Wang et al. 2024), SN2023ywc (Srivastav et al. 2023), and SN2022xkq (Pearson et al. 2024); see also works related to the Young Supernova Experiment (Jones et al. 2021; Aleo et al. 2023).

An overarching trend is that early-time lightcurves indicate that these supernovae probably did not originate from symbiotic-like (wide WD + RG) binaries (307 lightcurves from TESS, Fausnaugh et al. 2023).

We highlight here one interesting example: SN2019yvq, a slightly under-luminous SN Ia, exhibited an excess in the early lightcurve in the blue and UV (see Miller et al. 2020). It is one of the rare events known to exhibit a blue early flash but also additionally calcium emission in the nebular spectra (Siebert et al. 2020). Emission of [Ca II] in particular is consistent with this event having originated from a helium-shell detonation (see also Jiang et al. 2017), but no single progenitor scenario seems to be able to explain this event without introducing new discrepancies (Tucker et al. 2021).

Single degenerate scenarios are not the only formation scenario expected to give rise to early-time emission, and in fact the excess emission could be due to interaction with circumstellar material (Piro and Morozova 2016). Though typically the presence of early interaction emission is taken to mean we can exclude the possibility of a double degenerate progenitor, it turns out that mergers cannot be completely ruled out. Interaction between a tidal tail produced in a white dwarf merger interacting with the interstellar medium could give rise to a gas shell; such an interaction is predicted to produce spectral features, potentially across a wide range of wavelengths and timescales, with an early shock breakout phase giving rise to optical/UV emission (Raskin and Kasen 2013). Though useful for setting some limits on plausible progenitor scenarios (Hosseinzadeh et al. 2017), it appears very challenging to fully disentangle the possible SN Ia sub-classes with early excess emission (Jiang et al. 2018), as photometric data alone offer only modest constraints on progeni-

tor scenarios at best (see radiation hydrodynamical study by [Noebauer et al. 2017](#)).

2.1.2 Photospheric velocities

SNe Ia explosions give rise to a myriad of spectral lines in the optical regime. Some rather intriguing correlations exist, for example, [Garnavich et al. \(2004\)](#) showed that the depth of the 580 nm spectral feature, which has potential contributions from both Si II and then Ti II in cooler photospheres, correlates with luminosity for sub-luminous SNe Ia.

Before and around maximum light, the SN spectrum is characterized by broad emission and absorption line complexes. The observed photons are originating from a photosphere that moves inward in a Lagrangian sense. Since we are observing the part of the photosphere that is rapidly moving towards us (the view of the receding far side is obstructed by the optically thick core), the (blue-shifted) Doppler shifts of the lines can be measured. Such “expansion velocities” around maximum brightness are most prominently determined for Si II $\lambda 6355 \text{ \AA}$ (but also others, such as e.g. Ca II H&K).

[Benetti et al. \(2005\)](#) classified the diversity among SNe Ia by examining the time evolution of the Si II expansion velocity (the velocity gradient) and concluded that a population of 26 SNe could be broken into 3 ‘groups’: FAINT, high velocity gradient (HVG) and low velocity gradient (LVG), with the split occurring around $70 \text{ km s}^{-1} \text{ day}^{-1}$ (see lower panel of Fig. 4). The FAINT group, which include the well-known 1991bg event, tend to originate in older stellar populations (early type galaxies) and decline rather quickly in comparison to the other two groups, though were found to have velocity gradients similar to those of the HVG group in [Benetti et al. \(2005\)](#). Those authors speculated that HVG SNe could be delayed-detonation explosions in which variations in density at the time of deflagration-to-detonation transition is what may be causing the slight diversity among observed properties for this group (see Sect. 4 for a description of various explosion models in Chandrasekhar mass WDs). Speculation about the explosion mechanism for LVG SNe, which include the well-known SN 1991T event, was however less straightforward, though it was proposed this group is simply an extension of the HVG SNe in which ejecta mixing or circumstellar interaction could play some larger role. There is also evidence that explosions with high-velocity ($> 12,000 \text{ km/s}$) Si II $\lambda 6355 \text{ \AA}$ are found among more massive galaxies on average, with metallicity possibly being an affecting parameter ([Pan 2020](#), see Fig. 5).

Searching for correlations between observational properties, e.g. lightcurve decline rate and strengths of various absorption features at maximum light, has been explored with the aim of disentangling SN Ia physical processes. Some correlations have been found to give rise to a ‘spectral sequence’ ([Nugent et al. 1995](#)). Though some SNe Ia may show nearly identical lightcurve evolution, they have been known to exhibit a rather large dispersion in velocity gradient for certain features (i.e. Si II $\lambda 6355 \text{ \AA}$ line). The ratio of the depth of

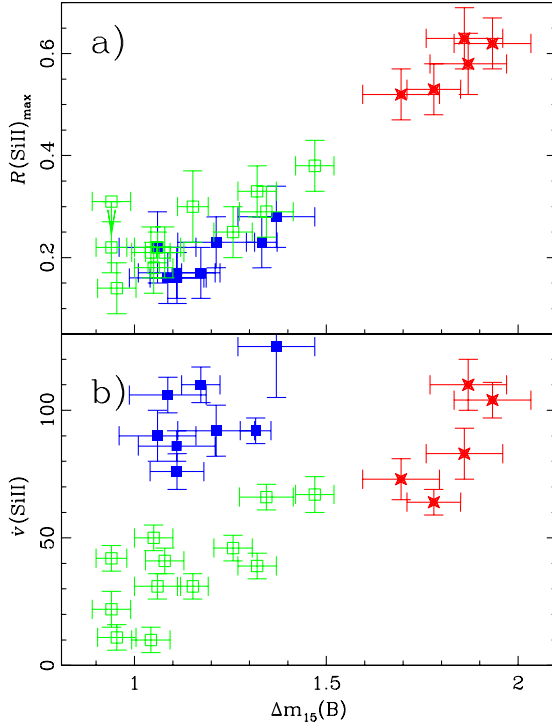


Fig. 4 Open symbols show LVG SNe, filled squares show HVG SNe, and starred symbols show FAINT SNe from [Benetti et al. \(2005\)](#). It was later shown by [Blondin et al. \(2012\)](#) that these groupings were less distinct when a stricter, more consistent definition of velocity gradient is used (see Sect. 5.2 of [Blondin et al. 2012](#)).

two absorption features against $\Delta m_{15}(B)$ is shown in the top panel of Fig. 4: $R(\text{Si II})_{\text{max}}$ represents the ratio of the depth of Si II 5972 Å and 6355 Å (rest wavelength) lines at maximum light (see also [Branch et al. 2006](#), where the term ‘core-normal’ originated from based on observations of 26 SNe Ia). In this parameter space, the FAINT SNe tend to show a clear separation from both LVG and HVG SNe. However when $\Delta m_{15}(B)$ is plotted against the expansion velocity evolution gradient \dot{v} (Fig. 4, bottom panel), the three groups are clustered in distinct regions, with the FAINT group more plausibly representing a different explosion pathway than the other two (LVG, HVG) groups, noting that the LVG SNe have lower Si II velocity gradients than the other two groups (see also [Wang et al. 2009b](#)). The \dot{v} parameter ($-\Delta v/\Delta t$) introduced by [Benetti et al. \(2005\)](#) measures the rate of decrease of the expanding ejecta, typically from the silicon line at 6355 Å which is usually prominent in the first \sim month after explosion. However, [Blondin et al. \(2012\)](#), who performed

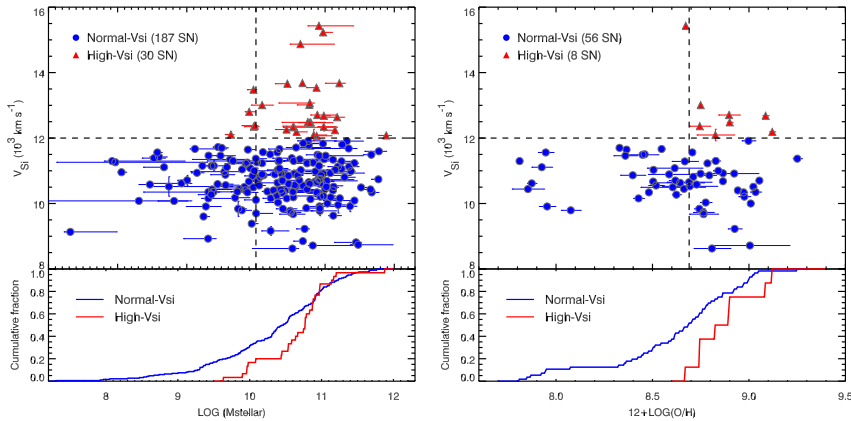


Fig. 5 Measured Si II $\lambda 6355$ \AA velocities as a function of host-galaxy stellar mass. The red triangles are the so-called high-velocity SNe Ia, and tend to be found among massive host galaxies, while the lower-velocity SNe are found over the entire range of galaxy masses. Image reproduced with permission from Pan (2020), copyright by AAS.

a detailed study of 462 SNe Ia, found that this definition of velocity gradient is not necessarily consistent since the value will depend on the interval of time over which the measurements are taken (see their Sect. 8). Nonetheless, when in possession of large amounts of high-quality data, it is useful to carefully explore potential underlying physical correlations that may hold tangible significance.

Maeda et al. (2010) investigated the LVG and HVG trend further, and came to the conclusion that the LVG and HVG grouping can be simply explained by a geometrical effect, and likely supported evidence for the existence of asymmetric (Chandrasekhar mass) SNe Ia explosions. They argue that viewing angle relative to the deflagration sparks, assumed to be initiated off-centre, will determine the amount of red- and/or blue-shifting of nebular lines [Fe II] (7155 \AA) and [Ni II] (7378 \AA), which trace the deflagration ash (also see the review by Jha et al. 2019, section 1, for recent discussion). In this context, LVG SNe can be explained as being viewed from an angle in which the deflagration was ignited on the nearside, and thus the deflagration ash, once visible, will display line-of-sight velocities that are blue-shifted; vice-versa for HVG events (see Figs. 2 and 4 of Maeda et al. 2010, for details).

With the well-known idea that the mass of the exploding white dwarf is likely connected to the SN Ia luminosity at peak brightness (Sim et al. 2010), to first order, one can assume that SNe Ia exploding from more massive WDs will exhibit lower ejecta velocities owing to having higher gravitational binding energies. Such a relationship – in this case increasing [Si II] velocity with M_{B} – was uncovered in the double-detonation simulations of Polin et al. (2019, see also Zingale et al. (2013)), who simulated double-detonations for different sub-Chandrasekhar mass models in 1D with $0.01 M_{\odot}$ shell masses

(see their Figs. 11 and 12). Polin et al. (2019) indeed found that a sub-set of the data from Zheng et al. (2018) followed this Si II – M_B relationship that would be anticipated for sub-Chandrasekhar events with a range of masses, while another group of SNe Ia clustered around $v \sim 11,000$ km/s and $M_B \sim -19.3$. The clumping group then are more likely to be arising from explosions of a common (Chandrasekhar) mass (see also Polin et al. 2021, for context regarding Ca-rich transients).

2.1.3 The importance of spectra in the nebular phase

After $\gtrsim 3$ months after explosion, the supernova is entering the nebular phase – where the expanding ejecta have decreased substantially in density such that photons can stream freely. This phase is extremely interesting since it allows us to ‘see’ both the near-side and far-side of the ejecta, as well as the low-velocity ejecta core. Since the outer ejecta are optically thin, we can directly probe the inner ejecta (species and their velocity red/blueshifts), which helps to constrain ignition model mechanism and geometry (Maeda et al. 2010). As the supernova enters the nebular phase, a large fraction of the radioactive nickel has decayed to cobalt, and it is the radioactive decay of $^{56}\text{Co} \rightarrow ^{56}\text{Fe}$ that powers the lightcurve at this stage. The spectrum transitions from one of continuous emission (with absorption features) to a spectrum dominated principally composed of emission lines from iron peak elements (Shingles et al. 2022), which allows for the determination of, among other properties, synthesized nickel mass (Childress et al. 2015, see also Sect. 3.3). It has been recently suggested that the near-infrared plateau observed during the nebular phase of some SNe Ia may be correlated with their peak luminosity, thus further similar studies could potentially give some insight into progenitor origin (Graur et al. 2020; Deckers et al. 2023).

An interesting way to probe the progenitor scenario is through the double-peaked velocity profile in the decay products of ^{56}Ni that is visible in some optical nebular spectra (Vallely et al. 2020). It has been argued that, given the \sim few thousand km/s spacing between the two velocity peaks, each peak could originate from an exploding white dwarf in the case of a double white dwarf collision (Dong et al. 2015) – though the same could be said for mergers, which are statistically more common than head-on collisions of white dwarfs (see Sect. 5.4). In such a scenario, to create the distinct velocity peaks, both stars would need to explode before a single, more massive (and more dense) white dwarf is formed.

2.1.4 $H\alpha$, circumstellar medium, and high-velocity features

It was noted by Leonard (2007) that should the donor star be hydrogen-rich, one should be able to detect $H\alpha$ emission in the nebular spectra of SNe Ia (see also Graham et al. 2017, and simulations by Marietta et al. 2000 and Pakmor et al. 2008). If a firm connection can be made between observed $H\alpha$ emission and the circumbinary material, then this would substantiate the assumption

that the SN Ia was produced by a Chandrasekhar mass white dwarf. A direct hydrogen signature, however, has only been found for a rare sub-class dubbed “Ia-CSM”, perhaps the most famous example is PTF-11kx (Dilday et al. 2012), but many other examples exist (e.g. Silverman et al. 2013; Sharma et al. 2023). Most SNe Ia however lack any sign of H α (Maguire et al. 2016; Graham et al. 2017; Tucker et al. 2020).

It has been known for almost 20 years that many (if not most) SNe Ia exhibit so-called “high-velocity features” (HVF) in their early, pre-maximum light spectra (Mazzali et al. 2005). These HVFs are mostly Si II and Ca II absorption lines that are at least several thousand km/s offset (faster) than the corresponding photospheric features. These HVFs allow us to study the high-velocity outer layers and the CSM (at length scales of $\sim 10^{15}$ cm) and there is hope that correlations with other SN properties yield further valuable insights into the explosion mechanism and environment (Childress et al. 2014; Silverman et al. 2015).

The CSM on even longer length scales ($\sim 10^{17}$ cm) surrounding the SN explosion site can also be probed with high-resolution spectroscopy, which sometimes reveals (mostly blue-shifted) time-varying Na I D absorption features (and also Ca II) (e.g. Patat et al. 2007; Sternberg et al. 2011). These are typically interpreted as coming from prior outflows of the pre-supernova system, yet while some correlations with other SN properties (e.g. photospheric velocities) exist, a consistent picture has not yet emerged (e.g. Hachinger et al. 2017). A recent attempt to establish whether there is a connection between the early HVFs and the time-varying Na I D features also showed that they appear unrelated (Clark et al. 2021).

2.2 Polarimetry

In the context of thermonuclear supernovae, the most important processes that can introduce a net polarization of the light observed on Earth are scattering and dichroic absorption on aligned interstellar dust grains. Both Rayleigh scattering by molecules and Mie scattering by small dust grains, either in the inter-stellar or circumstellar medium, can be significant. Finally, polarization induced by scattering of photons by electrons (Thomson scattering) is the key physical process that can lead to net intrinsic polarization of light emitted by the supernova. A monochromatic light wave, and in fact quantum-mechanically any individual photon, will have a fixed orientation of the oscillating electric field, and hence maximal polarization. These polarizations of the individual light waves (or photons) will however cancel each other out on average for light emitted (randomly) by an extended, spherically symmetric object with perfect symmetry in composition and structure (e.g. temperature, no preferred magnetic field direction). Since the different processes responsible for polarization have different signatures, we can sometimes disentangle whether it is asymmetries in the distribution of the chemical elements (e.g. clumps), overall departure from sphericity, scattering by circumstellar or interstellar dust, or

some combination thereof, that caused the polarization. For an introduction to supernova polarimetry see the review by Patat (2017).

As a class, Type Ia supernovae generally exhibit very low levels of polarization, often no significant polarization is detected down to the 0.2% level and below (e.g. Wang et al. 1996). This implies an overall high degree of spherical symmetry in Type Ia supernovae; for a review see Wang and Wheeler (2008). Polarization across strong spectral line features (line polarization) is a particularly useful probe of the inhomogeneity of the distribution of elements in an otherwise spherically symmetric explosion. The observational characteristics of line polarization can thus be compared to the predictions for different explosion model classes. For example, Wang et al. (2007) found a correlation between the lightcurve decline rate (Δm_{15}) and the polarization of the Si II $\lambda 6355$ Å line and they interpreted this result as strong support for the delayed-detonation (Chandrasekhar mass) explosion of Type Ia supernovae. Generally speaking, the low degree of polarization overall of most SNe Ia is in better agreement with typically more symmetrical near-Chandrasekhar mass explosions than the more globally asymmetric violent merger or double-detonation models (e.g. Bulla et al. 2016a,b, 2020). Interestingly, Cikota et al. (2019) find in a set of 35 SNe Ia observed with VLT/FORS2 that the linear polarization across the Si II $\lambda 6355$ Å line correlates with the pre-maximum line velocity, with suspected Chandrasekhar mass SNe having lower polarization compared to SNe Ia that are suspected to be sub-Chandrasekhar in nature (see their figures 14 and 15).

2.3 Direct imaging

While a number of works involving photometric surveys of SNe Ia abound, such as the Supernova Legacy Survey, or SNLS (Sullivan 2009), the Carnegie Supernova Project (Krisciunas et al. 2017), PanSTARRS (e.g. Scolnic et al. 2018), the Zwicky Transient Facility (ZTF Bellm et al. 2019), and the Dark Energy Survey (e.g. Abbott et al. 2019), the primary goal of such surveys has historically been to determine SN Ia distances (spectroscopic follow-up is often used to determine redshifts) to constrain the dark energy equation of state by setting limits on cosmological quantities such as the matter density parameter Ω_m , where $\Omega_m = 1 - \Omega_\Lambda$, and Ω_Λ is the density parameter for dark energy, in a flat Λ CDM Universe (Guy et al. 2010). For an up-to-date study on the data release of over 1500 SN Ia lightcurves with spectroscopic follow-up, see the Pantheon+ study of Scolnic et al. (2022); see also the recent study by the Dark Energy Survey (Abbott et al. 2024).

2.3.1 Companion searches

Though searches for stellar companions of SNe Ia relate more to constraining the nature of the progenitor system rather than constraining the explosion mechanism directly, a number of works have focused on searching for stellar

companions (ex-donors) of SN Ia exploders decades to 1000s of years after explosion. Though theoretical studies can be used as a guide to constrain expected observables from main sequence or evolved ex-donors (Marietta et al. 2000; Meng et al. 2007) and helium star ex-donors (Liu et al. 2021), So far, no unambiguous detection of an ex-donor has been achieved with absolute certainty (Ruiz-Lapuente et al. 2004; Kerzendorf et al. 2009; Schaefer and Pagnotta 2012; Do et al. 2021, see Sect. 3.5).

For recent SNe, ex-donor stars that are red giants would be more easily found for nearby supernova events such as SN2011fe or SN2014J, but small, compact donor stars like white dwarfs, low-mass main sequence stars or low-mass stripped helium-burning stars (Warner and Robinson 1972) are more difficult to detect and thus cannot unambiguously be ruled out as a plausible ex-donor (see Fig. 4 of Kelly et al. 2014, which considers the plausibility of different donor star types for nearby SNe Ia). Searches for signs of a stellar companion in the close vicinity (spatially and temporally) of the explosion (Li et al. 2011a; Kelly et al. 2014; Graur et al. 2014a; Graur and Woods 2019) have yielded some limits on what type of companion may have been allowed by the observations for a particular supernova. This type of study is well-suited to nearby SNe that are still in the early part of their ejecta-dominated phase.

With upcoming deep, optical synoptic sky surveys such as the Legacy Survey of Space and Time (LSST), which is proposed to begin collecting 10 years of data with the Vera C. Rubin Observatory, hereafter Rubin (Ivezić et al. 2019) in 2025, the number of pre-explosion images of SNe Ia is only going to grow. For now though, the number of pre-explosion images is relatively few, with one of the best examples being SN2012Z (McCully et al. 2014; Liu et al. 2015), where an intact blue (likely helium-rich) star companion is arguably detected in pre- and post-explosion images (McCully et al. 2022). SN2012Z is a well-known ‘‘SN Iax’’¹³ event and is thought to be the best candidate for a weak explosion of a Chandrasekhar mass white dwarf that is likely to have left behind a bound remnant (Vennes et al. 2017).

2.3.2 Lensed supernovae

Gravitational lensing offers a unique opportunity to observe very distant explosions, including supernovae. An intervening massive galaxy or cluster of galaxies may conspire to ‘magnify’ the supernova’s (intrinsic) luminosity such that it is detectable to us.

While lensed SNe with resolved images are fairly rare (iPTF16geu at $z = 0.409$, Goobar et al. 2017), there is a growing list of reported strongly-lensed and/or multiply-imaged SNe Ia (Patel et al. 2014; Rubin et al. 2018; Rodney et al. 2021; Goobar et al. 2023; Golubchik et al. 2023; Pierel et al. 2024; Pascale et al. 2024).

Strong gravitational lensing of an astrophysical object was first discovered in the 1970s (Walsh et al. 1979). ‘Double quasar’ QSO 0957+561 ‘components’

¹³ So-called SN Iax events are a broad sub-class of peculiar thermonuclear supernovae (Foley et al. 2014).

A and B were identified as having nearly identical spectral features and it was concluded that the most likely reason for this was a common origin. Though much less-commonly detected than lensed quasars, lensed SNe Ia are extremely valuable tools to study otherwise-undetectable (due to their high-redshift) explosions that occurred when the Universe was much younger. Since it is still not certainly known whether the nature of SN Ia progenitors evolves or changes with redshift, and given their critical importance in cosmological studies, these higher-redshift lensed events have become a coveted asset (Cano et al. 2018; Pielke et al. 2021). As we enter an era of synoptic sky surveys that go deep, detection of lensed supernovae will become more common, which also calls for the development of software that will enable rapid identification of events (Morgan et al. 2022). Oguri and Marshall (2010) predict on the order of 45 lensed SNe Ia to be detected over the decade-long lifetime of the Rubin LSST (see also Huber et al. 2019). Recent work by Cikota et al. (2023) demonstrates innovative methods that can be used to recover spectra of high-redshift supernovae through strong lensing.

3 Indirect constraints of the explosion

3.1 Host environment

It is well-known that some physical characteristics of SNe Ia are correlated with properties of their host galaxies. As far as various sub-classes go, low star-forming galaxies tend to host 1991bg-like and Ca-rich SNe while the more luminous 1991T-like and “SN Ia CSM” (CSM = circumstellar medium) SNe are more often found in active star-forming galaxies (Panther et al. 2019; Hakobyan et al. 2020; Chakraborty et al. 2024; Qin et al. 2024). It was noted decades ago that, at face value, more luminous SNe Ia (slow-decliners) tend to be found in younger, star-forming stellar populations, such as spiral or irregular galaxies, while fainter SNe (fast-decliners) are preferentially found in hosts with an older stellar population, e.g. ellipticals (e.g. Hamuy et al. 1995). Nowadays, correlations between supernova brightness and host galaxy properties are often quoted *after* having been standardized for luminosity-decline rate, the main reason being that such a process is needed to use SNe Ia as standardizable cosmological candles (Childress et al. 2013). In the context of cosmology, the term “Hubble residual” is used, which is simply the difference between the distance modulus of the SN inferred from its lightcurve via the standardization process and the expectation value of this SN at its redshift (Kelly et al. 2010). These Hubble residuals are known to correlate with a number of (often interrelated) host galaxy properties, such as galaxy mass, metallicity, star formation rate, stellar age, and dust (e.g. Sullivan et al. 2003; Howell et al. 2009; Sullivan et al. 2010; Childress et al. 2013; Rigault et al. 2020; Brout and Scolnic 2021; Meldorf et al. 2023; Wiseman et al. 2023; Grayling et al. 2024).

In a study by Uddin et al. (2017) of 1338 spectroscopically-confirmed SNe Ia from 4 surveys, it was determined that, *after standardization*, brighter SNe tend to be found in more massive host galaxies on average (although, of course, these events are intrinsically under-luminous). Further, these trends were not found to vary as a function of redshift. Generally speaking: more massive (and generally metal-rich) galaxies host fainter SNe with narrow lightcurves while less massive and star-forming host galaxies tend to harbour more luminous SNe Ia with slower-declining lightcurves; however, we reiterate that this correlation should not be confused with the seemingly inverse correlations that are found for the Hubble residuals (e.g. Sullivan et al. 2006, 2010; Meyers et al. 2012; Pruzhinskaya et al. 2020, see Fig. 6).

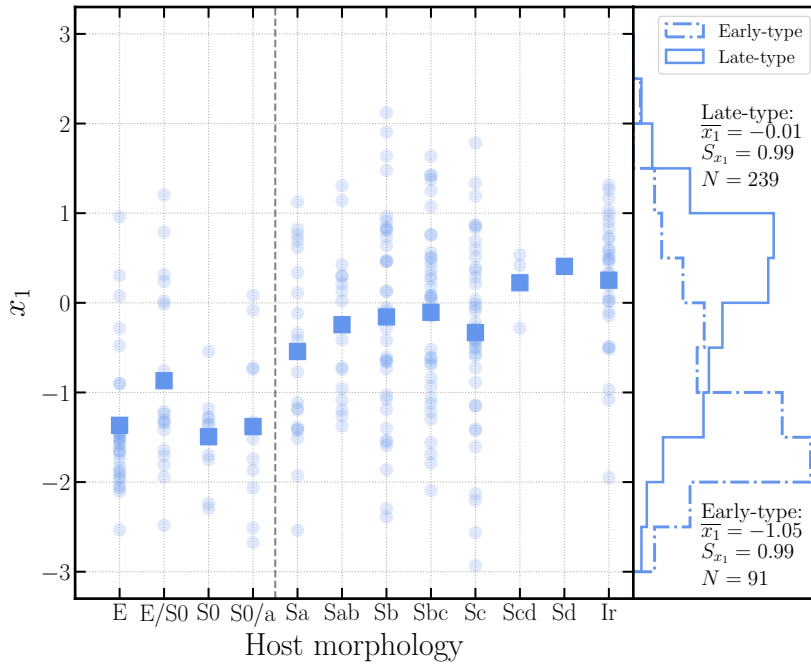


Fig. 6 SNe Ia from the PANTHEON survey showing SALT2 x_1 stretch parameter vs. galaxy host morphology (elliptical to lenticular to spiral types to irregular). In summary, SNe Ia in elliptical galaxies have lower stretch values, and in addition generally brighter SNe Ia but only *after* colour corrections are applied. Image reproduced with permission from Pruzhinskaya et al. (2020), copyright by the author(s).

Lower-metallicity intermediate mass stars on the AGB are expected to produce higher-mass stellar cores toward the end of their nuclear burning stage and therefore produce higher mass white dwarfs in single stellar evolution

models compared to their solar-metallicity counterparts, at least when considering stellar models up to approximately twice solar metallicity (Karakas 2010, 2014). Thus by the above logic, higher-metallicity (e.g. solar metal mass fraction) stars would form less massive white dwarfs compared to their metal-poor (e.g. higher redshift) counterparts. But as was pointed out, exploding white dwarf mass might be the dominant physical parameter that determines SN Ia peak luminosity (see Sect. 5.3.1), so if we expect to find more massive white dwarfs in binaries in some particular environment, then we would naively expect more luminous SNe Ia to occur there. Going in the same direction, Timmes et al. (2003) suggested that, in the context of Chandrasekhar mass explosions, SNe Ia from lower-metallicity progenitors would produce more ^{56}Ni , thus lower-metallicity progenitors should be more luminous, which follows the same general expected physically-motivated trend outlined above. But the face-value argument for more massive white dwarfs and thus brighter supernovae from lower-metallicity stars is not at all straightforward. Older, lower-metallicity massive white dwarf populations also tend to have lower carbon mass fractions (Umeda et al. 1999), thus plausibly make dimmer SNe Ia at least in the context of Chandrasekhar mass white dwarfs (see also Kang et al. 2020). In short, nothing is straightforward!

One crucial parameter to consider in linking SN Ia probability to environmental properties is the core mass at which the creation of a white dwarf becomes impossible owing to the core collapsing to a neutron star (or black hole) instead. One can investigate the plausible outcomes using detailed stellar evolution models of single stars in the mass range 8–10 M_{\odot} . A recent study of (single) AGB star nucleosynthesis uncovered an interesting trend: That, as a function of increasing metallicity (initial metal mass fraction) from $Z = 0.0025 - 0.05$, ignition of the carbon core to produce a core-collapse supernova would require higher initial stellar masses. However, at $Z \sim 0.04$, the trend reverses, and lower mass stars have a growing capacity to ignite as metallicity increases (see Cinquegrana et al. 2023, Fig. 1). We do not propose specific solutions to the challenges discussed here, but rather highlight that several factors crucial in stellar evolution, in particular metallicity, play a role in influencing the occurrence rate and host stellar population properties of Type Ia Supernovae.

We finally note that not all SNe Ia are connected to a known host: a recent example is the fast-declining event KSP-OT-201509b, for which no host galaxy has been discovered (Moon et al. 2021). Upcoming deep surveys that can allow for improved image-stacking capability should be able to shed more light (literally) on host environments of such sources.

3.2 Chemical evolution

Type Ia supernovae are important sites for the nucleosynthesis of heavy elements. With their unique (but delayed compared to core-collapse supernovae) nucleosynthesis signature they are a crucial ingredient for the chemical evolu-

tion of galaxies (e.g. [Matteucci and Greggio 1986](#)). For decades, Type Ia supernovae were approximated as a homogeneous, metallicity independent class of events, with a single yield set (typically W7) and delay time distribution (e.g. [Timmes et al. 1995](#); [Chiappini et al. 1997](#); [Kobayashi et al. 2006](#)). [Seitenzahl et al. \(2013a\)](#) relaxed this rigid assumption and considered different nucleosynthesis for different sub-channels of SNe Ia, thereby allowing for the impact of the diversity of SNe Ia on the chemical evolution of galaxies. A brief discussion of theoretical yields of iron-peak species can be found in Sect. 4.2.1.

3.2.1 Milky Way

It has been estimated that within the solar neighbourhood, more than half of the iron came from thermonuclear supernovae, with the rest coming from core-collapse events ([Maoz and Graur 2017](#)). Various works have estimated the relative fraction of different sub-classes of Type Ia supernovae with galactic chemical evolution models – initially breaking SNe Ia up into two main categories: Chandrasekhar mass explosions vs. sub-Chandrasekhar mass explosions, each with their own set of yield tables ([Seitenzahl et al. 2013b](#)). In general, including nucleosynthetic sources arising from products of binary star evolution has not been carried out extensively in the literature owing to the complex parameter space involved ([De Donder and Vanbeveren 2004](#)). Though nucleosynthetic yields for SNe Ia – including sub-Chandrasekhar mass models – started to be incorporated into galactic chemical evolution models once they were made available in the 1990s ([Samland et al. 1997](#)), there has been little, further advancement until recently. In recent years, galactic chemical evolution studies have started to incorporate a wider variety of SN Ia channel yields in an effort to reflect the observed diversity in observed properties, including incorporating chemical evolution feedback timescales by adopting different theoretical, or observationally-motivated, delay time distributions ([Lach et al. 2020](#); [Eitner et al. 2023](#); [Dubay et al. 2024](#)). The key result of [Seitenzahl et al. \(2013a\)](#), that explanation of the chemical evolution of the elemental ratios in the iron group (especially Mn/Fe, Cr/Fe, Ni/Fe) requires a mix of both near-Chandrasekhar and sub-Chandrasekhar mass progenitors, still holds, although non-LTE corrections ([Eitner et al. 2020](#)) and improved calculations of the central ignition density ([Bravo et al. 2022](#)) now favour a scenario where the sub-Chandrasekhar mass systems are the dominant channel. For a more comprehensive overview of Galactic chemical evolution, we refer the reader to [Matteucci \(2021\)](#).

3.2.2 Dwarf galaxies

The previous Sect. 3.2.1 outlines how the chemical evolution of our Milky Way Galaxy can provide meaningful constraints on the explosion mechanisms and progenitor scenarios of SNe Ia. While the large number of stars in the Milky Way that are bright enough for spectroscopy and atmospheric abundance modelling is an advantage, the Milky Way’s complicated star formation history,

past in-fall-, accretion-, and merger-events, and different stellar populations (e.g. thick disk, thin disk, bulge, halo) add much complexity. It was recently argued by [Sanders et al. \(2021\)](#) that there must have been a significant population of sub-Chandrasekhar supernovae that contributed to enriching the Gaia Enceladus (or ‘Sausage’) dwarf galaxy, which merged with our Milky Way over 8 Gyr ago. The support for sub-Chandrasekhar explosions in this (metal-poor) dwarf galaxy is evidenced by relatively low $[\text{Mn}/\text{Fe}]_{\text{In}}$ and $[\text{Ni}/\text{Fe}]_{\text{In}}$ abundance in stellar spectra (see Fig. 7).

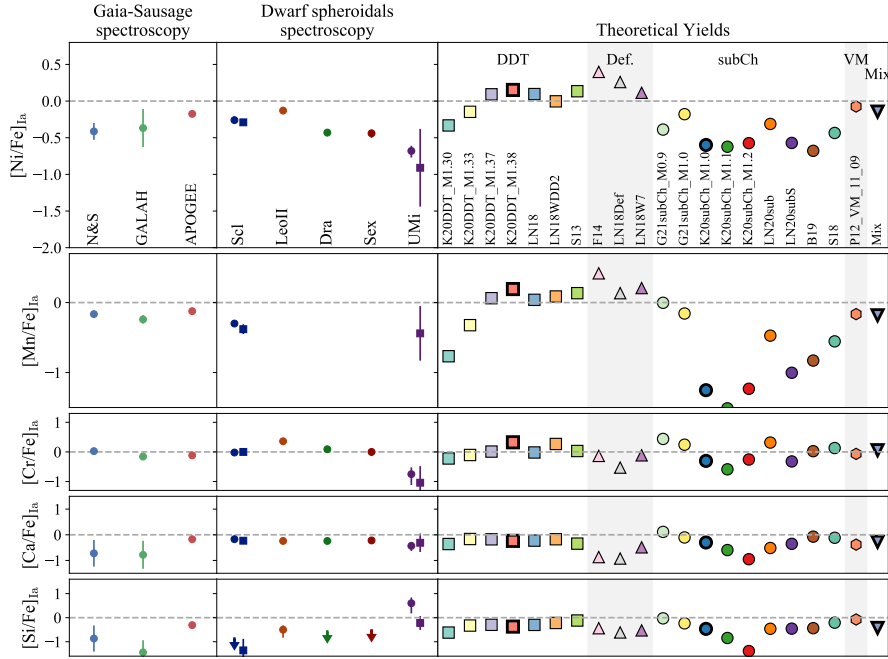


Fig. 7 Observed and theoretical SN Ia yields for the Gaia Sausage galaxy (observed; far left), other dwarf spheroidal galaxies (observed; middle column), and numerous SN Ia nucleosynthesis calculations from different explosion models: Chandrasekhar mass deflagration to detonation transition models (DDT), pure deflagration models (Def), and various sub-Chandrasekhar mass models. All dwarf spheroidals shown here exhibit sub-solar $[\text{Mn}/\text{Fe}]_{\text{In}}$ and $[\text{Ni}/\text{Fe}]_{\text{In}}$, as do the sub-Chandrasekhar mass theoretical yields. Image reproduced with permission from [Sanders et al. \(2021\)](#), copyright by the author(s).

Dwarf satellite galaxies of the Milky Way have much fewer stars accessible, but they tend to have much more simple star formation histories ([Tolstoy et al. 2009](#)), which offers unique opportunities to constrain SN Ia explosion models and progenitor channels via their distinct nucleosynthetic signatures and delay times. In the following paragraph, we discuss the prominent example of the element Mn in some detail.

The chemical evolution of Mn in dwarf satellite galaxies of the Milky Way, such as e.g. Fornax, Sculptor, Leo I, or Carina, has been known to exhibit

systematically different trends than that of our Galaxy (e.g. McWilliam et al. 2003; North et al. 2012), which had been attributed to a possible metallicity dependence of the Type Ia supernova Mn yield by these and other works (see also Cescutti et al. 2008). Seitzzahl et al. (2013a) suggest the alternative explanation that the different abundance trends of [Mn/Fe] in these dwarf galaxies could also be explained if SNe Ia did not arise from a unique channel (see also Kobayashi et al. 2015). If the more copiously Mn producing SN Ia channel had a longer delay time, then they might only begin to explode in dwarf galaxies after the gas has been depleted and star formation has ceased. The ‘textbook’ SN Ia progenitor consisting of a near-Chandrasekhar mass white dwarf and a hydrogen-rich donor is a natural candidate, as these systems do not explode at very short delay times according to some studies (see Fig. 2 of Hillebrandt et al. 2013). These Mn producing SNe Ia would have still exploded in these dwarf galaxies, however, their chemical signature would not be seen today in the atmospheric spectra of stars that formed at an earlier time. This is corroborated by the fact that [Mn/Fe] vs [Fe/H] in dwarf galaxies with early burst-like star formation histories, such as Sculptor (Kirby et al. 2019; de los Reyes et al. 2022) or Ursa Minor (McWilliam et al. 2018), differs qualitatively from dwarf galaxies with more extended star formation histories, such as Fornax or Leo I, which show significantly higher (about 0.2 dex) [Mn/Fe] at a given [Fe/H] (see e.g. de los Reyes et al. 2020). To be clear, we are not saying that (Mn-producing) long-delay time SNe Ia do not explode in dwarf galaxies like Sculptor. However, the nucleosynthetic signature of the long-delay time SNe Ia is not found in the atmospheric spectra of stars observed in such dwarfs today since star-formation had largely ceased at the time of the supernova explosion. The ejecta of any long-delay time SN Ia would escape the gravitational well of the small host galaxy before having a chance to be recycled into new generations of stars.

In the coming years, the 4MOST survey of dwarf galaxies and their stellar streams (4DWARFS, Skúladóttir et al. 2023) is anticipated to greatly increase the number of stars with spectroscopic abundances in these and other satellite dwarf galaxies and provide us with an incredible dataset to further test and refine these conclusions.

3.2.3 Intra-cluster medium

Measuring the abundances of elements in stellar atmospheres via spectroscopy is fundamental for constructing models of galactic chemical evolution. However, not all supernova ejecta remain within galaxies; both Type Ia and core-collapse supernova explosions drive outflows that enrich the intra-cluster medium (ICM) with synthesized elements, as noted by Finoguenov and Ponman (1999). In fact, the majority of the baryonic matter is not in stars and gas in galaxies but rather in the ICM (Giodini et al. 2009). Since the hot ICM gas is near collisional ionization equilibrium, it is possible to obtain precise determinations of abundance ratios by modelling X-ray spectra, as discussed in the review by Mernier et al. (2018). Initially, XMM-Newton-derived data suggested large

enhancements of Mn, Cr, and Ni relative to Fe, which led to the interpretation that near-Chandrasekhar mass primary WDs should have a dominant contribution to Type Ia supernovae (e.g. [Mernier et al. 2016](#)). A few years later, improvements to atomic models and much higher spectral resolution data from the Hitomi satellite revised these to near-solar ratios. Nonetheless, in the Perseus cluster, revised values still suggest significant contributions from near-Chandrasekhar mass white dwarfs to Type Ia supernovae ([Hitomi Collaboration et al. 2017](#); [Simionescu et al. 2019](#)). Similarly, for the Centaurus cluster, [Fukushima et al. \(2022\)](#) conclude that significant contributions from near-Chandrasekhar mass Type Ia supernovae are still required to explain near-solar [Mn/Fe] and [Cr/Fe] ratios. Another recent study by [Batalha et al. \(2022\)](#) also investigates the problem of which supernova explosion models are most likely to have contributed to the ICM metal enrichment. The authors present a non-parametric probability distribution function analysis to assess the likelihood of different SN yields from a large set of explosion models from the literature by making a comparison against observations of galaxy groups and galaxy clusters observed with Subaru. Regarding the role of Type Ia supernovae, [Batalha et al. \(2022\)](#) conclude that that 3D near-Chandrasekhar mass delayed-detonation models outperformed other tested combinations of supernova models.

3.3 Radioactive nickel and ejecta masses from lightcurves and spectra

Over the last few decades, a number of works were important in making progress toward understanding the structure of white dwarfs prior to explosion based on studies of the SN ejecta. As mentioned in Sect. 1.1, consideration of the radioactive decay law coupled with diffusion of light as it travels through the SN ejecta then allow us to make an estimate of ^{56}Ni mass from measuring SN Ia lightcurves around their maximum. The associated ‘‘Arnett’s rule’’ states that the instantaneous radioactive decay energy input (which is proportional to the ^{56}Ni mass) at the time of the lightcurve maximum is proportional to the peak luminosity ([Arnett 1979, 1982](#)). From UVOIR lightcurves, [Stritzinger et al. \(2006a\)](#) derived ejecta masses and applying Arnett’s rule (see their Sect. 3.2 and references therein) also derived ^{56}Ni masses for a set of 16 SNe Ia (see Fig. 8). [Stritzinger et al. \(2006a\)](#) thereby provided some of the first observationally derived evidence that the ejecta mass of SNe Ia varies by at least a factor of 2, and they suggested that sub-Chandrasekhar mass progenitors could be the reason.

In terms of sub-luminous SNe Ia, [Mazzali et al. \(1997\)](#) found that outer parts of ejecta in the sub-luminous SN1991bg were under-abundant in Fe-group, indicating the presence of some unburned material. They found that this supernova likely had an ejecta mass 0.4–1.0 M_{\odot} , with a total synthesized Ni mass of just 0.07 M_{\odot} . This ejecta mass is rather small in comparison to what is expected of SNe Ia at more typical peak luminosities. In terms of ejected nickel masses from the SN1991bg-like supernovae, [Stritzinger et al. \(2006b\)](#)

estimated a ^{56}Ni ejecta mass of $0.09 M_{\odot}$ for SN1991bg itself and $0.05 M_{\odot}$ for SN1999by from UVOIR data (see their Table 2). A ^{56}Ni ejecta mass in the range of $0.04\text{--}0.06 M_{\odot}$ was estimated for the fast-evolving SN2021qvv (Graur et al. 2023, Table 3), and a notably large $0.22 M_{\odot}$ for SN2022xkq (Pearson et al. 2024), a transitional/91bg-like.

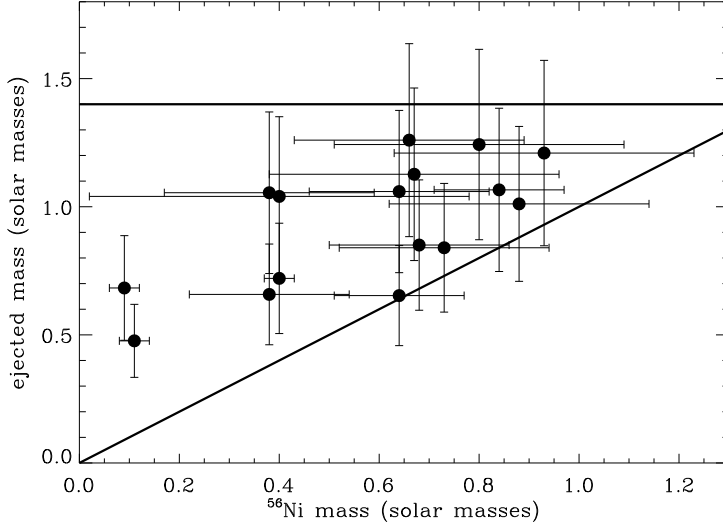


Fig. 8 Range of derived ejecta masses for 16 Type Ia supernovae as a function of estimated ^{56}Ni mass. Note the data points show that the inferred amount of synthesized ^{56}Ni varies within the sample by a factor of ten and the ejecta mass by more than a factor of two. Image reproduced with permission from Stritzinger et al. (2006a), copyright by ESO.

In the absence of conversion of kinetic energy to radiation via shock interaction, the energy source for the observed light output of the supernova are thus radioactive decays, and not the exothermic fusion reactions that power the explosion. One should keep in mind of course that there are complicated physical effects that may significantly affect the observed light curve evolution, including: magnetic field dependent positron transport and escape (Chan and Lingenfelter 1993; Penney and Hoefflich 2014; Kushnir and Waxman 2020); time-dependent delayed recombination (Fransson and Kozma 1993), an effect that depends on non-thermal excitation of ions (Fransson and Jerkstrand 2015); or light echoes (e.g. Schmidt et al. 1994; Patat et al. 2006). Effects like these complicate the derivation of radioactive isotope masses from late-time light curves (e.g. Kerzendorf and Sim 2014; Tucker et al. 2022).

Ejecta masses of “superluminous Type Ia supernovae” – stellar explosions assumed to be thermonuclear but exhibiting more luminous than standard peak luminosities and typically slower-declining lightcurves – have been estimated to be as high as $2.8 M_{\odot}$, with an inferred nickel mass of at least $1.2 M_{\odot}$

for SN2009dc (Taubenberger et al. 2011). Though, arguably, this is not a very precise way to estimate the ejecta mass in all cases, which renders the label of “Super-Chandrasekhar mass Type Ia supernova” misleading. In particular, it is very plausible that a significant fraction of such events may derive from a conversion of kinetic energy (via interaction) to light, which can explain “Super-Chandra SNe Ia” without an actual need for super-Chandrasekhar mass progenitors (Hachinger et al. 2012). However, other scenarios for super-Chandrasekhar mass explosions have indeed been proposed: spin-up / spin-down, or the merger of two white dwarfs resulting in a(n initially rapidly-spinning) white dwarf with a new mass above the Chandrasekhar mass limit (see Neunteufel et al. (2022, section 2.4)). Rapidly-rotating explosion models of super-Chandrasekhar mass explosions were investigated by Fink et al. (2018), and it was found their predicted observables did not match those of the observationally-labelled ‘super-Chandrasekhar’ events.

An approach to determining ^{56}Ni masses from the time evolution of the [Co III]5893 line during the nebular phase was pioneered by Childress et al. (2015). This method exploits the fact that the line flux of this nebular Co-line is proportional to two powers of the mass of ^{56}Co (and thus ^{56}Ni) as a function of time. The reason for this is that the observed line flux both scales with the number of available Co atom targets and the probability of exciting the line. As long as the ionization state of the ejecta does not significantly evolve, the flux of this Co-line thus decays much more rapidly than surrounding Fe-lines, which do not face the same problem of an exponentially decreasing target abundance. Childress et al. (2015) find that radioactive ^{56}Ni masses of SNe Ia fall into two regimes: i) SNe Ia with narrow lightcurves have low ^{56}Ni masses around $0.4 M_{\odot}$ with a weakly increasing yield as ejecta mass goes from $1.0 M_{\odot}$ to $1.4 M_{\odot}$, and ii) SNe Ia with broad lightcurves show a scatter in ^{56}Ni masses from around 0.6 to $1.2 M_{\odot}$, with ejecta masses clustering around $1.4 M_{\odot}$. Scalzo et al. (2014) find a similar bimodal distribution of ejecta and ^{56}Ni masses in their lightcurve analysis of 337 SNe Ia, corroborating the evidence for at least two distinct explosion mechanisms for normal SNe Ia.

3.4 Supernova abundance tomography

Supernova abundance tomography is a method to infer the abundance profiles (the radial distribution or distribution in velocity space) of chemical elements in the ejecta of supernovae. The technique was pioneered by Stehle et al. (2005b). In essence, the abundance tomography method takes advantage of the gradual shift of the photon emitting layer into deeper and deeper layers of the ejecta over time. In other words, as the supernova expands, the photosphere recedes (in a Lagrangian sense) deeper into the ejecta. Since spectral features form in the layers above the photosphere, the earliest spectra are sensitive to the chemical abundances in the outermost layers, whereas post-maximum light spectra probe much deeper layers of the ejecta. Therefore, by modelling a time series of spectra taken in succession, abundance profiles of chemical elements

that best reproduce the observed spectral evolution can be reconstructed from the outside in. Abundance tomography has been performed for several well-observed SNe Ia, including SN 2002bo (Stehle et al. 2005a; O’Brien et al. 2021), SN 2004eo (Mazzali et al. 2008), SN 2003du (Tanaka et al. 2011), SN 2009dc (Hachinger et al. 2012), SN 2010jn (Hachinger et al. 2013), SN 1991T (Sasdelli et al. 2014), SN 2011fe (Mazzali et al. 2015), SN 1986G (Ashall et al. 2016), and SN 1999aa (Aouad et al. 2022). For most of these studies, however, density profiles corresponding to a mass of the exploding white dwarf near the Chandrasekhar limit were a priori assumed. Mazzali et al. 2015 also used sub-Chandrasekhar mass profiles for SN 2011fe, Hachinger et al. 2012 also explored super-Chandrasekhar mass profiles for SN 2009dc, and O’Brien et al. 2021 used a larger variety of models in their Bayesian probabilistic modelling approach. Assuming a Chandrasekhar mass profile pre-emptively confines the derived white dwarf mass to $1.4 M_{\odot}$, which is currently not considered to be a valid assumption (Hillebrandt et al. 2013). In spite of this caveat, meaningful abundance profiles for individual SNe can be derived in this way. Such inferred abundance profiles can then be directly compared to the modelling predictions of different explosion models. To give one example, Aouad et al. (2022) performed abundance tomography for 3 (similar) density profiles (all Chandrasekhar mass models) for SN 1999aa and they found that the innermost $0.3 M_{\odot}$ consist of mostly stable IGE, then about $0.65 M_{\odot}$ radioactive nickel, then a thin layer of IMEs and then just over $0.2 M_{\odot}$ of an oxygen rich outer layer.

3.5 Potential surviving companions

In addition to efforts to look for SN Ia companions in present-day, nearby supernovae (Sect. 2.3.1), searching for companions of historical supernovae in the vicinity of supernova remnants has been ongoing (see Ruiz-Lapuente 2019). A star that survives the blast wave by its nearby stellar companion may appear to be observationally peculiar. Additionally, geometric effects on the supernova ejecta imparted by the surviving star have also been explored (Kasen et al. 2004). Certain observational signatures might be present even well after the remnant has entered its Taylor–Sedov phase, such as heavy-element enrichment (Liu et al. 2013), bloating leading to higher luminosity for both hydrogen-rich (Marietta et al. 2000; Shappee et al. 2013) and helium-rich (Pan et al. 2013) companions, and supernova kicks that result in higher-than-usual proper motion (Kerzendorf et al. 2009). We refer the interested reader to Liu et al. (2023), Sect. 5.2.1, for details regarding ejecta-companion interaction searches.

The search for surviving companions of SNe Ia has in the past mostly focused on the donor stars in single degenerate systems; for a recent review on the topic see Ruiz-Lapuente (2019). However, double-degenerate systems can have their own surviving companions if only one of the WDs explodes. For dynamically-driven mergers (see Sect. 5.3), the secondary star might sur-

vive the explosion (e.g. [Burmester et al. 2023](#)). For these double-degenerate systems, the orbital velocities are high (several hundred to a few thousand km/s) when the compact stars interact. As a result, the explosion of the primary leads to the expulsion of the secondary WD at high-velocity. Although these surviving companions are ejected largely unscathed, the expectation is that their composition is heavily altered by the interaction with the supernova ejecta (e.g. [Tanikawa et al. 2018](#)). The runaway stars thus carry a signature of the nucleosynthesis of the supernova explosion and they should present as chemically peculiar.

Modern spectroscopic surveys such as Gaia ([Gaia Collaboration et al. 2018](#)) have revealed very fast-moving chemically peculiar dwarf stars; some of these ‘runaway’ stars may be the surviving companions of SN Ia explosions from double degenerate binaries ([Shen et al. 2018](#); [Igoshev et al. 2023](#)). However, such runaways, if they originate from SN Ia exploding binaries – even if many are lurking in the Galaxy but eluding detection – are predicted to constitute only a small fraction of the total Galactic SN Ia population ([Neunteufel et al. 2022](#); [Pakmor et al. 2022](#)).

Chemically peculiar runaway stars carrying the nucleosynthetic signature of thermonuclear supernova explosion could also arise from near-Chandrasekhar mass explosions ([Raddi et al. 2018](#)), in particular from a pure deflagration scenario where the primary is not fully unbound by the thermonuclear runaway (cf. Sect. 4.4.1). Several candidate stars heavily enriched in O/Ne and showing signatures of high-density thermonuclear burning (e.g. super-solar Mn/Fe) that could be the stellar remnants of such thermonuclear supernovae have now been identified ([Raddi et al. 2019](#); [Igoshev et al. 2023](#)).

3.6 Supernova-remnant archaeology

Some SN Ia formation scenarios require extended periods of accretion from a secondary companion star onto the primary WD, growing the mass of the primary and increasing the central density leading up to the ignition. The required mass accretion rate to obtain stable burning on the surface and hence to grow the primary white dwarf mass results in a hot surface of the primary emitting strongly in soft X-rays and UV in a time window some 10 million years prior to explosion ([Kahabka and van den Heuvel 1997](#)). The paucity of such soft X-ray emission from nearby elliptical galaxies and bulges has been used by [Gilfanov and Bogdán \(2010\)](#) to limit the contribution of the H-accreting single-degenerate progenitor channel to less than 5% in these old stellar populations.

The ionizing radiation from SN Ia progenitor systems involving stably accreting white dwarfs would naturally also have an imprint on the interstellar medium surrounding the explosion site, and one could expect to detect signatures of ionized gas up to 100,000 years post-supernova from such progenitors. Despite efforts to reveal such signatures, thus far any strong evidence for such a progenitor through this detection method has not been found ([Woods et al.](#)

2017; Kuuttila et al. 2019; Souropanis et al. 2022). Specifically, the lack of a Strömgren sphere surrounding Tycho’s SNR (the remnant of SN 1576) has been used (Woods et al. 2017, 2018) to argue that this famous Galactic supernova more likely originated in a double degenerate merger.

3.7 Rates and delay time distributions

The observed rate of Type Ia supernovae, barring numerous observational biases, will be a convolution of the SN Ia delay time distributions and the star formation histories of the supernova-hosting environments. The empirically estimated Galactic SN Ia rate is ~ 0.5 per century (Li et al. 2011b; Wiseman et al. 2021, section 1, for a description of various methods used in deriving the SN Ia rate from observations).

The number of works focused on determining rates of SN Ia has grown substantially, and necessarily, as instrumentation has greatly improved, resulting in increased capability to detect events at higher redshift. Type Ia SN rates have been observationally-derived using various techniques, from data taken with different telescope facilities, with a range of sample sizes and host properties (Cappellaro et al. 1999; Tonry et al. 2003; Dahlen et al. 2004; Mannucci et al. 2005; Sullivan et al. 2006; Botticella et al. 2008; Li et al. 2011c; Graur et al. 2011; Maoz and Mannucci 2012; Graur et al. 2014b; Rodney et al. 2014; Friedmann and Maoz 2018; Brown et al. 2019; Strolger et al. 2020; Wiseman et al. 2021; Toy et al. 2023, to highlight a number of papers from the last quarter century). A relationship between the SN Ia rate and specific star formation rate out to a redshift of ~ 0.25 is shown in Fig. 9.

As mentioned already in Sect. 3.1, it has been well-known for decades that, without taking into account standardization for cosmological studies, the more luminous SNe Ia are those that occur among younger, star-forming galaxies, while dimmer SNe Ia are found among older stellar populations. The rate of SNe Ia is also much higher among young stellar populations, with the SN Ia rate in late-type (e.g. spiral) galaxies being larger by a factor of 20 or so when compared to early-type galaxies (Mannucci et al. 2005). Often, the supernova rate is expressed in SNum: ($\frac{\text{number of SN Ia}}{100\text{yr } 10^{10}M_{\odot}}$), though sometimes simply expressed in SNe $M_{\odot}^{-1} \text{ yr}^{-1}$, where the mass often represents the mass (born) in stars. The rate can also be expressed per unit volume (e.g. Cappellaro et al. 2015), or a volumetric rate that excludes mass but factors in the dependence of an assumed Hubble constant (SNe $\text{yr}^{-1} \text{ Mpc}^{-3} h_{70}^3$, e.g. Frohmaier et al. 2018).

Observations of SNe Ia in the mid-2000s indicated that SNe Ia were likely comprised of two main populations: a ‘prompt’ component with short delay times and a ‘tardy’ component with longer delay times that exploded over a wider age range (Mannucci et al. 2006). Motivated by the apparent existence of two populations of SNe Ia, Scannapieco and Bildsten (2005) came up with a simple 2-component analytical expression for the SN Ia rate as a function of both instantaneous star formation rate and total stellar mass: The

“A + B” model. This model however does not capture the full picture because observationally-inferred delay time distribution shapes clearly show a significant number of events at intermediate delay times (see e.g. Fig. 10).

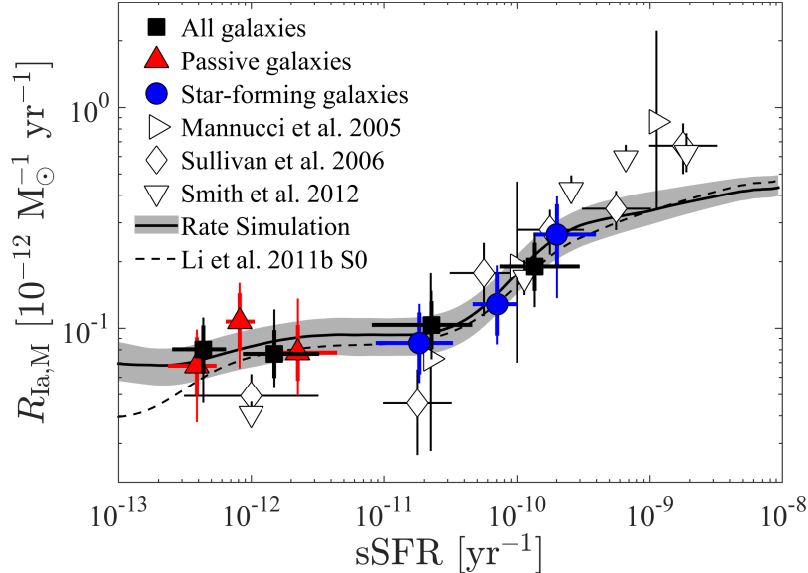


Fig. 9 SN Ia rate as a function of specific star formation rate (per unit stellar mass). Coloured data points have been mapped to galaxy types, either passive or star forming: A clear progression in SN Ia birthrate from passive galaxies to those that actively form stars is confirmed across a number of works. Image reproduced with permission from [Graur et al. \(2015\)](#), copyright by the author(s); (see also their Table 2).

In terms of more recent works, [Friedmann and Maoz \(2018\)](#) found that the rate of SNe Ia in galaxy clusters (at a mean redshift $z = 1.35$) is higher than that observed for field galaxies, with a cluster SN Ia rate of $2.6 \pm_{1.5}^{3.2} \times 10^{-13} \text{ yr}^{-1} \text{ M}_{\odot}^{-1}$, though the reason(s) for this higher efficiency are not clear. Already from observational studies of SN Ia rates and delay times over a decade ago ([Maoz et al. 2012](#)), it was apparent that the rate of SNe Ia per unit stellar mass in galaxy clusters is higher than in the local Universe. This finding was also recently re-confirmed by [Freundlich and Maoz \(2021\)](#), see Fig. 10); a similar figure can be found in [Strolger et al. \(2020\)](#), their Fig. 9.

Having said this, [Toy et al. \(2023\)](#) found the rate of SNe Ia in field galaxies to be quite similar to that of galaxy clusters (see their Fig. 8), plausibly at odds with the trend found by [Friedmann and Maoz \(2018\)](#). [Toy et al. \(2023\)](#) cite possible reasons for the difference (see their Sect. 4.2.1), however we note that the redshift range of cluster SNe in the [Toy et al. \(2023\)](#) study is significantly smaller ($0.1 \leq z < 0.7$) compared to the redshifts of galaxy clusters in [Friedmann and Maoz \(2018\)](#), so one could naively speculate that metallicity

plays some role. Employing a completely different method, [Wiseman et al. \(2021\)](#) derive a SN Ia rate from the Dark Energy Survey of $2.6 \pm 0.05 \times 10^{-13} \text{ yr}^{-1} M_{\odot}^{-1}$ (see their Sect. 5, and see Fig. 11, for the SN Ia rate as a function of galaxy stellar mass).

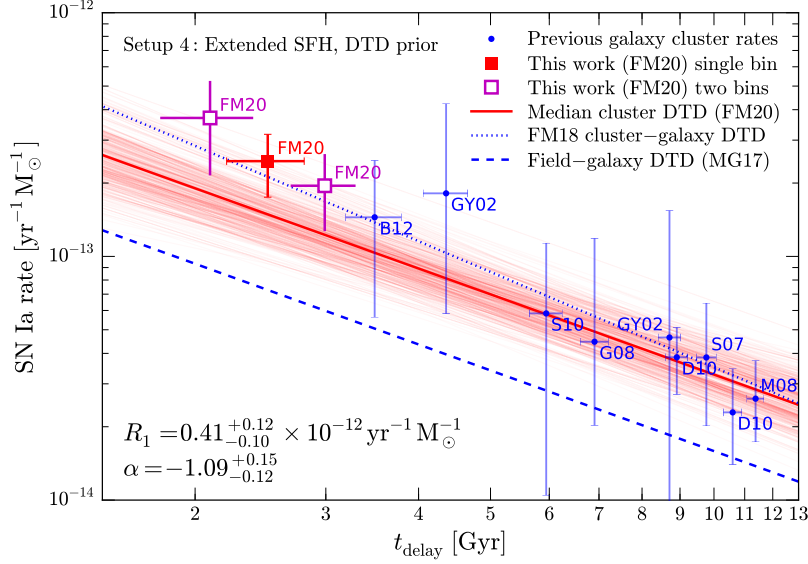


Fig. 10 Observationally-derived power-law DTD fits showing supernova rate per unit time per mass born in stars. Over-plotted are supernova rates from various works. The lower dashed blue line represents a fit based on field galaxies in the local universe, while the blue dotted line represents a best-fit based on the sample of higher-redshift galaxy clusters. Red lines represent DTD models from MCMC Bayesian inference from [Freundlich and Maoz \(2021\)](#), see paper for details). According to this work, for a given supernova age (or delay time), the overall supernova rate is higher in galaxy cluster environments compared to the local Universe by a factor of nearly 2 or more, with the discrepancy being higher at short delay times (see text). Figure from [Freundlich and Maoz \(2021\)](#).

There have also been several works dedicated to modelling the time from progenitor binary system birth to explosion: the delay time (i.e. [Yungelson and Livio 1998](#)). When this time is calculated for a number of supernovae, we uncover the delay time distribution (DTD). While it is possible to estimate the DTD of SNe Ia through analytic formulations ([Greggio 2005](#)), calculating delay time distributions from binary population synthesis models takes into account binary evolution physics in greater detail and thus enables the inclusion of a wider variety of possible outcomes ([Han and Podsiadlowski 2004](#); [Ruiter et al. 2009](#); [Bogomazov and Tutukov 2009](#); [Wang and Han 2010](#); [Mennekens et al. 2010](#); [Toonen et al. 2012](#); [Liu et al. 2015](#); [Yungelson and Kuranov 2017](#)). In BPS codes, the delay time is simply found by examining the time between

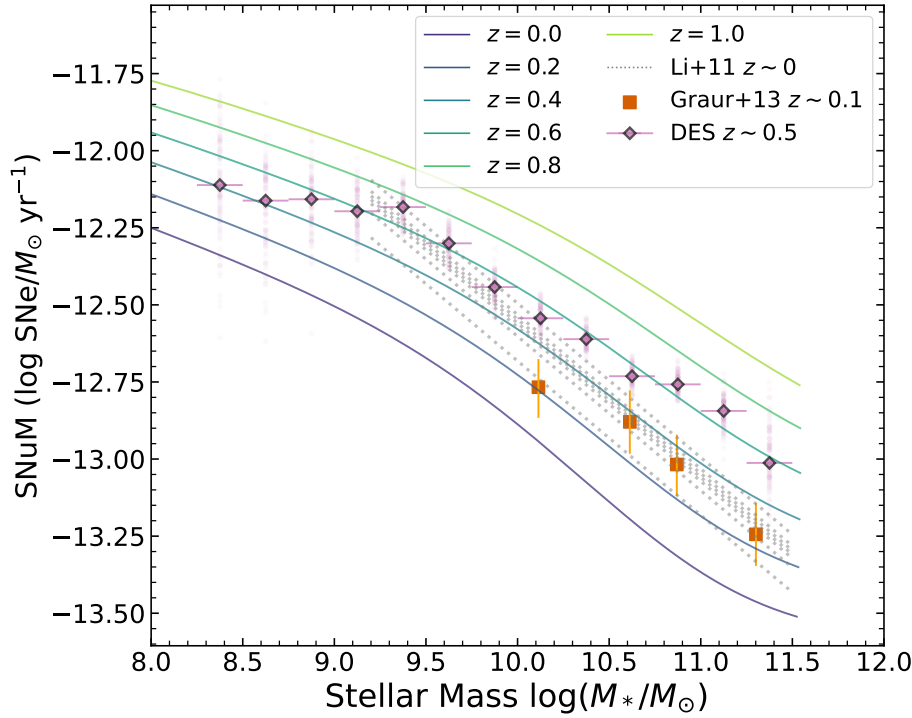


Fig. 11 Purple diamonds show the rate of SNe Ia per unit stellar mass as a function of galaxy stellar mass from [Wiseman et al. \(2021\)](#). Dotted lines and orange squares show previous rate estimates from earlier works. Image reproduced with permission from [Wiseman et al. \(2021\)](#), copyright by the author(s); see their Fig. 11 for details.

when the binary system is formed (usually assumed to be formed through field evolution, not through dynamical interactions in dense stellar environments) to when the supernova event occurs based on pre-set conditions (see [Claeys et al. 2014](#), for a parameter study). The DTD is rather powerful in that it sets a limit on SN Ia progenitor ages.

Since certain progenitor channels are predicted to only produce ‘prompt’ events with very short (e.g. well under 1 Gyr) delay times, we can then exclude such progenitors from explaining events occurring among old stellar populations, and vice-versa for any explosions that may be predicted to kick in only at long delay times. When considering the Chandrasekhar mass explosions from the single degenerate scenario, binary population synthesis calculations indicate there are two distinct age populations that emerge from the DTD: prompt events that stem from SNe Ia with hydrogen-stripped, helium-burning star donors, and the more canonical events where a WD accretes hydrogen-rich material from an unevolved or slightly evolved star, which have a longer average delay time distribution (see [Ruiter et al. 2011](#) Fig. 1; see also [Wang et al. 2009a](#)). Unlike white dwarf mergers whose DTD is primarily governed

by the timescale associated with gravitational wave radiation, the DTD of single-degenerate scenario SNe Ia is highly dependent on the evolutionary timescale of the (future) donor star. The H-stripped, He-burning donor stars that contribute to the prompt events derive from more massive progenitors than their H-rich donor counterparts, thus have shorter main sequence lifetimes (see [Ruiter et al. 2011](#), Sect. 4.1). We note however that, as with any result based on modelling assumptions, predicted DTDs may not be a true reflection of what actually happens in nature. Interestingly, varying certain parameters, such as common envelope efficiency, may not only affect the overall birthrates, but could uncover new evolutionary channels – and thus a differently-shaped DTD ([Ruiter et al. 2009](#), so-called AM CVn channel in their Fig. 1).

Observational delay time distributions on the other hand must be reconstructed, and there are a number of sources of uncertainty. One major assumption to be made is the star formation history of the stellar population associated with the supernova explosion, which is nearly impossible to know with any high accuracy, though is generally more straightforward for old stellar populations ([Totani et al. 2008](#)). Nonetheless, some clever methods have been developed to re-construct delay times – in other words, ages – of the stars responsible for the supernovae ([Maoz and Badenes 2010](#); [Maoz et al. 2011](#); [Graur and Maoz 2013](#); [Heringer et al. 2017](#); [Wiseman et al. 2021](#)). While several studies agree that the s parameter is on the order of 1 in the t^{-s} power-law fit to observational DTDs (e.g. [Maoz et al. 2012](#); [Sand et al. 2012](#); [Castrillo et al. 2021](#)), there is no reason to a priori assume that all SNe Ia must obey such behaviour (see recent study by [Palicio et al. 2024](#)). Some studies have demonstrated that, if indeed a single continuous power-law is assumed, s has some (unsurprisingly) apparent dependence on stellar environment (e.g. [Chen et al. 2021](#)). The power-law fit was found to be slightly shallower (steeper) if the DTD was derived from field (cluster) galaxies ([Maoz and Graur 2017](#), see also Fig. 10). Further, [Heringer et al. \(2017\)](#) found that supernovae with faster lightcurves were well-fit by a steeper DTD power-law ($t^{-1.27}$) whereas SNe Ia with broader lightcurves could not be fit by any single continuous power-law.

Figure 5 in [Wang and Han \(2012\)](#) gives an overall summary of model DTDs from BPS studies compared to observations. The model DTDs are separated into two groups: single-degenerate and double-degenerate (originally presented in [Nelemans et al. 2013](#)). The summary is that various BPS codes roughly agree in terms of producing DTDs from double white dwarf mergers (see Sect. 1.2.2 for more discussion). However, DTDs of single degenerate scenario Chandrasekhar mass SNe calculated with different codes greatly differ from one another, and in general do not match the observed DTD shape, and do a poorer job at coming close to the actual rate numbers, compared the DTD predicted for double degenerate¹⁴ systems. As discussed, building up the mass of a white dwarf toward the Chandrasekhar mass limit is a challenge for binary evolution. Other differences in the various code results are found to

¹⁴ The various authors were agnostic regarding the explosion mechanism for the DWD mergers in the DTD study.

simply arise from different assumptions on the treatment of binary evolution physics (Toonen et al. 2014). While not a cause for concern in terms of numerical accuracy, the lack of agreement between different codes does make it hard for the community to agree on which evolutionary channel(s) is/are most representative of single degenerate SNe Ia that would be found in nature.

4 Near-Chandrasekhar mass SN Ia explosion models

4.1 The central ignition problem

The Chandrasekhar mass limit is the maximum mass limit (a mathematical singularity where the radius approaches zero) of an idealized (zero-temperature) equation of state for a non-rotating white dwarf star supported by electron degeneracy pressure of a relativistic Fermi gas (Chandrasekhar 1931). The exact value of this mathematical mass limit depends on composition, with the mean molecular weight per electron fraction μ_e being the key parameter. The textbook value is $M_{\text{Ch}} = \frac{5.80}{\mu_e^2} M_{\odot}$ (see e.g. Clayton 1968). We note that for self-conjugate (nuclei with the same number of protons and neutrons) nuclear matter, such as ^4He , ^{12}C , ^{16}O , or ^{24}Mg , μ_e is very close to 2, leading to the familiar $M_{\text{Ch}} \approx 1.45 M_{\odot}$. Inclusion of neutron rich isotopes, such as ^{22}Ne or ^{56}Fe , leads to larger μ_e and thus to a smaller Chandrasekhar mass limit.

Since this is a review, we note here that the sometimes portrayed storyline that *a massive white dwarf accretes mass from a companion and when it reaches its limit of stability (the Chandrasekhar mass) it explodes* is incorrect. As a mathematical singularity of an idealized equation of state, an accreting white dwarf will not reach or exceed the Chandrasekhar mass, and if anything it should collapse to form an even more compact object, most likely a neutron star, which would result in a faint transient (Darbha et al. 2010).

What is true however is that the realistic equation of state of massive white dwarfs becomes very soft. What this means is that the star is more easily compressed, thus a small amount of additional mass leads to a large increase in compactness, and therefore a large increase in central density. For a composition rich in ^{12}C , realistic conditions lead to ignition of carbon burning (in the intermediate thermo-pycnonuclear regime) for densities around the range of $2 - 6 \times 10^9 \text{ g cm}^{-3}$, see e.g. Fig. 5 of Gasques et al. (2005). In this intermediate regime, where uncertainties surrounding the Coulomb screening of the reaction rate only add to the complexity, the nuclei contributing most to the fusion rate are either slightly bound or slightly unbound to the crystalline lattice (which is about to melt).

In addition to the inherent uncertainties in the nuclear reaction rate, the ignition problem is further complicated through heating and cooling processes. For example, heat produced by surface accretion can have a feed-back effect on the core-temperature, whereas cooling (dominated by neutrino losses) can delay the ignition (e.g. Lesaffre et al. 2006). Additionally, during the “simmering” phase lasting some 100 – 1000 years, nuclear reactions that lead up

to the thermonuclear runaway already modify the initial composition driving it more neutron-rich (Piro and Bildsten 2008). Furthermore, the impact of convective flows and turbulence on the birth of a thermonuclear deflagration flame (Höflich and Stein 2002; Nonaka et al. 2012) add considerable variance to the models as well. These effects all contribute to the complexity of the ignition problem of the deflagration. As a result, important parameters of the ignition remain uncertain, such as the central density when ignition occurs or the exact location of the ignition spot(s). Over the last few decades, many groups have explored the implications of the (stochastic) ignition mechanism, including ignition conditions, configuration, and whether and how the initial subsonic deflagration flame can transition to a supersonic detonation, on the observables of SNe Ia.

In what follows, we first give an overview of the characteristic nucleosynthesis occurring in such near-Chandrasekhar mass white dwarfs. Then we describe different types of binary systems in which central ignition of near-Chandrasekhar mass WDs can be achieved as described above. We conclude this section with a range of different possible explosion mechanisms that have been proposed to occur following the (near central) ignition of the deflagration flame.

4.2 Nuclear burning in Chandrasekhar mass white dwarfs

The explosions that are Type Ia supernovae are powered by the nuclear binding energy released that results from the transmutation of lighter, less-bound nuclear “fuel” species, such as ^{12}C , ^{16}O , ^{22}Ne , into heavier, more tightly-bound nuclear “ash” species, such as ^{32}S , ^{55}Co , or ^{56}Ni . The binding energy of ^{12}C is 7.68 MeV per nucleon (MeV/nuc), the binding energy of ^{16}O is 7.97 MeV/nuc, and the binding energy of ^{56}Ni is 8.64 MeV/nuc. Hypothetical fusion of a 50/50 mix (by mass) of ^{12}C and ^{16}O to ^{56}Ni thus would release about 0.82 MeV/nuc. Using this simple “back-of-the-envelope” calculation, we see that completely burning a $1.4 M_{\odot}$ 50/50 CO WD into ^{56}Ni would release:

$$\frac{1.4 \times 2 \times 10^{33} \text{g (WD mass)}}{1.66 \times 10^{-24} \text{g (mass per nuc)}} \rightarrow 1.67 \times 10^{59} \text{ nuc} \times 0.82 \text{ MeV/nuc}, \quad (2)$$

which is about 1.37×10^{57} MeV, or 2.2×10^{51} erg of nuclear energy, which is less than the approximately 3×10^{51} erg of gravitational binding energy of such a massive WD. So one may ask – how can the white dwarf actually become unbound from such an explosion?

To get the full picture, we must also account for the internal energy, which is dominated by the internal energy of the degenerate electron gas and already accounts for a large fraction of the gravitational binding energy. The nuclear binding energy released by the explosive nuclear fusion reactions only needs to overcome the difference in initial gravitational binding energy and the internal energy. Kinetic explosion energies around the canonical value of

10^{51} erg (1 Bethe) are thus readily achieved, even if only some fraction of the star is burned to the most tightly-bound iron group nuclear species, see e.g. Figure 12. As an aside, we note that the energy released by the thermonuclear fusion only powers the explosion but not the energy emitted by radiation – the lightcurve – which is powered by the radioactive decay of long-lived nuclear species produced in the explosion, such as ^{56}Ni and ^{56}Co at early and intermediate phases, and ^{57}Co and ^{55}Fe at late phases (Seitenzahl et al. 2009c).

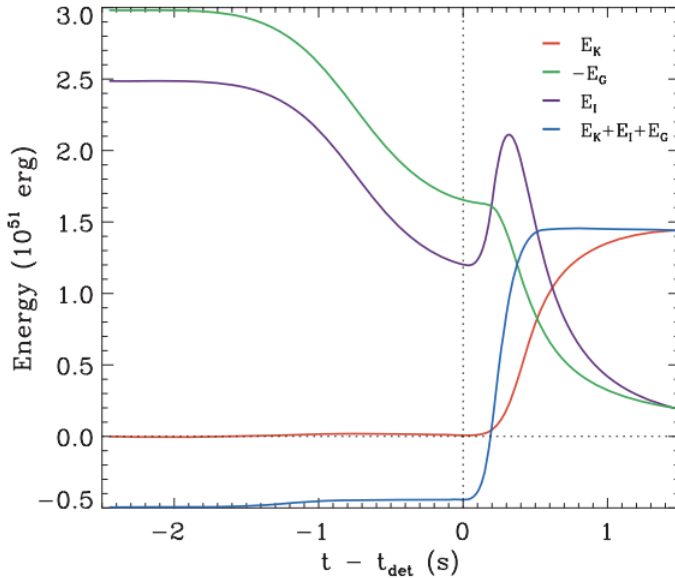


Fig. 12 The evolution of kinetic (red), internal (purple), and gravitational potential (green) energies for a gravitationally-confined detonation model (see Sect. 4.4.3) of a Type Ia supernova explosion. For this model, the flame bubble was ignited 25 km from the centre of the star. Post-detonation (dotted vertical line), nuclear binding energy gets rapidly converted to internal energy, which in turn converts to kinetic energy, and the star blows up. Image reproduced with permission from Meakin et al. (2009), copyright by AAS.

We have summarized above that it is the difference between the nuclear binding energy of the “fuel” and the “ash” that powers the explosion. But what determines the composition, and hence nuclear binding energy, of the “ash”? For a fixed fuel composition, the fuel density at the time of ignition is the key parameter that determines the outcome of the explosive nuclear burning, since it sets the peak temperature reached. Broadly, we can categorize the outcomes into different burning regimes. At high densities, nuclear fusion reactions are so rapid (compared to the expansion timescale) that the composition can reach a state of nuclear statistical equilibrium (NSE) (see Clifford and Tayler 1965; Woosley et al. 1973; Seitenzahl et al. 2009d), dominated by iron-group elements. At lower densities, expansion and cooling leads

to a “freeze-out” of nuclear reactions before the burning is complete, leading to partially burned ash states dominated by intermediate mass elements, such as Si, and S (e.g. [Iwamoto et al. 1999](#)). For fuel mostly composed of carbon and oxygen, we distinguish five different burning regimes (see e.g. figure 1 of [Seitenzahl and Townsley 2017](#)):

1. at the highest densities, $\rho \gtrsim 10^9 \text{g cm}^{-3}$: High-density allows efficient neutronization via electron captures, resulting in neutron-rich NSE, characterized by relatively high abundance of stable iron-group nuclei, such as ^{54}Fe , ^{56}Fe , or ^{58}Ni (stable nickel).
2. at the next lower densities, but $\rho \gtrsim 2 \times 10^8 \text{g cm}^{-3}$: “normal” (low-entropy) freeze-out from NSE composition, dominated by ^{56}Ni , and characterized by relatively high abundance of e.g. ^{55}Co , which ends up as stable manganese.
3. at the next lower densities, but $\rho \gtrsim 2 \times 10^7 \text{g cm}^{-3}$: “alpha-rich” (high-entropy) freeze-out from NSE composition, dominated by ^{56}Ni , and characterized by a paucity of e.g. ^{55}Co and increased relative abundance of nuclei past ^{56}Ni that are produced during the alpha-rich freeze-out, such as ^{64}Ga and ^{66}Ge (both decay to stable zinc), see e.g. Fig. 6 of [Lach et al. \(2020\)](#).
4. at the next lower densities, but $\rho \gtrsim 3 \times 10^6 \text{g cm}^{-3}$: Carbon and oxygen burn, but the silicon-burning is incomplete. This density range is therefore characterized by large abundances of intermediate mass element isotopes such as ^{28}Si and ^{32}S , and in addition some iron group isotopes characteristic for incomplete silicon-burning, such as ^{55}Co and ^{56}Ni .
5. at the next lower densities, but $\rho \gtrsim 3 \times 10^5 \text{g cm}^{-3}$: At such low densities, carbon and neon still burn, leading to a net production of oxygen, which is already largely inert, and slightly heavier intermediate mass elements.

We note that the transitions are not sudden and there is overlap between the different regimes. The densities given are only indicative and will vary somewhat for different explosion models (see e.g. figure 2 of [Lach et al. 2020](#)). For a review on how the detailed explosive nucleosynthesis is typically calculated from multi-dimensional hydrodynamical simulations via tracer particle methods see [Seitenzahl and Pakmor \(2023\)](#).

Detonations in helium-rich fuel are still viable at even lower density, and they carry a different characteristic nucleosynthetic signature. Most conspicuously, α -isotopes, such as ^{36}Ar , ^{40}Ca , ^{44}Ti , ^{48}Cr or ^{52}Fe are typically produced in much greater abundance compared to explosive carbon and oxygen burning. For introductions to the literature on explosive helium burning as it applies to thermonuclear supernovae (see [Timmes and Niemeyer 2000](#); [Moore et al. 2013](#)).

4.2.1 Recent comparison of observational iron-group element masses and isotope ratios with explosion model predictions (Chandrasekhar vs. sub-Chandrasekhar)

A recent study by [Blondin et al. \(2022\)](#) presented the amount of stable nickel produced (a year after SN explosion) as a function of the amount of radioactive

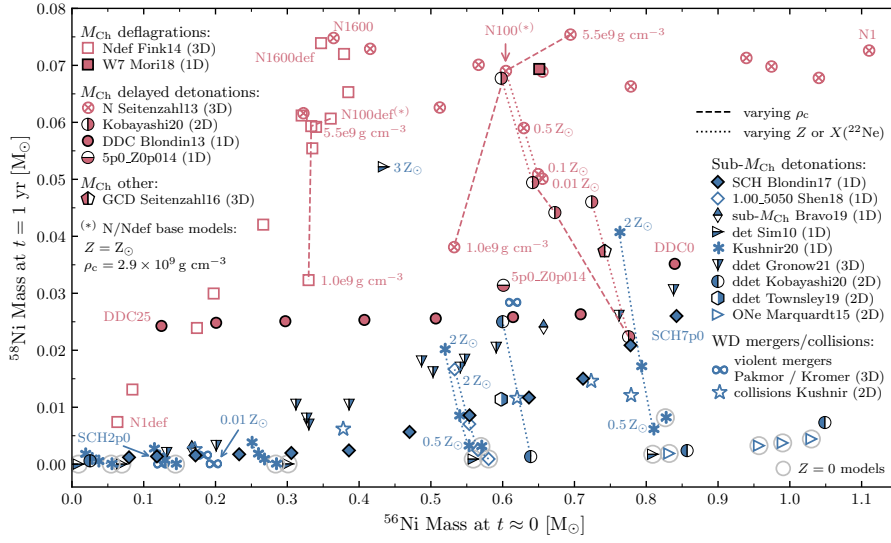


Fig. 13 Range of ^{56}Ni (radioactive nickel produced in explosion) vs. ^{58}Ni (decayed after 1 year; stable) for a number of simulated SN Ia explosions from the literature. Chandrasekhar mass models are shown in red while sub-Chandrasekhar mass models are shown in blue. Image reproduced with permission from [Blondin et al. \(2022\)](#), copyright by the author(s).

nickel produced in the explosion for a wide variety of 1D, 2D and 3D models, including Chandrasekhar- and sub-Chandrasekhar mass simulations (encompassing multiple assumed progenitor channels). A general trend is found such that Chandrasekhar mass SNe Ia tend to produce more stable nickel overall (with some exceptions), which would make for easier detection of forbidden nickel lines like $[\text{Ni II}]$ in late time spectra of SNe Ia for these systems (see Fig. 13).

In another study, [Tiwari et al. \(2022\)](#) analyze trends in $A=57$ to $A=56$ and $A=55$ to $A=56$ production ratios for a diverse selection of explosion models from different research groups. They find clear trends of these ratios as a function of metallicity and primary WD mass. Notably, the model-to-model variance of the sub-Chandrasekhar model category is insufficient to account for the full range of observationally-inferred production ratios, even when allowing for significantly super-solar initial metallicities. [Tiwari et al. \(2022\)](#) conclude both near-Chandrasekhar and sub-Chandrasekhar models are required to explain the observationally inferred production ratios of these iron group isobars.

4.3 Progenitor scenarios of near-Chandrasekhar mass explosions

4.3.1 Merging white dwarfs leading to near-Chandrasekhar mass WD ignition

The double degenerate channel of two merging carbon-oxygen white dwarfs has been considered a plausible progenitor scenario for many years (Webbink 1984; Iben and Tutukov 1984; Han et al. 1995; Postnov and Yungelson 2014). Until around 2010, it was assumed that in such a scenario the less massive (larger) degenerate dwarf would disrupt upon filling its Roche lobe and form a torus of material around the smaller, more massive dwarf, and this material would be accreted at a relatively high rate (up to $10^{-5} M_{\odot}$ per year, Yoon et al. 2007). If enough mass is present in the donor white dwarf, the more massive white dwarf – if allowed to continually accrete – would approach the Chandrasekhar mass limit. What happens at this stage depends on several factors, namely the accretion rate behaviour over the course of mass transfer evolution and subsequent burning of the freshly-accreted material.

One possibility is that the accreting white dwarf is ‘transformed’ from a carbon-oxygen white dwarf to one that contains heavier elements, i.e. an oxygen-neon-magnesium white dwarf (Miyaji et al. 1980; Saio and Nomoto 1985; Isern et al. 1991; Shen et al. 2012). This change in chemical make-up has a very important consequence: as an ONe(Mg) WD approaches the Chandrasekhar mass limit, it is more prone to electron captures on ^{24}Mg and ^{20}Ne which are produced in oxygen burning (see Jones et al. 2016, for more details). With electron capture rates increasing, degeneracy pressure loses its influence, and the ONe(Mg) white dwarf likely collapses to form a neutron star in what is called an accretion-induced collapse¹⁵ or more specific to this case – a merger-induced collapse (Ivanova et al. 2008; Ruitter et al. 2019; Schwab 2021). To be more confident of the outcome as to whether a massive ONe-rich white dwarf would definitely collapse to a neutron star or possibly explode, even partially, requires further study with multidimensional hydrodynamical simulations (see Jones et al. 2019).

On the other hand, if the CO white dwarf remains for the most part chemically unchanged and manages to approach the Chandrasekhar mass limit through accretion of its disrupted companion, it will explode, or possibly will accrete slightly above $1.4 M_{\odot}$ given the appropriate physical conditions (Pieranti et al. 2003; Di Stefano et al. 2011). In the case where the Chandrasekhar mass is approached, it is believed that the central ignition would take place in the manner as outlined above in Sect. 4.1, in essence in the same way as the ignition would occur in the core-degenerate or the single-degenerate Chandrasekhar mass scenarios discussed below. As mentioned in Sect. 3.3, ex-

¹⁵ Electron-capture supernovae (ECSNe Nomoto 1984) are often likened to accretion-induced collapse supernovae because both involve a stellar core accreting mass leading to a core-collapse neutron star, and both explosions produce relatively low energies compared to SNe Ia or core-collapse SNe (Dessart et al. 2006). ECSNe occur in stars with masses in the range between those that produce degenerate ONe white dwarfs and those that produce iron core-collapse neutron stars, and ECSN progenitors are referred to as Super-AGB stars (Doherty et al. 2017).

plosion models involving super-Chandrasekhar mass white dwarfs have yet to show significant promise in reproducing the observed properties of the so-called super-Chandrasekhar SNe Ia sub-class.

Over the last dozen years or so, a number of sophisticated three-dimensional white dwarf merger simulations from different research groups have revealed that robust thermonuclear explosions can occur in white dwarfs that are well-below the Chandrasekhar mass limit (see Sect. 5). Further, these explosions exhibit physical behaviour (ejecta velocities and nucleosynthesis) that are in agreement with those of observed SNe Ia – at least they are no worse than those models of exploding Chandrasekhar mass white dwarfs (Röpke et al. 2012). Since it has become clear in recent years that white dwarfs in mergers readily explode well before the more massive star has accreted much mass – through the ‘double-detonation’ rather than delayed detonation mechanism – for the rest of this section we do not discuss double degenerate white dwarf mergers in the context of Chandrasekhar mass explosions; we return to mergers in Sect. 5. Though our current understanding disfavours the Chandrasekhar white dwarf mass model in white dwarf mergers, we acknowledge that this could indeed be an incorrect assumption.

4.3.2 *The core-degenerate scenario*

It should be noted that the ‘core-degenerate scenario’ (Sparks and Stecher 1974; Livio and Riess 2003; Kashi and Soker 2011) is another potential, though less-studied (but see Aznar-Siguán et al. 2015) progenitor scenario of SNe Ia that involves the merger between a white dwarf and a relatively massive (non-degenerate) core of an evolved star during or following a common envelope episode. A central idea is that during the common envelope phase, not all material is ejected and $\sim 1\text{--}10\%$ of the envelope remains bound (Ilkov and Soker 2012) to the binary system. The resulting circumbinary disc can decrease the merger timescale between the AGB core and the white dwarf, which results in the (still hot) core becoming a relatively massive (possibly super-Chandrasekhar) object. We note here that binary star mergers have also been proposed as a channel for producing highly-magnetic, rather massive white dwarfs (Wickramasinghe and Ferrario 2000; Bogomazov and Tutukov 2009). In terms of explaining a large fraction of SNe Ia, the core degenerate scenario has drawn a lot of criticism owing to the fact that SN Ia explosions occurring during (or shortly after) a common envelope phase would likely exhibit tell-tale hydrogen features, and such features are only rarely seen in SNe Ia spectra (though there are exceptions, see Dilday et al. 2012; Kollmeier et al. 2019). It has been argued though that if a white dwarf + AGB core star merger does result in an eventual explosion, there could be a range of plausible delay times (between merger and explosion) spanning up to ~ 1 Gyr because magnetodipole radiation torques could delay the spin-down time of the newly-formed $\sim 1.4\text{--}1.5 M_{\odot}$ white dwarf (Ilkov and Soker 2012). Though this scenario is potentially promising (see also Soker and Bear 2023), and we indeed do expect these types of mergers to occur in nature, more numerical simulations of this

particularly challenging scenario are required before we can say more with a high degree of certainty.

4.3.3 *Single-degenerate near-Chandrasekhar mass scenario*

For decades, it was assumed that all SNe Ia occur in carbon-oxygen white dwarfs that have managed to approach the Chandrasekhar mass limit (Thielemann et al. 2004) due to accretion from a stellar companion. The companion is often assumed to be a hydrogen-rich main sequence or evolved star (either in the Hertzsprung gap or a red giant). However, though less common, the companion could instead be a hydrogen-stripped, helium-burning star (see Sect. 1.2.1).

The single-degenerate near-Chandrasekhar mass progenitor scenario for SNe Ia – regardless of how the explosion actually occurs – is the one that was made popular in numerous textbooks. It seemed attractive at first glance by offering a simple explanation as to how to evolve a binary system to ignition of an otherwise inert white dwarf, via mass accretion from a Roche-lobe filling non-degenerate companion onto a massive white dwarf primary. This scenario always leads to ignition of a more or less bare primary white dwarf just below the Chandrasekhar mass. This common mass was further seen as a natural explanation for the observation that many SNe Ia (at least historically) look similar to each other in terms of their lightcurve behaviour and general spectral properties (see Han and Podsiadlowski 2004, for some discussion on formation scenarios and birthrates).

One well-known issue with the canonical single-degenerate scenario of SNe Ia is the challenge of building up the mass of the white dwarf to the Chandrasekhar mass through accretion of hydrogen (Sutherland and Wheeler 1984; Wheeler and Harkness 1990). The issue is that the mass transfer rate has to be just right for the WD to gain mass, and this changes as the WD grows in mass, which appears as a fine-tuning problem (Han and Podsiadlowski 2004; Nomoto and Leung 2018). There is a small parameter space over which fully efficient hydrogen-rich burning, and thus sustained mass gain, on a CO WD can occur. This results in a rather narrow region in *white dwarf mass – mass accretion rate* parameter space over which fully efficient burning is possible. Outside of this parameter space the WD will experience thermally unstable burning resulting in novae for low accretion rates, or significant expansion of the WD atmosphere and optically thick winds for high accretion rates (the so-called ‘red giant’ configuration, Prialnik and Kovetz 1995; Nomoto et al. 2007). Potentially, the accreting WD may even experience mass erosion through nova eruptions in which case it would never attain near-Chandrasekhar mass (Patterson et al. 2017).

While the symbiotic channel has previously been investigated – in which a white dwarf accretes material from the wind of an evolved star (Munari and Renzini 1992), it was determined that such a binary configuration was unlikely to lead to the formation of a Chandrasekhar mass white dwarf over the course of the short lifetime of the symbiotic (Kenyon et al. 1993; Hachisu and Kato

2012), though such systems might contribute some small fraction of SN Ia events to the sub-Chandrasekhar mass scenario. However, given the existence of systems like RS Oph, which is estimated to host a white dwarf close to the Chandrasekhar mass limit, perhaps the jury is still out on the symbiotic question.

Now that we have broadly introduced the main binary star configurations (see also Sect. 1.2) and discussed pathways to central ignition of near-Chandrasekhar mass models, we next give a summary of the different explosion models in the context of explosions in modern Chandrasekhar mass WD models.

4.4 Explosion mechanisms

The near-Chandrasekhar mass models discussed in this section all start with the ignition of a deflagration (sub-sonic burning) near the centre of the WD (see Sect. 4.1). In the next Sect. 4.4.1, we present the characteristics of models where all of the nuclear burning occurs only in a deflagration. As discussed there, predictions of state-of-the-art 3D pure deflagration models proved to be irreconcilable with many features of normal SNe Ia, although they remain good candidates for certain sub-luminous sub-types of SNe Ia, in particular the 2002cx-like SNe. Both pure detonation models, which burn way too much of the WD to IGEs (see Sect. 1.2.4), and pure deflagration models, which, for realistic ignition conditions, burn far too little of the WD to IGEs, are therefore ruled out for the bulk of SNe Ia. Phrased in this way, it is not surprising that the attention turned to models that include a combination of the two: an initial deflagration phase that in one way or another transitions to a later detonation phase.

It was [Khokhlov \(1991a\)](#) that showed that an initial expansion of the white dwarf during a deflagration phase, followed by a transition of the mode of burning to a detonation at a time when the density of the unburned fuel had decreased to allow for production of intermediate mass elements, resulted in better agreement with observations. We refer to such models that pre-expand the star through an initial deflagration phase before detonating it when the central density has been lowered as “delayed-detonation models”. A few different main variants of delayed-detonation models exist: deflagration to detonation transition (DDT), gravitationally confined detonation (GCD), and pulsating reverse detonation models (PRD). We discuss these different variants in turn in the Sects. 4.4.2 – 4.4.4, following immediately the description of pure deflagration models in the next section.

4.4.1 Pure deflagrations (failed detonations)

It became very clear in the late 1960s that if the near-Chandrasekhar mass models were to work, the initial ignition had to occur as a subsonic deflagration (see Sect. 1.2.4). The successes of parameterized 1D fast-deflagration models

– most prominently the W7 model of [Nomoto et al. \(1984b\)](#) – in reproducing key observable features of normal SNe Ia, led to a focus of the thermonuclear modelling efforts on pure deflagration models for the next 20 – 30 years.

1D models however are un-physical, in that they do not capture the all-important effects of buoyancy, turbulence, and the Rayleigh–Taylor instability on the evolution of the flame front. In 1D, a deflagration ignited in a small central region simply burns outward in mass-coordinates and there are no pockets of unburned fuel left at high density. This produces an artificially large fuel consumption rate and leads to more energetic and luminous explosions than what is physical for the initial model. In 3D by contrast, a deflagration ignited in a small volume near the centre of the WD will be buoyant, since the energy release of the nuclear fusion reactions resulted in a small expansion and lower density of the hot ignition spot compared to the colder surrounding material. The bubble starts to float radially outwards in one direction towards the surface, accelerating and growing in size driven by the interaction of the flame front with the turbulent fluid flows and hydrodynamical instabilities (see e.g. the review by [Röpke and Sim 2018](#)). Consequentially, it was found that single spot ignition models only produced weak and faint explosions, unable to explain normal SNe Ia (e.g. [Reinecke et al. 1999](#)).

To obtain more energetic and luminous explosions in 3D models without suppressing buoyancy and hydrodynamical instabilities, central and multi-spot ignition models were introduced, which lead to a faster initial growth of the flame surface and a more complete incineration of the high density interior. This results in explosion models that produce a few tenths of a solar mass of ^{56}Ni and completely unbinds the white dwarf (e.g. [Gamezo et al. 2003, 2004](#); [Röpke and Hillebrandt 2005](#); [Röpke et al. 2006, 2007](#)).

It is worth noting that pure deflagration models produce high ratios of stable iron group isotopes (e.g. ^{54}Fe , ^{58}Ni) relative to radioactive ^{56}Ni and also high $[\text{Mn}/\text{Fe}]$. The reason for this is that the contribution of the detonation, which in DDT models produces several tenths of a solar mass of ^{56}Ni and intermediate mass elements, is missing. This occurs since the detonation in DDT models predominantly burns at densities where neutronization via electron captures is largely negligible and NSE is established in the high-entropy regime (see Sect. 4.2).

There was mounting evidence that the mixed ejecta of pure deflagration models are not in agreement with the more layered ejecta profiles inferred for normal SNe Ia (see e.g. [Stehle et al. 2005a](#); [Mazzali et al. 2007](#)) and that in any case the ignition of the deflagration is most likely occurring in a single, off-centre spot ([Zingale et al. 2009](#); [Nonaka et al. 2012](#)). Moreover, it was soon demonstrated that the turbulently mixed profiles of such pure deflagration models exhibit characteristics (e.g. colours, spectra) that are not reconcilable with observations of normal SNe Ia (see e.g. [Fink et al. 2014](#)). The pure deflagration model thus ceased to be a contender as a viable explosion model for normal SNe Ia, and the focus for the near-Chandrasekhar mass ignition paradigm shifted to models where the sub-sonic deflagration transitions to a super-sonic detonation, in one way or another (see the following sub-sections).

However, [Jordan et al. \(2012b\)](#) and [Kromer et al. \(2013\)](#) independently realized that, while too mixed and insufficiently energetic and luminous to explain the normal SNe Ia, single-spot, off-centre ignited pure-deflagration models are excellent candidates to explain the sub-luminous sub-class of 2002cx-like SNe of the SN Iax class. Notably, these models fail to unbind the whole white dwarf and they leave compact, high-velocity WD remnants behind that are polluted with some of the ashes of the thermonuclear fusion reactions (see e.g. [Fink et al. 2014](#)).

Off-centre, single-spot ignited pure-deflagrations in ‘hybrid’ CONe WDs can eject even less mass and produce even fainter events, with the explosion model of [Kromer et al. \(2015\)](#) producing only $3.4 \times 10^{-3} M_{\odot}$ and providing a good match to SNe Iax at the faint end of the SN Iax luminosity range, such as SN 2008ha. Taking this even further, such partial explosions may even be possible in ONeMg WDs (see e.g. [Jones et al. 2016](#)), where the high central densities near $10^{10} \text{ g cm}^{-3}$ lead to high neutronization rates and an over-production of neutron-rich Fe-group isotopes (e.g. [Jones et al. 2019](#)).

The chemically peculiar remnants that are left behind by such incomplete explosions or “thermonuclear eruptions” may already have been identified; see e.g. [Raddi et al. \(2019\)](#) for plausible high-velocity stellar remnants and [Zhou et al. \(2021\)](#) for a plausible Galactic supernova remnant.

4.4.2 Deflagration-to-detonation transition models

Often referred to as DDT models, deflagration-to-detonation transition (DDT) models used to be the most widely-accepted explosion models that can possibly explain normal (and maybe some abnormal) SNe Ia ([Hillebrandt and Niemeyer 2000](#)). In such DDT models, the ignition of the deflagration occurs as described above. The key ingredient for DDT models is then the spontaneous transition of the subsonic mode of nuclear burning (deflagration) to a supersonic mode of burning – a detonation. DDTs are frequently observed on Earth, such as the “knocking” in the cylinders of combustion engines. In these terrestrial cases, the DDTs are enabled by the walls of the confinement vessel. Stars do not have walls, however, and the problem of DDTs in an unconfined medium is more complicated. The basic idea, which goes back to [Zel’dovich et al. \(1980\)](#), is that a gradient in the induction times (auto-ignition delay-times to thermonuclear runaway) leads to a shock-formation and a detonation. [Lee et al. \(1978\)](#) refined this basic picture and the Shock-Wave-Amplification-through-Coherent-Energy-Release (SWACER) mechanism was born: sound waves created by small volumes of fuel that ignited propagate outwards, these sound waves reach other neighbouring volumes of fuel that by the time of their arrival are also igniting. With an appropriate spatial-gradient in these “induction” or auto-ignition timescales, the sound waves amplify and the pressure pulse can steepen into a shock, that for the right gradients can transform into a detonation, see e.g. [Seitenzahl et al. \(2009b\)](#) for a determination of critical induction time gradients relevant to the SN Ia problem. The mechanism of how a suitable induction-time gradient can be set up in a deflagration involves mixing

hot ash with cold fuel, when the deflagration enters the distributed burning regime, and strong turbulence, which intermittently produces small volumes with relatively large velocity (and temperature) fluctuations (e.g. [Khokhlov 1991b](#); [Niemeyer 1999](#); [Lisewski et al. 2000](#); [Woosley 2007](#); [Schmidt et al. 2010](#); [Ciaraldi-Schoolmann et al. 2013](#)). For alternative mechanisms to transition to a detonation see also [Fisher et al. \(2019\)](#) and [Poludnenko et al. \(2019\)](#).

[Khokhlov \(1991c\)](#) showed that the expansion of the star prior to the detonation results in the desired nuclear burning at densities where IMEs such as Si and S are synthesized. Early one-dimensional simulations (e.g. [Höflich 1995](#); [Höflich and Khokhlov 1996](#)) gave promising comparisons of the models against observations, however, key physical processes in the DDT explosion mechanism such as buoyancy, convection, and the turbulent cascade are inherently three-dimensional, requiring three-dimensional full-star simulations for a self-consistent approach to the problem (see e.g. [Pakmor et al. 2024](#)). [Gamezo et al. \(2005\)](#) showed first in a three-dimensional simulation that a period of sub-sonic burning (a deflagration) in an expanding white dwarf followed by a supersonic detonation led to kinetic energies that were on par with what was observed for typical SNe Ia ($\sim 1.3 - 1.6 \times 10^{51}$ erg), in contrast to the pure deflagration models which produced kinetic energies only about half of this range. Further, the resulting nucleosynthesis agreed more readily with observations compared to pure deflagration models, which would leave intermediate mass elements (i.e. oxygen, carbon) unburned near the white dwarf centre.

Parameterized model grids initially indicated that the width-luminosity relation may be recovered by DDT models ([Kasen et al. 2009](#)). However, [Sim et al. \(2013\)](#) demonstrated with 3D Monte Carlo radiative transfer calculations of the 3D model grid of [Seitenzahl et al. \(2013b\)](#) that DDT models tend to lie orthogonal to the width-luminosity relation, in spite of giving relatively good spectral matches to some observed SNe Ia. Varying secondary parameters, such as the carbon fraction, do not appear to change the orthogonality of the DDT models to the width-luminosity relation ([Ohlmann et al. 2014](#)).

4.4.3 Gravitationally confined detonation models

Another variant of near-Chandrasekhar mass explosion is the so-called “gravitationally confined detonation” (GCD) ([Plewa et al. 2004](#)). In GCD models, a deflagration ignites in a single bubble, typically some tens of km offset from the centre. Buoyancy drives the hot bubble towards the surface. As it grows in size and complexity due to the Rayleigh–Taylor instability, the rising plume accelerates to super-sonic speeds. Near the surface of the WD where the ambient pressure is sufficiently low, the hot ash can eventually spread laterally in all directions across the surface. While some material along the initial ignition axis reaches escape velocity, most of the hot ash material remains confined (bound) to the star as it rapidly spreads outwards, which is the origin of the somewhat misleading name “gravitationally confined detonation” scenario. The hot ashes then “collide” at the anti-podal point opposite to where

the plume of ash first broke out of the star. Nuclear fuel in the collision region may be sufficiently compressed and heated to trigger a detonation (see e.g. [Seitenzahl et al. 2009b,a](#)). Since the detonation is triggered only after energy release of the deflagration has allowed the WD to expand, this is also a type of delayed-detonation model.

The weak deflagrations arising from single ignition point models only allow for moderate expansion of the WD before the detonation is triggered. The further out the initial ignition spot is, the faster the plume rises (weaker deflagration phase) and the more compact the white dwarf when it detonates, leading to more ^{56}Ni and bright events. Moving the ignition spot closer to the centre reduces the initial buoyancy, allowing the deflagration to burn more mass. This increased energy release leads to more expansion and a weaker collision of the ash after break-out. For bubbles ignited close to the centre, a detonation becomes increasingly unlikely, limiting GCD models to the brighter end of the SN Ia distribution ([Fisher and Jumper 2015](#); [Byrohl et al. 2019](#)). The WD is thus still rather compact (relatively high density) when it detonates, which is the reason why these models are expected to be rather bright ([Fisher and Jumper 2015](#)), producing a lot of ^{56}Ni and relatively small amounts of IMEs. [Meakin et al. \(2009\)](#) calculated the first detailed nucleosynthesis for single ignition point (2D) GCD models, which indeed exhibit a large IGE/IME ratio. However, since only very little material is burned in the deflagration at the highest densities where electron captures drive the material neutron rich, compared to DDT models these GCD models also produce lower Mn/Fe and relatively fewer neutron-rich IGE. With a 3D simulation, detailed nucleosynthesis, and 3D Monte Carlo radiative transfer calculations, [Seitenzahl et al. \(2016\)](#) demonstrated that their GCD models do not match to normal SNe Ia. Further, although there are intriguing similarities with the 1991T-like SNe Ia, their models have a little too much high-velocity IGE and not enough low-velocity stable iron.

[Jordan et al. \(2012a\)](#) first introduced the pulsationally assisted gravitationally confined detonation variant of this class of explosion mechanisms. They ignited the deflagration more vigorously in multiple overlapping spots. As expected, the greater energy release leads to more expansion and the colliding ashes initially fail to produce detonation conditions. However, the energy release is too small to unbind the WD. After reaching a maximum radius, the WD contracts again and the additional compression and heating during the contraction phase leads to a detonation.

[Lach et al. \(2022\)](#) looked further into pulsationally assisted gravitationally confined detonations for a range of different ignition conditions. They produce models with ^{56}Ni masses from 0.257 to 1.057 M_{\odot} . Comparing their model spectra with observations, they conclude that although the models cover a range of ^{56}Ni masses all the way from sub-luminous to super-luminous SNe Ia, only the 1991T-like sub-type provides a good match to the bright end of the model distribution.

4.4.4 Pulsational reverse detonation models

The pulsating reverse detonation (PRD) model (Bravo and García-Senz 2006) is another variant of a delayed-detonation. Similar to the GCD models discussed in the previous section, the explosion begins with a (weak) deflagration that fails to unbind the star. The energy input however excites a pulsational mode. When the white dwarf contracts again, an accretion shock forms as the expanded outer layers fall back onto the CO core. The conversion of the pulsational kinetic energy may sufficiently compress and heat the underlying material to initiate a detonation (see Bravo and García-Senz 2009). Three-dimensional explosion simulations of the PRD variant show that energetic explosions with radioactive ^{56}Ni masses that match the brighter SNe Ia can be obtained (Bravo et al. 2009). However, this subclass of explosion models has deflagration ash at high velocity, and therefore large amounts of iron-group elements in the outer layers. The location of these iron-group elements in the ejecta leads to quite red colours and the predicted spectra are largely not in agreement with normal SNe Ia (e.g. Baron et al. 2008), although some viewing angles are better than others (Bravo et al. 2009). Compared to e.g. DDT models, there is also a lot more unburned carbon, which leads to a C II feature not typically seen in normal SNe Ia near maximum light (Baron et al. 2008; Dessart et al. 2014). Moreover, the relatively small mass burned at high density by the deflagration means that for the Bravo et al. (2009) model even $[\text{Mn}/\text{Fe}]$ is sub-solar. Overall, the PRD models are therefore not great candidates for SNe Ia.

4.4.5 Alternative models

There are some alternative explosion models in the literature that are less main-stream than the models discussed above, but nevertheless worth mentioning here. For example, it was pointed out by Horowitz and Caplan (2021) that actinides, including radioactive uranium, should preferentially crystallize in cooling massive white dwarfs first, owing to their high melting points. The authors entertain the idea that critical masses of radioactive actinides nuclei could condense, giving rise to a chain-reaction and ultimately fission-ignited thermonuclear supernovae, (see Deibel et al. 2022; Horowitz 2022). In a modification of the near-Chandrasekhar mass explosion models, Leung et al. (2015) and Chan et al. (2021) considered the effect of white dwarfs with dark-matter cores on the explosion properties, which generally lead to fainter but slower declining events. The energy released by annihilating dark matter particles in collapsing dark matter cores has even been hypothesized as a possible alternative ignition scenario for the nuclear fuel (Janish et al. 2019).

5 Sub-Chandrasekhar mass SN Ia explosion models

5.1 Historical context

As discussed in the previous chapter, the problem of building up the mass of a white dwarf toward the Chandrasekhar mass via mass-transfer is a well-known one. An advantage of sub-Chandrasekhar ($\text{sub}M_{\text{Ch}}$) WDs is that nature finds it easier to make them (see e.g. [Torres et al. 2021](#)). The idea that Type Ia supernovae could originate through a double-detonation mechanism in $\text{sub}M_{\text{Ch}}$ WDs was explored many decades ago ([Woosley et al. 1980](#); [Nomoto 1982b](#)), and significant work with hydrodynamical simulations involving helium shell detonations on $\text{sub}M_{\text{Ch}}$ mass WDs started to become more common-place throughout the 1990s. Explosive nucleosynthesis calculations and synthetic lightcurves indicated that $\text{sub}M_{\text{Ch}}$ mass explosions should be taken seriously as viable SN Ia progenitors. Though it was found that lower-mass WDs that explode via double-detonation are not capable of producing very large amounts of iron, they indeed produce large amounts of V, Cr, and Ti ([Woosley and Weaver 1994a](#); [Livne and Arnett 1995](#)). Two-dimensional models showed fairly good agreement with four real SN Ia explosions: the well-known super-luminous and sub-luminous SN 1991T and SN 1991bg, respectively, as well as SN 1989B and SN 1992A (see also [Woosley and Weaver 1995](#)). A main issue however was that these sub-Chandrasekhar mass explosion models from the 1990s involved rather massive helium-rich shells ($\sim 0.15 - 0.2 M_{\odot}$) acquired via accumulation from a stellar companion, sitting on the WD surface. The second detonation deeper within the WD – occurring at higher density – was necessary to achieve any reasonable nucleosynthetic outcome resembling SNe Ia. But when the first detonation occurs in a massive helium shell, helium-burning leads to a rather large amount of iron-group elements being synthesized, with too much iron-group material at high expansion velocities. A key issue with an abundance of IGEs in the outer layers is that fluorescence in elements like titanium and chromium redistributes blue photons to redder wavelengths and consequently, synthetic B-V colours are generally too red at peak and do not satisfy observational constraints (e.g. [Kromer et al. 2010](#)). It was confirmed with the advent of more sophisticated numerical models including 3D hydrodynamics, that such massive (or ‘thick’) helium shells were not actually necessary to achieve a double-detonation, putting the $\text{sub}M_{\text{Ch}}$ mass double-detonation scenario back on the table as a promising progenitor candidate ([Sim et al. 2010](#); [Kromer et al. 2010](#); [Fink et al. 2010](#); [Woosley and Kasen 2011](#); [Shen and Moore 2014](#)).

In this section, we discuss $\text{sub}M_{\text{Ch}}$ mass explosions in two parts: those where mass transfer is dynamically-driven (i.e. unstable), and those where the binary is undergoing stable mass transfer at the time of explosion; binaries involving a $\text{sub}M_{\text{Ch}}$ mass white dwarf that gathered mass either through RLOF, or even through winds, can potentially produce Type Ia supernovae. Both types of double-detonation configurations – dynamically unstable or stable mass transfer – require different modelling approaches.

‘Dynamically-driven’ (dynamically unstable mass transfer) implies that the rate at which mass is transferred between the stars leading up to the supernova proceeds on a dynamical timescale (rather than on a longer nuclear or thermal timescale). In the case of two white dwarfs of similar mass, mass transfer will be unstable and proceed rapidly and the stars will most certainly merge quickly (see [Marsh et al. 2004](#)). On the other hand, for binaries undergoing sustained RLOF, the mass gain rate, which is dependent upon the orbital configuration of the binary, determines whether the material captured by the accretor will undergo nuclear burning on the white dwarf or whether material will simply accumulate on the WD surface, building up the mass of the helium ‘shell’. In a nut ‘shell’, if enough helium-rich material is allowed to avoid burning and simply accumulate on the sub M_{Ch} WD at a relatively low rate ($\sim 10^{-8} M_{\odot} \text{yr}^{-1}$, i.e. [Hashimoto et al. 1986](#); [Piersanti et al. 2014](#)), a detonation will be initiated in the recently-accumulated helium-rich shell. This first detonation will subsequently trigger a second detonation in the central regions of the white dwarf, thus destroying the star. Such a mechanism is referred to as a ‘double-detonation’, and for about 4 decades has been the principle explosion mechanism thought to be responsible for sub M_{Ch} mass SNe Ia.¹⁶ In this context, semi-detached binaries undergoing non-dynamical mass-transfer have canonically been assumed to potentially undergo double-detonations under the right conditions, and we will discuss these systems first.

5.2 Non-dynamical mass transfer

Population synthesis calculations have indicated that thermonuclear supernovae triggered from helium-shell detonations in mass-transferring binaries in which a white dwarf steadily accumulates mass from a helium-rich star¹⁷ could match the empirically-derived SN Ia rate of the Galaxy, which is 0.54 ± 0.12 per century; see [Li et al. \(2011b\)](#) (see also [Tutukov and Yungelson 1996](#); [Cappellaro et al. 1997](#)). While symbiotic binaries involving a white dwarf accreting hydrogen (which burns to helium) have been considered as potential candidates for the sub M_{Ch} scenario ([Kenyon et al. 1993](#)), such a configuration – an accreting white dwarf with both a thin helium and hydrogen shell – leads to frequent unstable burning and the probability for shell detonations leading to a WD detonation before the evolved donor has left the giant phase is unlikely (see also [Kemp et al. 2021](#), in the context of hydrogen and helium novae). When considering binaries with WD accretors and corresponding predicted

¹⁶ Some recent simulations have explored the possibility of each star experiencing if not two, a minimum of one detonation each for a total of 3 or 4 detonations in the binary ([Tanikawa et al. 2019](#); [Pakmor et al. 2022](#), see their table 2 for subsequent abundance computations), but we do not discuss these systems here.

¹⁷ Steady here does not mean fully efficient. During stable mass transfer some fraction of the mass lost by the donor will be captured by the companion, either through an accretion disc or via direct accretion or accumulation onto the star, and this fraction of material that is burned (or accumulated) need not be close to 1, and likely will change with time as the system evolves.

delay time distributions and rates for double-detonation supernovae (Ruiter et al. 2011; Wang et al. 2013; Ruiter et al. 2014), favoured binary star configurations include a CO white dwarf gaining material via RLOF from either a helium-rich white dwarf or the helium-rich core of a previously ‘regular’ star that has had its envelope removed through binary interactions¹⁸. The AM CVn systems are a well-known sub-population of cataclysmic variables in which a (CO) white dwarf accretes from a small helium-rich star (Warner 1995). For some time AM CVn systems were considered as plausible progenitors of some fraction of the SN Ia population (Solheim and Yungelson 2005; Bildsten et al. 2007). However, theoretical estimates of AM CVn birthrates seem to be over-estimated in population synthesis studies, since predictions of the AM CVn population numbers were typically an order of magnitude above those observationally-determined values, albeit with limited sample size (Nelemans et al. 2001; Roelofs et al. 2007).

Galactic AM CVn binaries, of which more than 55 are known (Ramsay et al. 2018), will be crucial targets for future space-based gravitational wave detectors like *LISA* (Kupfer et al. 2018; Amaro-Seoane et al. 2023), given their exceptional capability as multi-messenger (GW and electromagnetic) sources. Though earlier works concluded the donor star was likely a degenerate object and thus the ‘double white dwarf’ formation scenario for AM CVn systems was the most popular of the three main proposed scenarios, recent, detailed studies have demonstrated that at least some (if not the majority) of AM CVn donor stars are actually non-degenerate, or only partially degenerate (see Green 2019). The majority of AM CVn systems appear to harbour rather ‘run of the mill’ CO WD accretors in terms of mass, with very low-mass companions, thus they are not deemed as particularly likely SN Ia progenitors, even for the sub-Chandrasekhar mass events. However, a sub-set of AM CVn-like binaries involving more massive WDs accreting from subdwarf B/O stars (Heber 2016) could potentially reach sufficient physical conditions to produce double-detonations, though the SN Ia birthrate of this channel is expected to be rather low (see also Pelisoli et al. 2021, for discussion of HD265435, a binary consisting of a white dwarf and a hot subdwarf). It was recently estimated that such systems could be responsible for a rather small fraction ($\lesssim 1\%$) of Galactic SNe Ia (Zhou et al. 2014; Neunteufel et al. 2022).

5.2.1 Double-detonation models in binaries undergoing non-dynamical mass transfer

In binary evolution physics, the inter-connection between changing orbital quantities (masses and mass ratio, separation, eccentricity) and evolving stellar properties (phase of stellar evolution e.g. size and density; composition) make predicting final states from initial states extremely challenging – even for a simple stellar population having one metallicity! Rapid binary population

¹⁸ Such objects can encompass a range of level of degeneracy and are often referred to in various ways in the literature: naked helium star, helium main sequence star, hydrogen-stripped helium-burning star, (semi-)degenerate helium core, etc.

synthesis studies, simulating between $\sim 10^5 - 10^9$ stars in one go, have greatly improved our ability to set limits on which binary star configurations plausibly produce a Type Ia supernova in the first place, thereby guiding computationally expensive hydrodynamical and radiative transfer simulations that focus on the most crucial part of the evolution: pre-explosion and/or explosive phase (see also [Neunteufel et al. 2016](#)).

In detailed hydrodynamical simulations of double-detonations in binaries undergoing stable mass transfer, the donor itself is generally not simulated. Such simulations offer an approach about the binary configuration and thus progenitor scenario. Despite the lack of information about binary interactions preceding the detonations in these models, such simulations can be indicative of what might occur in the case of a WD merger (see next sub-section).

The amount of helium that is collected on the WD surface before the initial helium shell ignition is dependent on the mass of the underlying white dwarf ([Iben and Tutukov 1989](#); [Shen and Bildsten 2009](#)). If the helium shell ignites but fails to drive a second detonation deeper in the star, the result would be a so-called .Ia (*‘dot one Eh’*, [Bildsten et al. 2007](#)). A potential observed counterpart of such a transient could be SN2002bj ([Poznanski et al. 2010](#)). As mentioned in Sect. 4.3.3, a white dwarf accreting helium-rich matter can on the other hand approach the Chandrasekhar mass limit, thus surpassing the opportunity to explode as a sub M_{Ch} event. The overall outcome (either Chandra or sub-Chandra) will depend heavily on the accretion rate, with higher rates leading to hotter envelopes that facilitate nuclear burning of helium, either stably or via a series of helium-shell flashes ([Kato and Hachisu 2004](#)). [Piersanti et al. \(2014\)](#) carried out a comprehensive investigation of helium-accreting white dwarfs, taking into account the thermal response of the accretor using a modified version of the FRANEC evolutionary code ([Chieffi et al. 1998](#)). Figure 14 depicts a summary of their findings, which breaks down He-accreting WD systems into various regimes. Chandrasekhar mass white dwarf explosions may be achieved for relatively high accretion rates when the white dwarf undergoes stable burning, while sub M_{Ch} explosions are only achievable for accumulation rates on the order of $\sim \text{few} \times 10^{-8} M_{\odot} \text{ yr}^{-1}$ or less.

The overall picture is that the initial detonation is ignited in a helium-rich layer that has been convectively burning helium for a few days. For vigorous convection, conditions can be such that at the inflow of a convective shell a He-detonation can ignite ([Glasner et al. 2018](#)). This helium detonation in turn creates a propagating shock wave that travels through the core, closes in on itself, and ultimately ignites a detonation in the core. Where exactly the helium shell detonation takes place, in terms of scale height and geometry, and then how and precisely where the second detonation in the white dwarf occurs, are still not completely clear ([Moll and Woosley 2013](#)). When a helium shell detonation, which could arise by compressional heating during mass accumulation, leads directly to a second detonation at the shell-WD core interface, the mechanism is often referred to as an ‘edge-lit’ detonation ([Livne and Glasner 1990](#); [Sim et al. 2012](#)). However, another, possibly more favoured model occurs when the initial helium detonation shock wave does not immediately

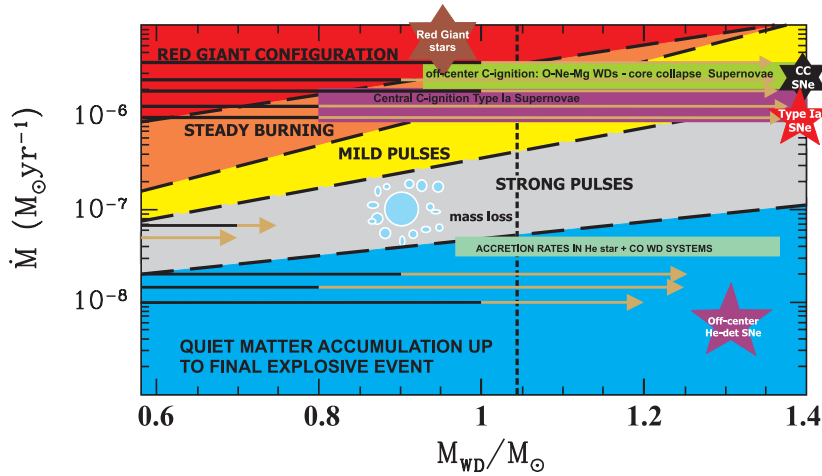


Fig. 14 Rate of accretion of helium as a function of white dwarf mass with various accretion regimes. In the Red Giant regime (red) the white dwarf cannot accept the large amount mass transferred and thus develops a red giant-like envelope (i.e. [Nomoto et al. 2007](#)). For slightly lower accretion rates, nuclear burning on the white dwarf becomes fully efficient (orange region), and the star may become massive enough to explode as a near-Chandrasekhar mass WD. For even lower accretion rates (yellow and grey), mild or strong helium flashes develop ([Kato and Hachisu 2003](#)), thereby decreasing mass retention efficiency; it is not fully clear whether accreting white dwarfs in this regime will erode in mass or ultimately gain mass (see [Starrfield et al. 1985](#), for the hydrogen-accretion context). Finally, for rates below $\sim \text{few} \times 10^{-8} M_{\odot} \text{ yr}^{-1}$, the build-up of a helium shell (no flashes) is possible, which may lead to a detonation in the helium shell once sufficient conditions are met ([Fink et al. 2010](#)). Image reproduced with permission from [Piersanti et al. \(2014\)](#), copyright by the author(s).

initiate a detonation near the shell-core boundary, but rather travels through the star and converges somewhere off-centre on the far side of the WD (on the opposite side of the initial ignition spot), resulting in a second detonation close to the WD centre ([Livne 1990](#)), where densities are rather high ($\gtrsim 10^7 \text{ g cm}^{-3}$). Such a ‘convergent shock scenario’ for double-detonations with rather small helium shell masses have shown to be extremely promising when comparing synthetic lightcurves and spectra of those with observed SNe Ia ([Townesley et al. 2012](#)). Using high-resolution 3D hydrodynamical simulations with Arepo ([Pakmor et al. 2016](#)), [Gronow et al. \(2020\)](#) found that even before the convergent shock mechanism occurs, double-detonations can already occur via the ‘scissor mechanism’ (see also e.g. [Livne and Arnett 1995](#); [García-Senz et al. 1999](#); [Forcada et al. 2006](#)), in which a carbon detonation is ignited during the convergence of the detonation wave at the base of the helium shell. Such a mechanism highlights the importance of mixing in (3D) simulations: helium shells that contain some fraction of carbon not only produce synthetic observables that are in better agreement with observations ([Kromer et al. 2010](#); [Shen and Moore 2014](#)), but enhance the He burning rate thus leading to stronger shocks.

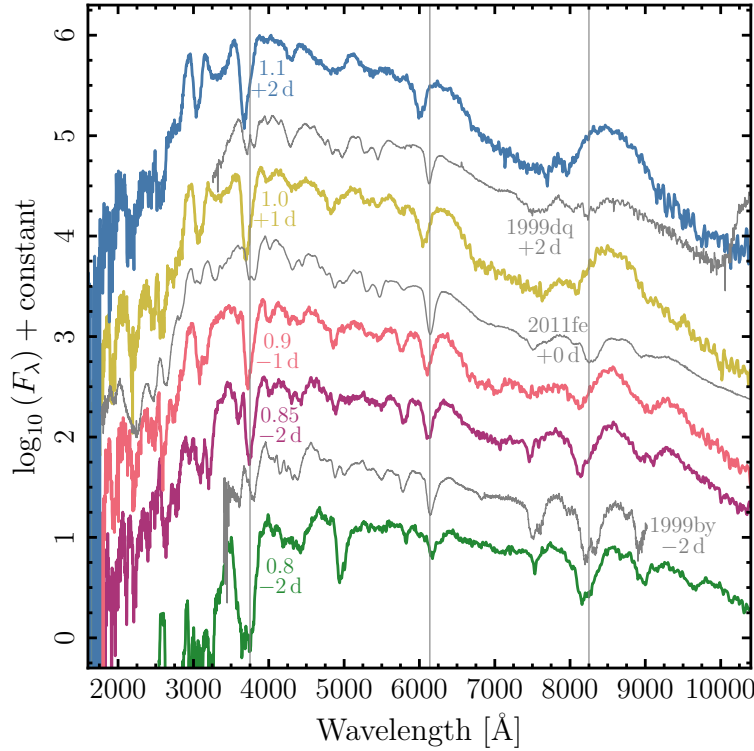


Fig. 15 Observed (grey) and synthetic (colours; 50/50 C/O fraction assumed) spectra near B-band maximum light. Exploding WD masses are indicated along with time in days before or after maximum. The Si II 6355 and Ca II H&K and near-infrared triplet regions are indicated by vertical lines. All spectra are offset on the y-axis by arbitrary constants. Image reprinted with permission from Shen et al. (2018), copyright by AAS.

Townsley et al. (2019) studied double-detonations in sub M_{Ch} mass white dwarfs (2D: $1 M_{\odot}$ WD with a $0.02 M_{\odot}$ helium shell) confirming that these explosions can produce normal SNe Ia spectra, with higher ejecta velocities being found in the simulations where the supernova is analyzed at higher latitudes. It was noted however that the lightcurve decline rate in this particular study was somewhat lower than those of observed SNe Ia like SN2011fe. Computing detonations in sub M_{Ch} WDs with an extensive reaction network, Shen et al. (2018) found that exploding WDs with mass $\sim 1 M_{\odot}$ produced nucleosynthetic observables in very good agreement with observations of normal SNe Ia (see Fig. 15), even following the Phillip's relation. Shen et al. (2021) found WDs in the mass range $\sim 0.9 - 1.1 M_{\odot}$ exhibit features very similar to normal SNe Ia, while less massive WDs $\sim 0.85 M_{\odot}$ fared rather well in explaining the sub-luminous events (see their Figs. 8 and 20).

Boos et al. (2021) performed a parameter study of 2D full star detonations using FLASH and a 55-species reaction network (Townesley et al. 2019). In their study they included both the preferred thin-shell models as well as thick-shell models, which are plausibly good representatives of other exotic thermonuclear transients (Polin et al. 2019; De et al. 2019). A notable point of the Boos et al. (2021) study is that the secondary detonation did not always occur at a consistent location relative to the WD centre, with the thickest shell (0.1 M_{\odot} helium shell model on a 1.0 M_{\odot} WD) resulting in a detonation most off-set from the symmetry axis, i.e. closer to the core-shell boundary. The different models exhibited a range in nucleosynthetic yields ranging a factor of ~ 2 in intermediate mass elements and a factor of ~ 7 in ^{56}Ni (see their Table 2).

While 3D hydrodynamical studies of double-detonations are now feasible at high-resolution, much of the parameter space remains to be explored. One emerging trend appears to be that at least some sub M_{Ch} explosion models (and their associated radiative transfer calculations and predictions of nucleosynthetic structure) are promising for explaining some SNe Ia of the more peculiar sub-classes (Collins et al. 2022). On the other hand, in a parameter study of 3D double-detonations of varying shell (0.02–0.1 M_{\odot}) and core mass (0.8–1.1 M_{\odot}), Gronow et al. (2021) found that bolometric properties of simulated double-detonations were a fairly good match to faint and normal Type Ia supernovae (see Fig. 16).

Finally, while canonical models assume a CO WD as the exploding star, other situations have been explored for accretors of different composition. White dwarfs with significant amounts of helium are generally not massive enough (thus do not harbour the right density) to readily synthesize elements near the iron peak (Hashimoto et al. 1986). On the other hand, sub M_{Ch} oxygen-neon white dwarfs possess sufficient densities, and could plausibly account for some small fraction of events (Marquardt et al. 2015). However, ONe WDs are likely harder to ignite in the first place (see Shen and Moore 2014, for an overview of challenges and various works associated with achieving core detonations in double-detonation simulations). Other more exotic means of producing double-detonation SNe Ia have also been explored, for example tidally-induced double-detonations in white dwarfs that pass close to intermediate-mass black holes and become tidally disrupted (Tanikawa 2018). One can be hopeful that in the near-future, we will be able to learn more about these types of transient events with dedicated deep surveys such as Rubin (Ivezić et al. 2019), in particular if such transients can be optimized for multi-messenger follow-up over the electromagnetic (and in some cases gravitational wave) spectrum.

5.3 Dynamically-driven

When the orbital separation of two white dwarfs becomes too small for both stars to remain within their Roche lobes, the larger (less massive) white dwarf

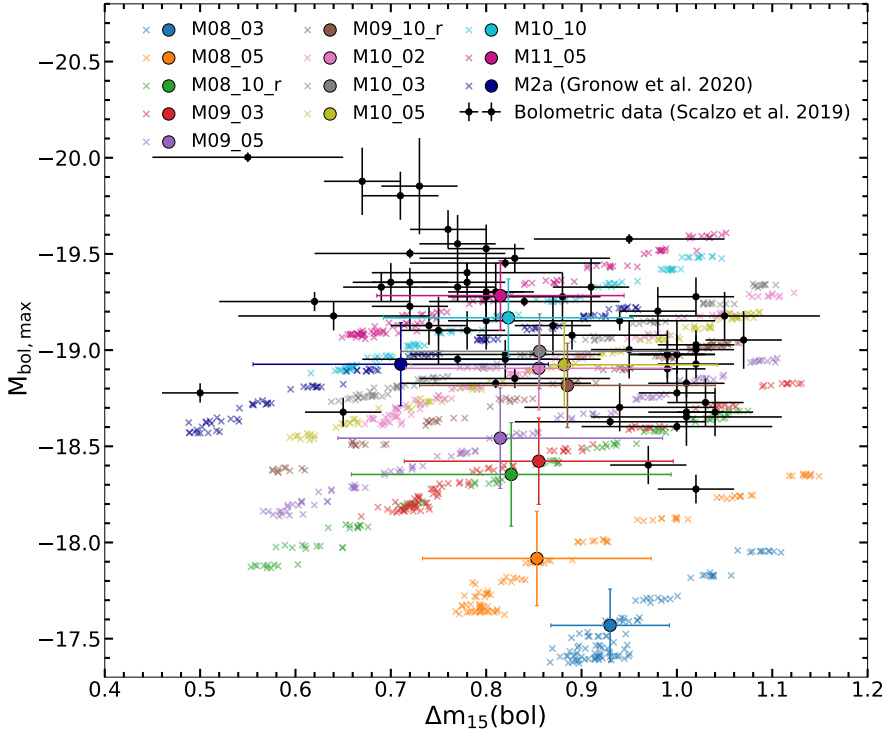


Fig. 16 Coloured dots represent angle-averaged (over 100 viewing angles) $\Delta m_{15, \text{bol}}$ vs. peak bolometric magnitude for various double-detonation explosion models. In the legend, M11.05 means the white dwarf ‘core’ mass was $1.1 M_{\odot}$ while the helium shell had a mass of $0.05 M_{\odot}$. The models with more massive white dwarfs and less massive shells more readily cover the range of observed SNe Ia in this parameter space. The sample of nearby SNe Ia from Scalzo et al. (2019) are represented by black cross symbols. Image reprinted with permission from Gronow et al. (2021), copyright by ESO.

will fill its Roche lobe and matter will be transferred away from it. In the ideal (easily to treat numerically) case, matter flows from the donor through the inner Lagrangian point between the stars toward the accretor, which then accepts the new material. However, in the case of dynamically-driven mass transfer, the transfer of material is too fast: the donor is unable to stay within its Roche lobe and structurally re-adjust itself in a short-enough timescale, and the accretor is unable to accept this influx of material. When the mass-losing star (donor) has a relatively distinct core-envelope structure, its envelope engulfs both stars in a common envelope (see Röpke and De Marco 2023, for a recent review on numerical techniques). However, in the case of two stellar cores with no envelope(s), the stars merge. The precise timescale on which the merger occurs depends on the properties of the system, as there are many competing processes to consider (Piersanti et al. 2003; Shen et al. 2012). These

merging white dwarfs are the systems we discuss next in the context of SN Ia progenitors.

5.3.1 Mergers of white dwarfs

Simulations of white dwarf mergers are very computationally demanding, and have only become possible relatively recently at a resolution where length scales relevant to the detonation physics are starting to be resolved (e.g. [Morán-Fraile et al. 2024](#)). Smoothed Particle Hydrodynamical simulations of white dwarf mergers initially indicated that conditions necessary for a carbon detonation were not likely to be met ([Guerrero et al. 2004](#)), but exceptions were indeed possible ([Yoon et al. 2007](#)). [Pakmor et al. \(2010\)](#) demonstrated with 3D hydrodynamical simulations coupled with radiative transfer modelling that two CO white dwarfs with roughly equal mass ($\sim 0.9 M_{\odot}$) would merge violently to create an explosion through direct carbon ignition near the core of the primary white dwarf without the requirement for a double-detonation.¹⁹ In addition, synthetic spectra and lightcurves matched those of 1991bg-like (sub-luminous) SNe extremely well. The [Pakmor et al. \(2010\)](#) study also concluded that such mergers could occur in young and old galaxies alike, thus discounting the perception that such mergers are rare, ‘niche’ events. Additional simulations of carbon-ignited WD mergers soon followed ([Pakmor et al. 2011](#); [Pakmor et al. 2012](#); [Sato et al. 2015](#)), demonstrating that some of these explosions could plausibly reach peak luminosities comparable to normal SNe Ia (see [Fig. 17](#) for snapshots of the merger process). While successful SN Ia explosions are mostly expected to only occur in double white dwarf systems above a critical mass ratio ([Sato et al. 2016](#)) and only for systems above a critical mass threshold for the primary star (but see [van Kerkwijk et al. 2010](#)), some of the first detailed WD merger simulations ([Guillochon et al. 2010](#)) demonstrated that the primary white dwarf density, and thus primary WD mass, plays the dominant role in determining the amount of iron-group elements that are synthesized in the explosion. In other words: *The primary white dwarf mass offered an elegant explanation for the observed diversity in SN Ia peak luminosity*, with more massive primaries giving rise to a higher production of radioactive nickel, resulting in more luminous events at peak ([Ruiter et al. 2013](#); [Shen et al. 2017](#)).

It was soon realized that explosion of the primary white dwarf is much more readily achieved if the binary system contained some (even small) amount of helium, for example on the white dwarf surface. How would the helium have gotten there? This could be achieved either through rapid mass transfer from a helium or hybrid white dwarf (see [Guillochon et al. 2010](#)), or could be a thin layer of helium that is left over from previous stellar evolution, pre-existing well before the final binary interaction phase ([Pakmor et al. 2013](#)). Such ‘helium-ignited’ mergers then quickly became the poster child as the

¹⁹ In the carbon-ignited merger scenario, the merger occurs violently enough such that the primary WD suffers sufficient compressional heating in its central regions and undergoes a prompt detonation there, completely unbinding the star.

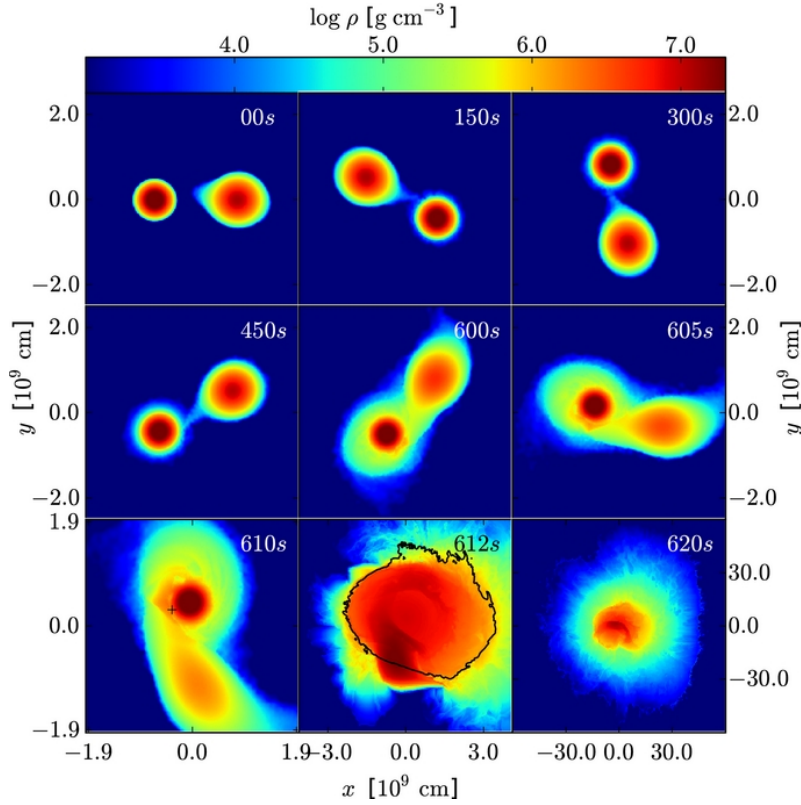


Fig. 17 A white-dwarf merger simulated with GADGET resulting in a carbon-ignited detonation (marked with black cross) of the primary white dwarf; the LEAFS code is used to model the detonation flames (Reinecke et al. 1999). Mass transfer proceeds stably initially but after ~ 10 minutes, mass transfer becomes dynamically unstable. The masses of the primary and secondary CO WDs are 1.1 and $0.9 M_{\odot}$, respectively, and the primary remains mostly fully intact throughout the interaction, thus retaining much of its initial density profile, until after the detonation. The black line in the bottom row (middle panel) shows the detonation front, which engulfs both stars, leaving no surviving companion in this case. Image reproduced with permission from Pakmor et al. (2012), copyright by AAS.

favoured sub-Chandrasekhar mass progenitor channel of SNe Ia. Over the last dozen years, simulations of white dwarf mergers, and studies investigating post-merger configurations in the context of SNe Ia, have been active areas of research by different groups employing a variety of numerical techniques: (Schwab et al. 2012; Ji et al. 2013; Dan et al. 2014; Moll et al. 2014; Dan et al. 2015; Raskin et al. 2014; Kashyap et al. 2015; Zhu et al. 2015; Kashyap et al. 2018; Pakmor et al. 2021; Roy et al. 2022; Pakmor et al. 2022; Zenati et al. 2023; Burmester et al. 2023). Despite the increasing number of works in this area, much of the parameter space of 3-dimensional white dwarf mergers still remains largely unexplored. One challenge to the field is that the learning curve associated with understanding how to use and additionally correctly

interpret output from a 3D hydrodynamical codes is quite steep and time-consuming. We note that white dwarf mergers nonetheless are increasingly an extremely promising progenitor scenario, potentially for normal SNe Ia as well as other sub-classes, and we strongly encourage further numerical studies in this area. Such studies will be useful in the larger context of white dwarf merger research (not limited to SNe Ia progenitors) with prospective work supported by future space-based gravitational wave observatory missions that are projected to come online starting in the 2030s.

5.4 WD+WD collisions

Distinct from white dwarf mergers where gravitational wave radiation emission is what drives the stars together – white dwarf collisions refer to white dwarfs crossing each other’s path before total orbital decay. Such coalescing of white dwarfs that may occur in dense stellar environments, such as in the cores of globular clusters. In a white dwarf collision (similar to the case of mergers), the combined stellar mass need not be above the Chandrasekhar mass limit: white dwarf densities can rise significantly due to shock compression, in particular if the collision occurs head-on (see [Rosswog et al. 2009](#), who performed a parameter study in WD mass and composition). The range of impact conditions results in a range of ^{56}Ni that comfortably encompasses the expected range of normal SNe Ia, though [Raskin et al. \(2009\)](#), who conducted 3D smoothed-particle hydrodynamical simulations, found a more modest ($\sim 0.4 M_{\odot}$; i.e. sub-luminous) amount of nickel produced for their explored (thought to be most probable) case of two $0.6 M_{\odot}$ white dwarfs.

Using 2D hydrodynamical simulations, [Kushnir et al. \(2013\)](#) found that collisions of white dwarfs with a range of masses and impact parameters bracket the observed properties of SNe Ia, and argue that this channel could be relatively common if triple star systems are considered (see also [Iben and Tutukov 1999](#); [Thompson 2011](#); [Hamers et al. 2022](#); [Rajamuthukumar et al. 2023](#)). However, no population synthesis nor dynamical studies were performed in that work to confirm this. A population study is needed to properly quantify the probability of such systems being successfully produced in nature; stars increase dramatically in size as they evolve, and so avoiding a merger prior to the double white dwarf phase could be a major hurdle for the triple scenario. [Piro et al. \(2014\)](#) found that colliding white dwarf masses would need to be relatively large to produce sufficient amounts of ^{56}Ni in an explosion. Thus, we should only expect normal SNe Ia via collisions to be found among young stellar populations (i.e. with short delay times), which does not fit the general trend of SNe Ia, with normal events occurring among a large range of stellar environments and ages.

[Toonen et al. \(2018\)](#) explored a range of models using triple star evolution coupled with dynamical secular evolution and found the rate of WD+WD collisions plausibly leading to SNe Ia is on the order of 0.1%. A recent parameter study by [Rajamuthukumar et al. \(2023\)](#) that incorporated stellar evolution

and dynamical interactions of triple star systems found that WD+WD collisions could account for 0.4–4% of SNe Ia.

6 Final remarks

The current state of the field is that white dwarf mergers leading to sub-Chandrasekhar mass explosions are an extremely promising channel that seem to be able to account for a large fraction, if not the majority, of Type Ia supernovae. In terms of various model predictions, double white dwarf mergers fare extremely well in terms of delay time distribution and rates (see Sect. 3.7), and perhaps more importantly, the expected range in exploding white dwarf mass provides a natural, simple explanation for the observed diversity among SN Ia peak luminosity (Sect. 5.3.1). Whether the companion explodes too, or not, is not clear. However, some modern 3D hydrodynamical simulations indicate that the predicted differences between the two cases would not be immediately apparent, and any differences would not be extreme (Pakmor et al. 2022). The fact that deeper searches for potential hyper-velocity ‘fly away’ white dwarf companions did not recover a large amount of candidates might give credence to the idea that, in the case of WD mergers leading to SNe Ia, both WDs are likely destroyed more often than not. However, it could be that a large fraction of such high-velocity ex-donors are still eluding detection (El-Badry et al. 2023). On the other hand, taking into account constraints set by stellar abundance data from the solar neighbourhood, it is likely that at least some SNe Ia must have had to originate in massive white dwarfs around the Chandrasekhar mass to have produced sufficient amounts of IGEs, in particular Mn (Sect. 3.2), which is more supportive of a single-degenerate origin. Taken together, the over-arching theme has been that sub-Chandrasekhar mass SNe Ia, in particular coming from white dwarf mergers, are slowly emerging as the most-favoured progenitor scenario, but they cannot be the only progenitor.

We are entering a phase in which the rate of the discovery of new transients will continue to increase even more drastically in the coming years. Rubin will detect about 10 million transients per night; an overflow of data unlike any we have encountered before. Since it is not feasible for humans to efficiently sift through this rapid data-deluge in real time using traditional methods – separating the useful data into distinct categories (asteroids/fireballs, exoplanets, core-collapse and thermonuclear supernovae, gamma ray bursts etc.) – several stream alert ‘brokers’ have been in development by a variety of teams. The brokers²⁰, many of which are actively receiving and processing alerts from the Zwicky Transient Facility (Bellm et al. 2019; Patterson et al. 2019), each have their own unique set of priorities, objectives, and methods for identifying and rapidly prioritizing diverse transient data for the scientific community, who can then initiate further, detailed (e.g. spectral) follow-up. Among the Rubin brokers, Fink (Möller et al. 2021) has the capability of SN Ia classification even

²⁰ <https://www.lsst.org/scientists/alert-brokers>

several days before peak magnitude, using a deep learning framework based on SuperNNova classifier scores (Möller and de Boissière 2020; Leoni et al. 2022).

Other than refining rate estimates for various SN sub-classes, gathering numbers and statistics of SN explosions as a function of host environment (metallicity, galaxy Hubble type) will be useful particularly for high-redshift supernovae where, currently, it is not always possible to resolve a host. The deep (over 10 year) Legacy Survey of Space and Time that Rubin will conduct will offer an unprecedented opportunity to drill the environments of high-redshift supernovae. Combined with data from the Euclid mission, it will be possible to increase the sample of events even further (Bailey et al. 2023). Going a few years into the future, Nancy Grace Roman Telescope NIR data will play an important role in detecting SNe out to higher redshifts, which will be important for future studies in precision cosmology (e.g. Dettman et al. 2021).

One question to ask is: how will increasing the number of SN lightcurves from deep surveys enable us to learn more about their physics? We are already at a stage where the acquisition of observational data far exceeds (and will continue to exceed) the development of mature models that describe the very phenomena we see through their light. Recent, nearby SNe (like SN 2011fe and SN 2014J) have enabled astronomers to set strict likelihood limits on progenitor scenarios for these individual events. Likewise, historic, nearby young supernova remnants such as Kepler, Tycho, and SNRs in the LMC have enabled astronomers to put some constraints on the nature of the explosion and the progenitor system (Decourchelle 2017; Vink 2017; Seitenzahl et al. 2019).

While nearby supernovae are rare, they offer an unprecedented opportunity to probe explosion physics which is not possible with the majority of events. High-quality SN Ia spectra obtained during the nebular phase can give valuable and constraining information on SN physics, but as mentioned already (Sect. 2.1) one must be careful when interpreting the observations to draw conclusions about progenitor structure. This is because while no model is flawless, some simulations may not incorporate all the relevant physics required to fully capture intrinsic 3D behaviour (Shingles et al. 2020; Pakmor et al. 2024). Investment in 3D spectral modelling of the nebular phase, ideally arising from different explosion conditions, could be a promising approach toward making stronger connections between observed SN Ia sub-classes and progenitor origin.

Acknowledgements AJR acknowledges financial support from the Australian Research Council under award number FT170100243. This research was supported in part by the National Science Foundation grant PHY-1748958 to the Kavli Institute for Theoretical Physics (KITP). AJR is grateful for helpful discussions with A. Cikota, D. Hamacher, A. Karakas, A. Möller, and R. Pakmor, and thanks the anonymous referees for their comments and suggestions that helped to improve this manuscript. AJR also acknowledges her late PhD supervisor, Chris Belczynski, who helped to foster her interest in studying SN Ia progenitors and actively encouraged her to participate in the first SN Ia meeting of her career in Arcetri, Italy, in 2008. Chris was passionate about life and science, and embraced challenges with great enthusiasm and tenacity.

Conflict of interest The authors declare no competing interests.

References

- Abbott TMC, Allam S, Andersen P, et al. (2019) First Cosmology Results using Type Ia Supernovae from the Dark Energy Survey: Constraints on Cosmological Parameters. *ApJ Lett.* 872(2):L30. <https://doi.org/10.3847/2041-8213/ab04fa>. [arXiv:1811.02374](https://arxiv.org/abs/1811.02374) [astro-ph.CO]
- Abbott TMC, Acevedo M, Aguena M, et al. (2024) The Dark Energy Survey: Cosmology Results with ~ 1500 New High-redshift Type Ia Supernovae Using the Full 5 yr Data Set. *ApJ Lett.* 973(1):L14. <https://doi.org/10.3847/2041-8213/ad6f9f>. [arXiv:2401.02929](https://arxiv.org/abs/2401.02929) [astro-ph.CO]
- Aleo PD, Malanchev K, Sharief S, et al. (2023) The Young Supernova Experiment Data Release 1 (YSE DR1): Light Curves and Photometric Classification of 1975 Supernovae. *ApJS* 266(1):9. <https://doi.org/10.3847/1538-4365/acbfba>. [arXiv:2211.07128](https://arxiv.org/abs/2211.07128) [astro-ph.HE]
- Amaro-Seoane P, Andrews J, Arca Sedda M, et al. (2023) Astrophysics with the Laser Interferometer Space Antenna. *Living Rev Relativ* 26:2. <https://doi.org/10.1007/s41114-022-00041-y>. [arXiv:2203.06016](https://arxiv.org/abs/2203.06016) [gr-qc]
- Aouad CJ, Mazzali PA, Hachinger S, et al. (2022) Abundance stratification in Type Ia supernovae – VI. The peculiar slow decliner SN 1999aa. *MNRAS* 515(3):4445–4463. <https://doi.org/10.1093/mnras/stac2024>. [arXiv:2207.08947](https://arxiv.org/abs/2207.08947) [astro-ph.HE]
- Arnett WD (1969) A possible model of supernovae: Detonation of ^{12}C . *Astrophys. Space Sci.* 5:180–212. <https://doi.org/10.1007/BF00650291>
- Arnett WD (1979) On the theory of Type I supernovae. *ApJ Lett.* 230:L37–L40. <https://doi.org/10.1086/182957>
- Arnett WD (1982) Type I supernovae. I. analytic solutions for the early part of the light curve. *ApJ* 253:785–797. <https://doi.org/10.1086/159681>
- Arnett WD, Truran JW, Woosley SE (1971) Nucleosynthesis in supernova models. II. The ^{12}C detonation model. *ApJ* 165:87–103
- Arunachalam P, Hughes JP, Hovey L, Eriksen K (2022) A Hydro-based MCMC Analysis of SNR 0509-67.5: Revealing the Explosion Properties from Fluid Discontinuities Alone. *ApJ* 938(2):121. <https://doi.org/10.3847/1538-4357/ac927c>. [arXiv:2208.07693](https://arxiv.org/abs/2208.07693) [astro-ph.HE]
- Ashall C, Mazzali PA, Pian E, James PA (2016) Abundance stratification in Type Ia supernovae – V. SN 1986G bridging the gap between normal and subluminous SNe Ia. *MNRAS* 463(2):1891–1906. <https://doi.org/10.1093/mnras/stw2114>. [arXiv:1608.05244](https://arxiv.org/abs/1608.05244) [astro-ph.HE]
- Aznar-Siguán G, García-Berro E, Lorén-Aguilar P, Soker N, Kashi A (2015) Smoothed particle hydrodynamics simulations of the core-degenerate scenario for Type Ia supernovae. *MNRAS* 450(3):2948–2962. <https://doi.org/10.1093/mnras/stv824>. [arXiv:1503.02444](https://arxiv.org/abs/1503.02444) [astro-ph.HE]
- Baade W (1938) The Absolute Photographic Magnitude of Supernovae. *ApJ* 88:285. <https://doi.org/10.1086/143983>

- Baade W, Zwicky F (1934a) On Super-novae. Proceedings of the National Academy of Science 20(5):254–259. <https://doi.org/10.1073/pnas.20.5.254>
- Baade W, Zwicky F (1934b) Remarks on super-novae and cosmic rays. Phys Rev 46:76–77. <https://doi.org/10.1103/PhysRev.46.76.2>
- Badenes C, Maoz D (2012) The merger rate of binary white dwarfs in the galactic disk. ApJ Lett. 749:L11. <https://doi.org/10.1088/2041-8205/749/1/L11>. [arXiv:1202.5472](https://arxiv.org/abs/1202.5472) [astro-ph.SR]
- Bailey AC, Vincenzi M, Scolnic D, et al. (2023) Type Ia supernova observations combining data from the Euclid mission and the Vera C. Rubin Observatory. MNRAS 524(4):5432–5441. <https://doi.org/10.1093/mnras/stad2179>. [arXiv:2211.01206](https://arxiv.org/abs/2211.01206) [astro-ph.CO]
- Baron E, Jeffery DJ, Branch D, et al. (2008) Detailed spectral modeling of a three-dimensional Pulsating Reverse Detonation model: Too much nickel. ApJ 672:1038–1042. <https://doi.org/10.1086/524009>. [arXiv:0709.4177](https://arxiv.org/abs/0709.4177)
- Batalha RM, Dupke RA, Jiménez-Teja Y (2022) Ranking Theoretical Supernovae Explosion Models from Observations of the Intra-cluster Gas. ApJS 262(1):27. <https://doi.org/10.3847/1538-4365/ac7de1>. [arXiv:2207.00601](https://arxiv.org/abs/2207.00601) [astro-ph.HE]
- Belczynski K, Kalogera V, Rasio FA, et al. (2008) Compact object modeling with the startrack population synthesis code. ApJS 174:223–260. <https://doi.org/10.1086/521026>. [arXiv:astro-ph/0511811](https://arxiv.org/abs/astro-ph/0511811)
- Bellm EC, Kulkarni SR, Graham MJ, et al. (2019) The Zwicky Transient Facility: System Overview, Performance, and First Results. PASP 131(995):018002. <https://doi.org/10.1088/1538-3873/aacbe>. [arXiv:1902.01932](https://arxiv.org/abs/1902.01932) [astro-ph.IM]
- Benetti S, Cappellaro E, Mazzali PA, et al. (2005) The diversity of Type Ia supernovae: Evidence for systematics? ApJ 623:1011–1016. <https://doi.org/10.1086/428608>. [arXiv:astro-ph/0411059](https://arxiv.org/abs/astro-ph/0411059)
- Bildsten L, Shen KJ, Weinberg NN, Nelemans G (2007) Faint thermonuclear supernovae from am canum venaticorum binaries. ApJ Lett. 662:L95–L98. <https://doi.org/10.1086/519489>. [arXiv:astro-ph/0703578](https://arxiv.org/abs/astro-ph/0703578)
- Blondin S, Matheson T, Kirshner RP, et al. (2012) The Spectroscopic Diversity of Type Ia Supernovae. AJ 143(5):126. <https://doi.org/10.1088/0004-6256/143/5/126>. [arXiv:1203.4832](https://arxiv.org/abs/1203.4832) [astro-ph.SR]
- Blondin S, Bravo E, Timmes FX, Dessart L, Hillier DJ (2022) Stable nickel production in type Ia supernovae: A smoking gun for the progenitor mass? A&A 660:A96. <https://doi.org/10.1051/0004-6361/202142323>. [arXiv:2109.13840](https://arxiv.org/abs/2109.13840) [astro-ph.SR]
- Bogomazov AI, Tutukov AV (2009) Merging of components in close binaries: Type Ia supernovae, massive white dwarfs, and Ap stars. Astronomy Reports 53(3):214–222. <https://doi.org/10.1134/S1063772909030032>. [arXiv:0901.4899](https://arxiv.org/abs/0901.4899) [astro-ph.SR]
- Boos SJ, Townsley DM, Shen KJ, Caldwell S, Miles BJ (2021) Multidimensional Parameter Study of Double Detonation Type Ia Supernovae Originating from Thin Helium Shell White Dwarfs. ApJ 919(2):126. <https://doi.org/10.3847/1538-4357/ac07a2>. [arXiv:2101.12330](https://arxiv.org/abs/2101.12330) [astro-ph.HE]

- Bora Z, Vinkó J, Könyves-Tóth R (2022) Initial Ni-56 Masses in Type Ia Supernovae. *PASP* 134(1035):054201. <https://doi.org/10.1088/1538-3873/ac63e7>
- Botticella MT, Riello M, Cappellaro E, et al. (2008) Supernova rates from the Southern Intermediate Redshift ESO Supernova Search (STRESS). *A&A* 479(1):49–66. <https://doi.org/10.1051/0004-6361/20078011>. [arXiv:0710.3763](https://arxiv.org/abs/0710.3763) [astro-ph]
- Bours MCP, Toonen S, Nelemans G (2013) Single degenerate supernova type Ia progenitors. studying the influence of different mass retention efficiencies. *A&A* 552:A24. <https://doi.org/10.1051/0004-6361/201220692>
- Brachwitz F, Dean DJ, Hix WR, et al. (2000) The role of electron captures in Chandrasekhar-mass models for type Ia supernovae. *ApJ* 536:934–947. <https://doi.org/10.1086/308968>. [arXiv:astro-ph/0001464](https://arxiv.org/abs/astro-ph/0001464)
- Branch D, Doggett JB, Nomoto K, Thielemann FK (1985) Accreting white dwarf models for the type I supernovae. IV. The optical spectrum of a carbon-deflagration supernova. *ApJ* 294:619–625. <https://doi.org/10.1086/163329>
- Branch D, Fisher A, Nugent P (1993) On the relative frequencies of spectroscopically normal and peculiar type Ia supernovae. *AJ* 106:2383–2391. <https://doi.org/10.1086/116810>
- Branch D, Romanishin W, Baron E (1996) Statistical Connections between the Properties of Type IA Supernovae and the $B - V$ Colors of Their Parent Galaxies, and the Value of H_0 . *ApJ* 465:73–78. <https://doi.org/10.1086/177402>. [arXiv:astro-ph/9510071](https://arxiv.org/abs/astro-ph/9510071)
- Branch D, Dang LC, Hall N, et al. (2006) Comparative direct analysis of Type Ia supernova spectra. II. maximum light. *PASP* 118:560–571. <https://doi.org/10.1086/502778>. [arXiv:astro-ph/0601048](https://arxiv.org/abs/astro-ph/0601048)
- Bravo E, García-Senz D (2006) Beyond the bubble catastrophe of Type Ia supernovae: Pulsating reverse detonation models. *ApJ Lett.* 642:L157–L160. <https://doi.org/10.1086/504713>. [arXiv:astro-ph/0604025](https://arxiv.org/abs/astro-ph/0604025)
- Bravo E, García-Senz D (2009) Pulsating reverse detonation models of type Ia supernovae. i. detonation ignition. *ApJ* 695:1244–1256. <https://doi.org/10.1088/0004-637X/695/2/1244>. [arXiv:0901.3008](https://arxiv.org/abs/0901.3008) [astro-ph.SR]
- Bravo E, García-Senz D, Cabezón RM, Domínguez I (2009) Pulsating Reverse Detonation Models of Type Ia Supernovae. II. Explosion. *ApJ* 695(2):1257–1272. <https://doi.org/10.1088/0004-637X/695/2/1257>. [arXiv:0901.3013](https://arxiv.org/abs/0901.3013) [astro-ph.SR]
- Bravo E, Piersanti L, Blondin S, et al. (2022) Chandrasekhar-mass white dwarfs are the progenitors of a small fraction of Type Ia supernovae according to nucleosynthesis constraints. *MNRAS* 517(1):L31–L35. <https://doi.org/10.1093/mnrasl/slac103>. [arXiv:2209.04020](https://arxiv.org/abs/2209.04020) [astro-ph.SR]
- Broersen S, Chiotellis A, Vink J, Bamba A (2014) The many sides of RCW 86: a Type Ia supernova remnant evolving in its progenitor’s wind bubble. *MNRAS* 441(4):3040–3054. <https://doi.org/10.1093/mnras/stu667>. [arXiv:1404.5434](https://arxiv.org/abs/1404.5434) [astro-ph.HE]
- Brout D, Scolnic D (2021) It’s Dust: Solving the Mysteries of the Intrinsic

- Scatter and Host-galaxy Dependence of Standardized Type Ia Supernova Brightnesses. *ApJ* 909(1):26. <https://doi.org/10.3847/1538-4357/abd69b>. [arXiv:2004.10206](https://arxiv.org/abs/2004.10206) [astro-ph.CO]
- Brown JS, Stanek KZ, Holoiu TWS, et al. (2019) The relative specific Type Ia supernovae rate from three years of ASAS-SN. *MNRAS* 484(3):3785–3796. <https://doi.org/10.1093/mnras/stz258>. [arXiv:1810.00011](https://arxiv.org/abs/1810.00011) [astro-ph.GA]
- Bruenn SW (1971) The Effect of Beta Processes on the Dynamic Evolution of Carbon-Detonation Supernovae. *ApJ* 168:203. <https://doi.org/10.1086/151075>
- Buchler JR, Mazurek TJ, Truran JW (1974) The Afterclap of Degenerative Carbon Ignition. *Comments on Astrophysics and Space Physics* 6:45–55
- Bulla M, Sim SA, Kromer M, et al. (2016a) Predicting polarization signatures for double-detonation and delayed-detonation models of Type Ia supernovae. *MNRAS* 462(1):1039–1056. <https://doi.org/10.1093/mnras/stw1733>. [arXiv:1607.04081](https://arxiv.org/abs/1607.04081) [astro-ph.HE]
- Bulla M, Sim SA, Pakmor R, et al. (2016b) Type Ia supernovae from violent mergers of carbon-oxygen white dwarfs: polarization signatures. *MNRAS* 455(1):1060–1070. <https://doi.org/10.1093/mnras/stv2402>. [arXiv:1510.04128](https://arxiv.org/abs/1510.04128) [astro-ph.HE]
- Bulla M, Liu ZW, Röpke FK, et al. (2020) White dwarf deflagrations for Type Iax supernovae: polarisation signatures from the explosion and companion interaction. *A&A* 635:A179. <https://doi.org/10.1051/0004-6361/201937245>. [arXiv:2002.11134](https://arxiv.org/abs/2002.11134) [astro-ph.HE]
- Burbidge EM, Burbidge GR, Fowler WA, Hoyle F (1957) Synthesis of the elements in stars. *Reviews of Modern Physics* 29:547–650. <https://doi.org/10.1103/RevModPhys.29.547>
- Burmester UP, Ferrario L, Pakmor R, et al. (2023) AREPO white dwarf merger simulations resulting in edge-lit detonation and run-away hypervelocity companion. *MNRAS* 523(1):527–544. <https://doi.org/10.1093/mnras/stad1394>. [arXiv:2305.05192](https://arxiv.org/abs/2305.05192) [astro-ph.SR]
- Byrohl C, Fisher R, Townsley D (2019) The Intrinsic Stochasticity of the ^{56}Ni Distribution of Single-degenerate Near-Chandrasekhar-mass SN Ia. *ApJ* 878(1):67. <https://doi.org/10.3847/1538-4357/ab1f73>. [arXiv:1810.08203](https://arxiv.org/abs/1810.08203) [astro-ph.SR]
- Cameron AGW (1957) Nuclear Reactions in Stars and Nucleogenesis. *PASP* 69(408):201. <https://doi.org/10.1086/127051>
- Cano Z, Selsing J, Hjorth J, et al. (2018) A spectroscopic look at the gravitationally lensed Type Ia supernova 2016geu at $z = 0.409$. *MNRAS* 473(3):4257–4267. <https://doi.org/10.1093/mnras/stx2624>. [arXiv:1708.05534](https://arxiv.org/abs/1708.05534) [astro-ph.HE]
- Cao Y, Kulkarni SR, Howell DA, et al. (2015) A strong ultraviolet pulse from a newborn type Ia supernova. *Nature* 521(7552):328–331. <https://doi.org/10.1038/nature14440>. [arXiv:1505.05158](https://arxiv.org/abs/1505.05158) [astro-ph.SR]
- Cappellaro E, Turatto M, Tsvetkov DY, et al. (1997) The rate of supernovae from the combined sample of five searches. *A&A* 322:431–441. [arXiv:astro-ph/9611191](https://arxiv.org/abs/astro-ph/9611191)

- Cappellaro E, Evans R, Turatto M (1999) A new determination of supernova rates and a comparison with indicators for galactic star formation. *A&A* 351:459–466. [arXiv:astro-ph/9904225](https://arxiv.org/abs/astro-ph/9904225)
- Cappellaro E, Botticella MT, Pignata G, et al. (2015) Supernova rates from the SUDARE VST-OmegaCAM search. I. Rates per unit volume. *A&A* 584:A62. <https://doi.org/10.1051/0004-6361/201526712>. [arXiv:1509.04496](https://arxiv.org/abs/1509.04496) [astro-ph.CO]
- Castrillo A, Ascasibar Y, Galbany L, et al. (2021) The delay time distribution of supernovae from integral-field spectroscopy of nearby galaxies. *MNRAS* 501(3):3122–3136. <https://doi.org/10.1093/mnras/staa3876>. [arXiv:2012.11958](https://arxiv.org/abs/2012.11958) [astro-ph.GA]
- Cescutti G, Matteucci F, Lanfranchi GA, McWilliam A (2008) The chemical evolution of manganese in different stellar systems. *A&A* 491(2):401–405. <https://doi.org/10.1051/0004-6361:200810537>. [arXiv:0807.1463](https://arxiv.org/abs/0807.1463) [astro-ph]
- Chakraborty S, Sadler B, Hoefflich P, et al. (2024) Type Ia Supernova Progenitor Properties and their Host Galaxies. *ApJ* 969(2):80. <https://doi.org/10.3847/1538-4357/ad4702>. [arXiv:2311.03473](https://arxiv.org/abs/2311.03473) [astro-ph.HE]
- Chan HS, Chu Mc, Leung SC, Lin LM (2021) Delayed Detonation Thermonuclear Supernovae with an Extended Dark Matter Component. *ApJ* 914(2):138. <https://doi.org/10.3847/1538-4357/abfd32>. [arXiv:2012.06857](https://arxiv.org/abs/2012.06857) [astro-ph.HE]
- Chan KW, Lingenfelter RE (1993) Positrons from supernovae. *ApJ* 405:614–636. <https://doi.org/10.1086/172393>
- Chandrasekhar S (1931) The maximum mass of ideal white dwarfs. *ApJ* 74:81–82
- Chen X, Hu L, Wang L (2021) Constraining Type Ia Supernova Delay Time with Spatially Resolved Star Formation Histories. *ApJ* 922(1):15. <https://doi.org/10.3847/1538-4357/ac178d>. [arXiv:2101.06242](https://arxiv.org/abs/2101.06242) [astro-ph.GA]
- Chiappini C, Matteucci F, Gratton R (1997) The Chemical Evolution of the Galaxy: The Two-Infall Model. *ApJ* 477(2):765–780. <https://doi.org/10.1086/303726>. [arXiv:astro-ph/9609199](https://arxiv.org/abs/astro-ph/9609199) [astro-ph]
- Chieffi A, Limongi M, Straniero O (1998) The Evolution of a 25 M_{\odot} Star from the Main Sequence up to the Onset of the Iron Core Collapse. *ApJ* 502(2):737–762. <https://doi.org/10.1086/305921>
- Childress M, Aldering G, Antilogus P, et al. (2013) Host Galaxy Properties and Hubble Residuals of Type Ia Supernovae from the Nearby Supernova Factory. *ApJ* 770:108. <https://doi.org/10.1088/0004-637X/770/2/108>. [arXiv:1304.4720](https://arxiv.org/abs/1304.4720)
- Childress MJ, Filippenko AV, Ganeshalingam M, Schmidt BP (2014) High-velocity features in Type Ia supernova spectra. *MNRAS* 437(1):338–350. <https://doi.org/10.1093/mnras/stt1892>. [arXiv:1307.0563](https://arxiv.org/abs/1307.0563) [astro-ph.CO]
- Childress MJ, Hillier DJ, Seitzzahl I, et al. (2015) Measuring nickel masses in Type Ia supernovae using cobalt emission in nebular phase spectra. *MNRAS* 454(4):3816–3842. <https://doi.org/10.1093/mnras/stv2173>. [arXiv:1507.02501](https://arxiv.org/abs/1507.02501) [astro-ph.HE]
- Chomiuk L, Soderberg AM, Chevalier RA, et al. (2016) A Deep Search for

- Prompt Radio Emission from Thermonuclear Supernovae with the Very Large Array. *ApJ* 821(2):119. <https://doi.org/10.3847/0004-637X/821/2/119>. [arXiv:1510.07662](https://arxiv.org/abs/1510.07662) [astro-ph.HE]
- Ciaraldi-Schoolmann F, Seitenzahl IR, Röpke FK (2013) A subgrid-scale model for deflagration-to-detonation transitions in Type Ia supernova explosion simulations. Numerical implementation. *A&A* 559:A117. <https://doi.org/10.1051/0004-6361/201321480>. [arXiv:1307.8146](https://arxiv.org/abs/1307.8146) [astro-ph.SR]
- Cikota A, Patat F, Wang L, et al. (2019) Linear spectropolarimetry of 35 Type Ia supernovae with VLT/FORS: an analysis of the Si II line polarization. *MNRAS* 490(1):578–599. <https://doi.org/10.1093/mnras/stz2322>. [arXiv:1908.07526](https://arxiv.org/abs/1908.07526) [astro-ph.HE]
- Cikota A, Bertolla IT, Huang X, et al. (2023) DESI-253.2534+26.8843: A New Einstein Cross Spectroscopically Confirmed with Very Large Telescope/MUSE and Modeled with GIGA-Lens. *ApJ Lett.* 953(1):L5. <https://doi.org/10.3847/2041-8213/ace9da>. [arXiv:2307.12470](https://arxiv.org/abs/2307.12470) [astro-ph.GA]
- Cinquegrana GC, Joyce M, Karakas AI (2023) Bridging the gap between intermediate and massive stars II: M_{mas} for the most metal-rich stars and implications for Fe CCSNe rates. *MNRAS* 525(3):3216–3235. <https://doi.org/10.1093/mnras/stad2461>. [arXiv:2308.06002](https://arxiv.org/abs/2308.06002) [astro-ph.SR]
- Claeys JSW, Pols OR, Izzard RG, Vink J, Verbunt FWM (2014) Theoretical uncertainties of the Type Ia supernova rate. *A&A* 563:A83. <https://doi.org/10.1051/0004-6361/201322714>. [arXiv:1401.2895](https://arxiv.org/abs/1401.2895) [astro-ph.SR]
- Clark P, Maguire K, Bulla M, et al. (2021) Probing the progenitors of Type Ia supernovae using circumstellar material interaction signatures. *MNRAS* 507(3):4367–4388. <https://doi.org/10.1093/mnras/stab2038>. [arXiv:2107.09034](https://arxiv.org/abs/2107.09034) [astro-ph.HE]
- Clayton DD (1968) Principles of stellar evolution and nucleosynthesis. University of Chicago Press
- Clayton DD (1999) Radiogenic iron. *Meteorit Planet Sci* 34(S4):A145–A160. <https://doi.org/10.1111/j.1945-5100.1999.tb01760.x>
- Clifford FE, Tayler RJ (1965) The equilibrium distribution of nuclides in matter at high temperatures. *Mem. RAS* 69:21
- Colgate SA, McKee C (1969) Early supernova luminosity. *ApJ* 157:623–643
- Collins CE, Gronow S, Sim SA, Röpke FK (2022) Double detonations: variations in Type Ia supernovae due to different core and He shell masses – II. Synthetic observables. *MNRAS* 517(4):5289–5302. <https://doi.org/10.1093/mnras/stac2665>. [arXiv:2209.04305](https://arxiv.org/abs/2209.04305) [astro-ph.SR]
- Dahlen T, Strolger LG, Riess AG, et al. (2004) High-Redshift Supernova Rates. *ApJ* 613(1):189–199. <https://doi.org/10.1086/422899>. [arXiv:astro-ph/0406547](https://arxiv.org/abs/astro-ph/0406547) [astro-ph]
- Dan M, Rosswog S, Brüggen M, Podsiadlowski P (2014) The structure and fate of white dwarf merger remnants. *MNRAS* 438:14–34. <https://doi.org/10.1093/mnras/stt1766>. [arXiv:1308.1667](https://arxiv.org/abs/1308.1667) [astro-ph.HE]
- Dan M, Guillochon J, Brüggen M, Ramirez-Ruiz E, Rosswog S (2015) Thermonuclear detonations ensuing white dwarf mergers. *MNRAS* 454:4411–4428. <https://doi.org/10.1093/mnras/stv2289>. [arXiv:1508.02402](https://arxiv.org/abs/1508.02402) [astro-

- ph.HE]
- Darbha S, Metzger BD, Quataert E, et al. (2010) Nickel-rich outflows produced by the accretion-induced collapse of white dwarfs: light curves and spectra. *MNRAS* p 1254. <https://doi.org/10.1111/j.1365-2966.2010.17353.x>. [arXiv:1005.1081](https://arxiv.org/abs/1005.1081) [astro-ph.HE]
- De K, Kasliwal MM, Polin A, et al. (2019) ZTF 18aaqesu (SN2018byg): A Massive Helium-shell Double Detonation on a Sub-Chandrasekhar-mass White Dwarf. *ApJ Lett.* 873(2):L18. <https://doi.org/10.3847/2041-8213/ab0aec>. [arXiv:1901.00874](https://arxiv.org/abs/1901.00874) [astro-ph.HE]
- De K, Kasliwal MM, Tzanidakis A, et al. (2020) The Zwicky Transient Facility Census of the Local Universe. I. Systematic Search for Calcium-rich Gap Transients Reveals Three Related Spectroscopic Subclasses. *ApJ* 905(1):58. <https://doi.org/10.3847/1538-4357/abb45c>. [arXiv:2004.09029](https://arxiv.org/abs/2004.09029) [astro-ph.HE]
- De Donder E, Vanbeveren D (2004) The influence of binaries on galactic chemical evolution. *New Astronomy Reviews* 48:861–975. <https://doi.org/10.1016/j.newar.2004.07.001>. [arXiv:astro-ph/0410024](https://arxiv.org/abs/astro-ph/0410024)
- de los Reyes MAC, Kirby EN, Seitzzahl IR, Shen KJ (2020) Manganese Indicates a Transition from Sub- to Near-Chandrasekhar Type Ia Supernovae in Dwarf Galaxies. *ApJ* 891(1):85. <https://doi.org/10.3847/1538-4357/ab736f>. [arXiv:2001.01716](https://arxiv.org/abs/2001.01716) [astro-ph.SR]
- de los Reyes MAC, Kirby EN, Ji AP, Nuñez EH (2022) Simultaneous Constraints on the Star Formation History and Nucleosynthesis of Sculptor dSph. *ApJ* 925(1):66. <https://doi.org/10.3847/1538-4357/ac332b>. [arXiv:2110.01690](https://arxiv.org/abs/2110.01690) [astro-ph.GA]
- de Vaucouleurs G, Corwin J H G (1985) S Andromedae 1885: A Centennial Review. *ApJ* 295:287. <https://doi.org/10.1086/163374>
- Deckers M, Maguire K, Magee MR, et al. (2022) Constraining Type Ia supernova explosions and early flux excesses with the Zwicky Transient Factory. *MNRAS* 512(1):1317–1340. <https://doi.org/10.1093/mnras/stac558>. [arXiv:2202.12914](https://arxiv.org/abs/2202.12914) [astro-ph.HE]
- Deckers M, Graur O, Maguire K, et al. (2023) Photometric study of the late-time near-infrared plateau in Type Ia supernovae. *MNRAS* 521(3):4414–4430. <https://doi.org/10.1093/mnras/stad841>. [arXiv:2303.09548](https://arxiv.org/abs/2303.09548) [astro-ph.HE]
- Decourchelle A (2017) Supernova of 1572, Tycho’s Supernova. In: Alsabti AW, Murdin P (eds) *Handbook of Supernovae*. Springer, p 117. https://doi.org/10.1007/978-3-319-21846-5_48
- Deibel A, Caplan ME, Horowitz CJ (2022) Nuclear fission reaction simulations in compact stars. *Phys. Rev. C* 106(4):045803. <https://doi.org/10.1103/PhysRevC.106.045803>. [arXiv:2109.14714](https://arxiv.org/abs/2109.14714) [astro-ph.SR]
- Denissenkov PA, Herwig F, Truran JW, Paxton B (2013) The C-flame Quenching by Convective Boundary Mixing in Super-AGB Stars and the Formation of Hybrid C/O/Ne White Dwarfs and SN Progenitors. *ApJ* 772(1):37. <https://doi.org/10.1088/0004-637X/772/1/37>. [arXiv:1305.2649](https://arxiv.org/abs/1305.2649) [astro-ph.SR]
- Dessart L, Hillier DJ (2015) One-dimensional non-LTE time-dependent radia-

- tive transfer of an He-detonation model and the connection to faint and fast-decaying supernovae. *MNRAS* 447(2):1370–1382. <https://doi.org/10.1093/mnras/stu2520>. [arXiv:1411.7397](https://arxiv.org/abs/1411.7397) [astro-ph.SR]
- Dessart L, Burrows A, Ott CD, et al. (2006) Multidimensional Simulations of the Accretion-induced Collapse of White Dwarfs to Neutron Stars. *ApJ* 644:1063–1084. <https://doi.org/10.1086/503626>. [astro-ph/0601603](https://arxiv.org/abs/astro-ph/0601603)
- Dessart L, Blondin S, Hillier DJ, Khokhlov A (2014) Constraints on the explosion mechanism and progenitors of Type Ia supernovae. *MNRAS* 441(1):532–550. <https://doi.org/10.1093/mnras/stu598>. [arXiv:1310.7747](https://arxiv.org/abs/1310.7747) [astro-ph.SR]
- Dettman KG, Jha SW, Dai M, et al. (2021) The Foundation Supernova Survey: Photospheric Velocity Correlations in Type Ia Supernovae. *ApJ* 923(2):267. <https://doi.org/10.3847/1538-4357/ac2ee5>. [arXiv:2102.06524](https://arxiv.org/abs/2102.06524) [astro-ph.HE]
- Di Stefano R, Voss R, Claeys JSW (2011) Spin-up/Spin-down Models for Type Ia Supernovae. *ApJ Lett.* 738(1):L1. <https://doi.org/10.1088/2041-8205/738/1/L1>. [arXiv:1102.4342](https://arxiv.org/abs/1102.4342) [astro-ph.HE]
- Dilday B, Howell DA, Cenko SB, et al. (2012) PTF 11kx: A Type Ia Supernova with a Symbiotic Nova Progenitor. *Science* 337(6097):942. <https://doi.org/10.1126/science.1219164>. [arXiv:1207.1306](https://arxiv.org/abs/1207.1306) [astro-ph.CO]
- Dimitriadis G, Maguire K, Karambelkar VR, et al. (2023) SN 2021zny: an early flux excess combined with late-time oxygen emission suggests a double white dwarf merger event. *MNRAS* 521(1):1162–1183. <https://doi.org/10.1093/mnras/stad536>. [arXiv:2302.08228](https://arxiv.org/abs/2302.08228) [astro-ph.HE]
- Do A, Shappee BJ, De Cuyper JP, et al. (2021) Blast from the past: constraining progenitor models of SN 1972E. *MNRAS* 508(3):3649–3662. <https://doi.org/10.1093/mnras/stab2660>. [arXiv:2102.07796](https://arxiv.org/abs/2102.07796) [astro-ph.HE]
- Doherty CL, Gil-Pons P, Siess L, Lattanzio JC (2017) Super-AGB Stars and their Role as Electron Capture Supernova Progenitors. *PASA* 34:e056. <https://doi.org/10.1017/pasa.2017.52>. [arXiv:1703.06895](https://arxiv.org/abs/1703.06895) [astro-ph.SR]
- Dong S, Katz B, Kushnir D, Prieto JL (2015) Type Ia supernovae with bimodal explosions are common - possible smoking gun for direct collisions of white dwarfs. *MNRAS* 454:L61–L65. <https://doi.org/10.1093/mnrasl/slv129>. [arXiv:1401.3347](https://arxiv.org/abs/1401.3347) [astro-ph.HE]
- Dubay LO, Johnson JA, Johnson JW (2024) Galactic Chemical Evolution Models Favor an Extended Type Ia Supernova Delay-time Distribution. *ApJ* 973(1):55. <https://doi.org/10.3847/1538-4357/ad61df>. [arXiv:2404.08059](https://arxiv.org/abs/2404.08059) [astro-ph.GA]
- Eggleton PP (1983) Approximations to the radii of Roche lobes. *ApJ* 268:368. <https://doi.org/10.1086/160960>
- Einstein A (1917) Kosmologische Betrachtungen zur allgemeinen Relativitätstheorie. *Sitzungsber K Preuss Akad Wiss* pp 142–152
- Eitner P, Bergemann M, Hansen CJ, et al. (2020) Observational constraints on the origin of the elements. III. Evidence for the dominant role of sub-Chandrasekhar SN Ia in the chemical evolution of Mn and Fe in the Galaxy. *A&A* 635:A38. <https://doi.org/10.1051/0004-6361/201936603>. [arXiv:2003.01721](https://arxiv.org/abs/2003.01721) [astro-ph.GA]

- Eitner P, Bergemann M, Ruiter AJ, et al. (2023) Observational constraints on the origin of the elements. V. NLTE abundance ratios of [Ni/Fe] in Galactic stars and enrichment by sub-Chandrasekhar mass supernovae. *A&A* 677:A151. <https://doi.org/10.1051/0004-6361/202244286>. arXiv:2206.10258 [astro-ph.GA]
- El-Badry K, Shen KJ, Chandra V, et al. (2023) The fastest stars in the Galaxy. *The Open Journal of Astrophysics* 6:28. <https://doi.org/10.21105/astro.2306.03914>. arXiv:2306.03914 [astro-ph.SR]
- Fausnaugh MM, Vallely PJ, Tucker MA, et al. (2023) Four Years of Type Ia Supernovae Observed by TESS: Early-time Light-curve Shapes and Constraints on Companion Interaction Models. *ApJ* 956(2):108. <https://doi.org/10.3847/1538-4357/aceaf>. arXiv:2307.11815 [astro-ph.HE]
- Fesen RA, Schaefer BE, Patchick D (2023) Discovery of an Exceptional Optical Nebulosity in the Suspected Galactic SN Iax Remnant Pa 30 Linked to the Historical Guest Star of 1181 CE. *ApJ Lett.* 945(1):L4. <https://doi.org/10.3847/2041-8213/acbb67>. arXiv:2301.04809 [astro-ph.HE]
- Filippenko AV (1997) Optical spectra of supernovae. *ARA&A* 35:309–355. <https://doi.org/10.1146/annurev.astro.35.1.309>
- Fink M, Hillebrandt W, Röpke FK (2007) Double-detonation supernovae of sub-Chandrasekhar mass white dwarfs. *A&A* 476:1133–1143. <https://doi.org/10.1051/0004-6361:20078438>. arXiv:0710.5486
- Fink M, Röpke FK, Hillebrandt W, et al. (2010) Double-detonation sub-Chandrasekhar supernovae: can minimum helium shell masses detonate the core? *A&A* 514:A53. <https://doi.org/10.1051/0004-6361/200913892>
- Fink M, Kromer M, Seitenzahl IR, et al. (2014) Three-dimensional pure deflagration models with nucleosynthesis and synthetic observables for Type Ia supernovae. *MNRAS* 438(2):1762–1783. <https://doi.org/10.1093/mnras/stt2315>. arXiv:1308.3257 [astro-ph.SR]
- Fink M, Kromer M, Hillebrandt W, et al. (2018) Thermonuclear explosions of rapidly differentially rotating white dwarfs: Candidates for superluminous Type Ia supernovae? *A&A* 618:A124. <https://doi.org/10.1051/0004-6361/201833475>. arXiv:1807.10199 [astro-ph.HE]
- Finoguenov A, Ponman TJ (1999) Constraining the role of Type IA and Type II supernovae in galaxy groups by spatially resolved analysis of ROSAT and ASCA observations. *MNRAS* 305(2):325–337. <https://doi.org/10.1046/j.1365-8711.1999.02403.x>. arXiv:astro-ph/9901100 [astro-ph]
- Finzi A, Wolf RA (1967) Type I Supernovae. *ApJ* 150:115. <https://doi.org/10.1086/149317>
- Fisher R, Jumper K (2015) Single-degenerate Type Ia Supernovae Are Preferentially Overluminous. *ApJ* 805(2):150. <https://doi.org/10.1088/0004-637X/805/2/150>. arXiv:1504.00014 [astro-ph.SR]
- Fisher R, Mozumdar P, Casabona G (2019) Carbon Detonation Initiation in Turbulent Electron-degenerate Matter. *ApJ* 876(1):64. <https://doi.org/10.3847/1538-4357/ab15d8>. arXiv:1807.03786 [astro-ph.SR]
- Foley RJ, McCully C, Jha SW, et al. (2014) Possible Detection of the Stellar Donor or Remnant for the Type Iax Supernova 2008ha. *ApJ*

- 792(1):29. <https://doi.org/10.1088/0004-637X/792/1/29>. arXiv:1408.1091 [astro-ph.HE]
- Forcada R, Garcia-Senz D, José J (2006) Single point off-center helium ignitions as origin of some Type Ia supernovae. In: International Symposium on Nuclear Astrophysics - Nuclei in the Cosmos IX. Proc. Sci., vol PoS(NIC-IX). <https://doi.org/10.22323/1.028.0096>
- Fransson C, Jerkstrand A (2015) Reconciling the Infrared Catastrophe and Observations of SN 2011fe. *ApJ Lett.* 814(1):L2. <https://doi.org/10.1088/2041-8205/814/1/L2>. arXiv:1511.00245 [astro-ph.SR]
- Fransson C, Kozma C (1993) The freeze-out phase of sn 1987a - implications for the light curve. *ApJ Lett.* 408:L25–L28. <https://doi.org/10.1086/186822>
- Freundlich J, Maoz D (2021) The delay time distribution of Type-Ia supernovae in galaxy clusters: the impact of extended star-formation histories. *MNRAS* 502(4):5882–5895. <https://doi.org/10.1093/mnras/stab493>. arXiv:2012.00793 [astro-ph.GA]
- Friedmann M, Maoz D (2018) The rate of Type-Ia supernovae in galaxy clusters and the delay-time distribution out to redshift 1.75. *MNRAS* 479(3):3563–3581. <https://doi.org/10.1093/mnras/sty1664>. arXiv:1803.04421 [astro-ph.GA]
- Frieman JA, Turner MS, Huterer D (2008) Dark energy and the accelerating universe. *ARA&A* 46:385–432. <https://doi.org/10.1146/annurev.astro.46.060407.145243>. arXiv:0803.0982 [astro-ph]
- Frohmaier C, Sullivan M, Maguire K, Nugent P (2018) The Volumetric Rate of Calcium-rich Transients in the Local Universe. *ApJ* 858(1):50. <https://doi.org/10.3847/1538-4357/aabc0b>. arXiv:1804.03103 [astro-ph.HE]
- Fryer CL, Belczynski K, Wiktorowicz G, et al. (2012) Compact Remnant Mass Function: Dependence on the Explosion Mechanism and Metallicity. *ApJ* 749:91. <https://doi.org/10.1088/0004-637X/749/1/91>. arXiv:1110.1726 [astro-ph.SR]
- Fukushima K, Kobayashi SB, Matsushita K (2022) Chemical enrichment in the cool core of the Centaurus cluster of galaxies. *MNRAS* 514(3):4222–4238. <https://doi.org/10.1093/mnras/stac1590>. arXiv:2206.03749 [astro-ph.GA]
- Gaia Collaboration, Brown AGA, Vallenari A, et al. (2018) Gaia Data Release 2. Summary of the contents and survey properties. *A&A* 616:A1. <https://doi.org/10.1051/0004-6361/201833051>. arXiv:1804.09365 [astro-ph.GA]
- Gal-Yam A (2017) Observational and Physical Classification of Supernovae. In: Alsabti AW, Murdin P (eds) *Handbook of Supernovae*. Springer, Cham, p 195. https://doi.org/10.1007/978-3-319-21846-5_35
- Gal-Yam A, Mazzali PA, Manulis I, Bishop D (2013) Supernova Discoveries 2010-2011: Statistics and Trends. *PASP* 125(929):749. <https://doi.org/10.1086/671483>. arXiv:1103.5165 [astro-ph.CO]
- Gamezo VN, Khokhlov AM, Oran ES, Chtchelkanova AY, Rosenberg RO (2003) Thermonuclear supernovae: Simulations of the deflagration stage and their implications. *Science* 299:77–81. <https://doi.org/10.1126/science.1078129>. arXiv:astro-ph/0212054
- Gamezo VN, Khokhlov AM, Oran ES (2004) Deflagrations and detonations in

- thermonuclear supernovae. *Phys Rev Lett* 92(21):211102. <https://doi.org/10.1103/PhysRevLett.92.211102>. [arXiv:astro-ph/0406101](https://arxiv.org/abs/astro-ph/0406101)
- Gamezo VN, Khokhlov AM, Oran ES (2005) Three-dimensional delayed-detonation model of Type Ia supernovae. *ApJ* 623:337–346. <https://doi.org/10.1086/428767>. [arXiv:astro-ph/0409598](https://arxiv.org/abs/astro-ph/0409598)
- García-Senz D, Woosley SE (1995) Type Ia supernovae: The flame is born. *ApJ* 454:895–900. <https://doi.org/10.1086/176542>
- García-Senz D, Bravo E, Woosley SE (1999) Single and multiple detonations in white dwarfs. *A&A* 349:177–188
- Garnavich PM, Bonanos AZ, Krisciunas K, et al. (2004) The Luminosity of SN 1999by in NGC 2841 and the Nature of “Peculiar” Type Ia Supernovae. *ApJ* 613:1120–1132. <https://doi.org/10.1086/422986>. [arXiv:astro-ph/0105490](https://arxiv.org/abs/astro-ph/0105490)
- Gasques LR, Afanasjev AV, Aguilera EF, et al. (2005) Nuclear fusion in dense matter: Reaction rate and carbon burning. *Phys. Rev. C* 72(2):025806. <https://doi.org/10.1103/PhysRevC.72.025806>. [arXiv:astro-ph/0506386](https://arxiv.org/abs/astro-ph/0506386)
- Gilfanov M, Bogdán Á (2010) An upper limit on the contribution of accreting white dwarfs to the type Ia supernova rate. *Nature* 463:924–925. <https://doi.org/10.1038/nature08685>. [arXiv:1002.3359](https://arxiv.org/abs/1002.3359)
- Giodini S, Pierini D, Finoguenov A, et al. (2009) Stellar and Total Baryon Mass Fractions in Groups and Clusters Since Redshift 1. *ApJ* 703(1):982–993. <https://doi.org/10.1088/0004-637X/703/1/982>. [arXiv:0904.0448](https://arxiv.org/abs/0904.0448) [astro-ph.CO]
- Glasner SA, Livne E, Steinberg E, Yalinewich A, Truran JW (2018) Ignition of detonation in accreted helium envelopes. *MNRAS* 476(2):2238–2248. <https://doi.org/10.1093/mnras/sty421>
- Golubchik M, Zitrin A, Pierel J, et al. (2023) A search for transients in the Reionization Lensing Cluster Survey (RELICS): Three new supernovae. *MNRAS* <https://doi.org/10.1093/mnras/stad1238>. [arXiv:2302.11158](https://arxiv.org/abs/2302.11158) [astro-ph.GA]
- Goobar A, Amanullah R, Kulkarni SR, et al. (2017) iPTF16geu: A multiply imaged, gravitationally lensed type Ia supernova. *Science* 356(6335):291–295. <https://doi.org/10.1126/science.aal2729>. [arXiv:1611.00014](https://arxiv.org/abs/1611.00014) [astro-ph.CO]
- Goobar A, Johansson J, Schulze S, et al. (2023) Uncovering a population of gravitational lens galaxies with magnified standard candle SN Zwicky. *Nature Astronomy* 7:1098–1107. <https://doi.org/10.1038/s41550-023-01981-3>. [arXiv:2211.00656](https://arxiv.org/abs/2211.00656) [astro-ph.CO]
- Graham ML, Harris CE, Fox OD, et al. (2017) PTF11kx: A Type Ia Supernova with Hydrogen Emission Persisting after 3.5 Years. *ApJ* 843(2):102. <https://doi.org/10.3847/1538-4357/aa78ee>. [arXiv:1706.02266](https://arxiv.org/abs/1706.02266) [astro-ph.HE]
- Graur O (2024) Underluminous 1991bg-like Type Ia supernovae are standardizable candles. *MNRAS* 530(4):4950–4960. <https://doi.org/10.1093/mnras/stae949>. [arXiv:2311.16245](https://arxiv.org/abs/2311.16245) [astro-ph.HE]
- Graur O, Maoz D (2013) Discovery of 90 type Ia supernovae among 700 000 sloan spectra: the type Ia supernova rate versus galaxy mass and star formation rate at redshift ~ 0.1 . *MNRAS* 430:1746–1763. <https://doi.org/10.1093/mnras/sts718>. [arXiv:1209.0008](https://arxiv.org/abs/1209.0008) [astro-ph.CO]

- Graur O, Woods TE (2019) Progenitor constraints on the Type Ia supernova SN 2014J from Hubble Space Telescope H β and [O III] observations. *MNRAS* 484(1):L79–L84. <https://doi.org/10.1093/mnras/slz005>. [arXiv:1811.04944](https://arxiv.org/abs/1811.04944) [astro-ph.HE]
- Graur O, Poznanski D, Maoz D, et al. (2011) Supernovae in the Subaru deep field: the rate and delay-time distribution of type Ia supernovae out to redshift 2. *MNRAS* 417:916–940. <https://doi.org/10.1111/j.1365-2966.2011.19287.x>. [arXiv:1102.0005](https://arxiv.org/abs/1102.0005) [astro-ph.CO]
- Graur O, Maoz D, Shara MM (2014a) Progenitor constraints on the Type-Ia supernova SN2011fe from pre-explosion Hubble Space Telescope HeII narrow-band observations. *MNRAS* 442:L28–L32. <https://doi.org/10.1093/mnras/flu052>. [arXiv:1403.1878](https://arxiv.org/abs/1403.1878) [astro-ph.GA]
- Graur O, Rodney SA, Maoz D, et al. (2014b) Type-Ia Supernova Rates to Redshift 2.4 from CLASH: The Cluster Lensing And Supernova Survey with Hubble. *ApJ* 783(1):28. <https://doi.org/10.1088/0004-637X/783/1/28>. [arXiv:1310.3495](https://arxiv.org/abs/1310.3495) [astro-ph.CO]
- Graur O, Bianco FB, Modjaz M (2015) A unified explanation for the supernova rate-galaxy mass dependence based on supernovae detected in Sloan galaxy spectra. *MNRAS* 450(1):905–925. <https://doi.org/10.1093/mnras/stv713>. [arXiv:1412.7991](https://arxiv.org/abs/1412.7991) [astro-ph.HE]
- Graur O, Zurek D, Shara MM, et al. (2016) Late-time Photometry of Type Ia Supernova SN 2012cg Reveals the Radioactive Decay of ^{57}Co . *ApJ* 819:31. <https://doi.org/10.3847/0004-637X/819/1/31>. [arXiv:1505.00777](https://arxiv.org/abs/1505.00777) [astro-ph.HE]
- Graur O, Bianco FB, Modjaz M, et al. (2017) LOSS Revisited. II. The Relative Rates of Different Types of Supernovae Vary between Low- and High-mass Galaxies. *ApJ* 837(2):121. <https://doi.org/10.3847/1538-4357/aa5eb7>. [arXiv:1609.02923](https://arxiv.org/abs/1609.02923) [astro-ph.HE]
- Graur O, Maguire K, Ryan R, et al. (2020) A year-long plateau in the late-time near-infrared light curves of type Ia supernovae. *Nature Astronomy* 4:188–195. <https://doi.org/10.1038/s41550-019-0901-1>. [arXiv:1910.03614](https://arxiv.org/abs/1910.03614) [astro-ph.HE]
- Graur O, Padilla Gonzalez E, Burke J, et al. (2023) No plateau observed in late-time near-infrared observations of the underluminous Type Ia supernova 2021qvv. *MNRAS* 526(2):2977–2990. <https://doi.org/10.1093/mnras/stad2960>. [arXiv:2306.12858](https://arxiv.org/abs/2306.12858) [astro-ph.HE]
- Grayling M, Thorp S, Mandel KS, et al. (2024) Scalable hierarchical BayeSN inference: investigating dependence of SN Ia host galaxy dust properties on stellar mass and redshift. *MNRAS* 531(1):953–976. <https://doi.org/10.1093/mnras/stae1202>. [arXiv:2401.08755](https://arxiv.org/abs/2401.08755) [astro-ph.CO]
- Green M (2019) The Evolution of AM CVn Binary Systems. PhD thesis, University of Warwick, UK
- Greggio L (2005) The rates of type Ia supernovae. I. Analytical formulations. *A&A* 441(3):1055–1078. <https://doi.org/10.1051/0004-6361:20052926>. [arXiv:astro-ph/0504376](https://arxiv.org/abs/astro-ph/0504376) [astro-ph]
- Gronow S, Collins C, Ohlmann ST, et al. (2020) SNe Ia from double detona-

- tions: Impact of core-shell mixing on the carbon ignition mechanism. *A&A* 635:A169. <https://doi.org/10.1051/0004-6361/201936494>. [arXiv:2002.00981](https://arxiv.org/abs/2002.00981) [astro-ph.SR]
- Gronow S, Collins CE, Sim SA, Röpke FK (2021) Double detonations of sub- M_{Ch} CO white dwarfs: variations in Type Ia supernovae due to different core and He shell masses. *A&A* 649:A155. <https://doi.org/10.1051/0004-6361/202039954>. [arXiv:2102.06719](https://arxiv.org/abs/2102.06719) [astro-ph.SR]
- Guerrero J, García-Berro E, Isern J (2004) Smoothed Particle Hydrodynamics simulations of merging white dwarfs. *A&A* 413:257–272. <https://doi.org/10.1051/0004-6361:20031504>
- Guillochon J, Dan M, Ramirez-Ruiz E, Rosswog S (2010) Surface detonations in double degenerate binary systems triggered by accretion stream instabilities. *ApJ Lett.* 709:L64–L69. <https://doi.org/10.1088/2041-8205/709/1/L64>. [arXiv:0911.0416](https://arxiv.org/abs/0911.0416)
- Guy J, Sullivan M, Conley A, et al. (2010) The Supernova Legacy Survey 3-year sample: Type Ia supernovae photometric distances and cosmological constraints. *A&A* 523:A7. <https://doi.org/10.1051/0004-6361/201014468>. [arXiv:1010.4743](https://arxiv.org/abs/1010.4743) [astro-ph.CO]
- Hachinger S, Mazzali PA, Taubenberger S, et al. (2012) Spectral modelling of the ‘super-Chandrasekhar’ Type Ia SN 2009dc - testing a $2 M_{\odot}$ white dwarf explosion model and alternatives. *MNRAS* 427(3):2057–2078. <https://doi.org/10.1111/j.1365-2966.2012.22068.x>. [arXiv:1209.1339](https://arxiv.org/abs/1209.1339) [astro-ph.SR]
- Hachinger S, Mazzali PA, Sullivan M, et al. (2013) The UV/optical spectra of the Type Ia supernova SN 2010jn: a bright supernova with outer layers rich in iron-group elements. *MNRAS* 429(3):2228–2248. <https://doi.org/10.1093/mnras/sts492>. [arXiv:1208.1267](https://arxiv.org/abs/1208.1267) [astro-ph.SR]
- Hachinger S, Röpke FK, Mazzali PA, et al. (2017) Type Ia supernovae with and without blueshifted narrow Na I D lines - how different is their structure? *MNRAS* 471(1):491–506. <https://doi.org/10.1093/mnras/stx1578>. [arXiv:1707.00700](https://arxiv.org/abs/1707.00700) [astro-ph.SR]
- Hachisu I, Kato M (2012) A Extremely Massive White Dwarf of the Symbiotic Classical Nova V407 Cyg as Suggested by the RS Oph and U Sco Models. *Baltic Astronomy* 21:68–75. <https://doi.org/10.1515/astro-2017-0360>
- Hakobyan AA, Barkhudaryan LV, Karapetyan AG, et al. (2020) Supernovae and their host galaxies - VII. The diversity of Type Ia supernova progenitors. *MNRAS* 499(1):1424–1440. <https://doi.org/10.1093/mnras/staa2940>. [arXiv:2009.02135](https://arxiv.org/abs/2009.02135) [astro-ph.GA]
- Hamacher D, Garcia B, Gangui A, et al. (2022) IAU Working Group for Ethnoastronomy & Intangible Heritage: Triennial Report, 2018-2021. *Journal of Astronomical History and Heritage* 25(2):318–321
- Hamacher DW (2014) Are supernovae recorded in indigenous astronomical traditions? *J Astron History Heritage* 17(2):161–170. <https://doi.org/10.48550/arXiv.1404.3253>. [arXiv:1404.3253](https://arxiv.org/abs/1404.3253) [physics.hist-ph]
- Hamers AS, Perets HB, Thompson TA, Neunteufel P (2022) Return of the TEDI: Revisiting the Triple Evolution Dynamical Instability Channel in Triple Stars. *ApJ* 925(2):178. <https://doi.org/10.3847/1538-4357/ac400b>.

- [arXiv:2107.13620](#) [astro-ph.SR]
- Hamuy M, Pinto PA (2002) Type II Supernovae as Standardized Candles. *ApJ Lett.* 566(2):L63–L65. <https://doi.org/10.1086/339676>. [arXiv:astro-ph/0201279](#) [astro-ph]
- Hamuy M, Phillips MM, Maza J, et al. (1995) A hubble diagram of distant type ia supernovae. *AJ* 109:1–13. <https://doi.org/10.1086/117251>
- Hamuy M, Phillips MM, Suntzeff NB, et al. (1996) The Morphology of Type IA Supernovae Light Curves. *AJ* 112:2438. <https://doi.org/10.1086/118193>. [arXiv:astro-ph/9609063](#) [astro-ph]
- Hamuy M, Trager SC, Pinto PA, et al. (2000) A Search for Environmental Effects on Type IA Supernovae. *AJ* 120(3):1479–1486. <https://doi.org/10.1086/301527>. [arXiv:astro-ph/0005213](#) [astro-ph]
- Han Z, Podsiadlowski P (2004) The single-degenerate channel for the progenitors of Type Ia supernovae. *MNRAS* 350:1301–1309. <https://doi.org/10.1111/j.1365-2966.2004.07713.x>. [arXiv:astro-ph/0309618](#)
- Han Z, Podsiadlowski P, Eggleton PP (1995) The formation of bipolar planetary nebulae and close white dwarf binaries. *MNRAS* 272(4):800–820. <https://doi.org/10.1093/mnras/272.4.800>
- Han ZW, Ge HW, Chen XF, Chen HL (2020) Binary Population Synthesis. *Res Astron Astrophys* 20(10):161. <https://doi.org/10.1088/1674-4527/20/10/161>. [arXiv:2009.08611](#) [astro-ph.SR]
- Hansen CJ, Wheeler JC (1969) A Calculation of a White Dwarf Supernova. *Astrophys. Space Sci.* 3(3):464–474. <https://doi.org/10.1007/BF00653366>
- Hashimoto MA, Hanawa T, Sugimoto D (1983) Explosive helium burning at constant pressures. *PASJ* 35:1–15
- Hashimoto MA, Nomoto KI, Arai K, Kaminisi K (1986) The $^{14}\text{N}(e^-, \nu)$ $^{14}\text{C}(\alpha, \gamma)$ ^{18}O Reaction and Helium Flashes in Accreting Helium White Dwarfs. *ApJ* 307:687. <https://doi.org/10.1086/164453>
- Hayden BT, Garnavich PM, Kessler R, et al. (2010) The Rise and Fall of Type Ia Supernova Light Curves in the SDSS-II Supernova Survey. *ApJ* 712:350–366. <https://doi.org/10.1088/0004-637X/712/1/350>. [arXiv:1001.3428](#) [astro-ph.CO]
- Heber U (2016) Hot Subluminous Stars. *PASP* 128(966):082001. <https://doi.org/10.1088/1538-3873/128/966/082001>. [arXiv:1604.07749](#) [astro-ph.SR]
- Heringer E, Pritchett C, Kezwer J, et al. (2017) Type Ia Supernovae: Colors, Rates, and Progenitors. *ApJ* 834(1):15. <https://doi.org/10.3847/1538-4357/834/1/15>. [arXiv:1611.01162](#) [astro-ph.HE]
- Hernanz M, Isern J, Canal R, Labay J, Mochkovitch R (1988) The final stages of evolution of cold, mass-accreting white dwarfs. *ApJ* 324:331–344. <https://doi.org/10.1086/165898>
- Hillebrandt W, Niemeyer JC (2000) Type Ia supernova explosion models. *ARA&A* 38:191–230. <https://doi.org/10.1146/annurev.astro.38.1.191>. [arXiv:astro-ph/0006305](#)
- Hillebrandt W, Kromer M, Röpke FK, Ruiter AJ (2013) Towards an understanding of type ia supernovae from a synthesis of theory and observations. *Frontiers of Physics* 8:116–143. <https://doi.org/10.1007/s11467-013-0303-2>

- [arXiv:1302.6420](#) [astro-ph.CO]
- Hitomi Collaboration, Aharonian F, Akamatsu H, et al. (2017) Solar abundance ratios of the iron-peak elements in the Perseus cluster. *Nature* 551(7681):478–480. <https://doi.org/10.1038/nature24301>. [arXiv:1711.10035](#) [astro-ph.HE]
- Höflich P (1995) Analysis of the type Ia supernova SN 1994D. *ApJ* 443:89–108. <https://doi.org/10.1086/175505>
- Höflich P, Khokhlov A (1996) Explosion Models for Type Ia Supernovae: A Comparison with Observed Light Curves, Distances, H_0 , and q_0 . *ApJ* 457:500. <https://doi.org/10.1086/176748>. [arXiv:astro-ph/9602025](#)
- Höflich P, Stein J (2002) On the thermonuclear runaway in Type Ia supernovae: How to run away? *ApJ* 568:779–790. <https://doi.org/10.1086/338981>. [arXiv:astro-ph/0104226](#)
- Horowitz CJ (2022) Ignition of Carbon Burning from Nuclear Fission in Compact Stars. *ApJ Lett.* 935(1):L2. <https://doi.org/10.3847/2041-8213/ac8552>. [arXiv:2208.00053](#) [astro-ph.SR]
- Horowitz CJ, Caplan ME (2021) Actinide Crystallization and Fission Reactions in Cooling White Dwarf Stars. *Phys. Rev. Lett.* 126(13):131101. <https://doi.org/10.1103/PhysRevLett.126.131101>. [arXiv:2103.02122](#) [astro-ph.SR]
- Hosseinzadeh G, Sand DJ, Valenti S, et al. (2017) Early Blue Excess from the Type Ia Supernova 2017cbv and Implications for Its Progenitor. *ApJ Lett.* 845(2):L11. <https://doi.org/10.3847/2041-8213/aa8402>. [arXiv:1706.08990](#) [astro-ph.HE]
- Hosseinzadeh G, Sand DJ, Sarbadhickey SK, et al. (2023) The Early Light Curve of SN 2023bee: Constraining Type Ia Supernova Progenitors the Apian Way. *ApJ Lett.* 953(1):L15. <https://doi.org/10.3847/2041-8213/ace7c0>. [arXiv:2305.03071](#) [astro-ph.HE]
- Howell DA, Sullivan M, Brown EF, et al. (2009) The Effect of Progenitor Age and Metallicity on Luminosity and ^{56}Ni Yield in Type Ia Supernovae. *ApJ* 691:661–671. <https://doi.org/10.1088/0004-637X/691/1/661>. [arXiv:0810.0031](#)
- Hoyle F, Fowler WA (1960) Nucleosynthesis in supernovae. *ApJ* 132:565–590
- Hubble E (1929) A Relation between Distance and Radial Velocity among Extra-Galactic Nebulae. *Proceedings of the National Academy of Science* 15:168–173. <https://doi.org/10.1073/pnas.15.3.168>
- Huber S, Suyu SH, Noebauer UM, et al. (2019) Strongly lensed SNe Ia in the era of LSST: observing cadence for lens discoveries and time-delay measurements. *A&A* 631:A161. <https://doi.org/10.1051/0004-6361/201935370>. [arXiv:1903.00510](#) [astro-ph.IM]
- Iben I Jr, Tutukov AV (1984) Supernovae of type I as end products of the evolution of binaries with components of moderate initial mass (M not greater than about 9 solar masses). *ApJS* 54:335–372. <https://doi.org/10.1086/190932>
- Iben I Jr, Tutukov AV (1989) Model stars with degenerate dwarf cores and helium-burning shells - A stationary-burning approximation. *ApJ* 342:430–

448. <https://doi.org/10.1086/167603>
- Iben J Jr, Tutukov AV (1991) Helium star cataclysmics. *ApJ* 370:615–629. <https://doi.org/10.1086/169848>
- Iben J I, Renzini A (1983) Asymptotic giant branch evolution and beyond. *ARA&A* 21:271–342. <https://doi.org/10.1146/annurev.aa.21.090183.001415>
- Iben J I, Tutukov AV (1985) On the evolution of close binaries with components of initial mass between $3 M_{\odot}$ and $12 M_{\odot}$. *ApJS* 58:661–710. <https://doi.org/10.1086/191054>
- Iben J Icko, Tutukov AV (1987) Evolutionary Scenarios for Intermediate-Mass Stars in Close Binaries. *ApJ* 313:727. <https://doi.org/10.1086/165011>
- Iben J Icko, Tutukov AV (1999) On the Evolution of Close Triple Stars That Produce Type Ia Supernovae. *ApJ* 511(1):324–334. <https://doi.org/10.1086/306672>
- Igoshev AP, Perets H, Hallakoun N (2023) Hyper-runaway and hypervelocity white dwarf candidates in Gaia Data Release 3: Possible remnants from Ia/Iax supernova explosions or dynamical encounters. *MNRAS* 518(4):6223–6237. <https://doi.org/10.1093/mnras/stac348810.48550> [arXiv:2209.09915](https://arxiv.org/abs/2209.09915) [astro-ph.SR]
- Ilkov M, Soker N (2012) Type Ia supernovae from very long delayed explosion of core-white dwarf merger. *MNRAS* 419:1695–1700. <https://doi.org/10.1111/j.1365-2966.2011.19833.x> [arXiv:1106.2027](https://arxiv.org/abs/1106.2027) [astro-ph.SR]
- Immler S, Brown PJ, Milne P, et al. (2006) X-Ray Observations of Type Ia Supernovae with Swift: Evidence of Circumstellar Interaction for SN 2005ke. *ApJ Lett.* 648(2):L119–L122. <https://doi.org/10.1086/507947> [arXiv:astro-ph/0607620](https://arxiv.org/abs/astro-ph/0607620) [astro-ph]
- Inserra C, Smartt SJ (2014) Superluminous Supernovae as Standardizable Candles and High-redshift Distance Probes. *ApJ* 796(2):87. <https://doi.org/10.1088/0004-637X/796/2/87> [arXiv:1409.4429](https://arxiv.org/abs/1409.4429) [astro-ph.SR]
- Isern J, Canal R, Labay J (1991) The outcome of explosive ignition of ONeMg cores - Supernovae, neutron stars, or 'iron' white dwarfs? *ApJ Lett.* 372:L83–L86. <https://doi.org/10.1086/186029>
- Ivanov VD, Hamuy M, Pinto PA (2000) On the Relation between Peak Luminosity and Parent Population of Type IA Supernovae: A New Tool for Probing the Ages of Distant Galaxies. *ApJ* 542(2):588–596. <https://doi.org/10.1086/317060> [arXiv:astro-ph/0006047](https://arxiv.org/abs/astro-ph/0006047) [astro-ph]
- Ivanova LN, Imshennik VS, Chechetkin VM (1974) Pulsation regime of the thermonuclear explosion of a star's dense carbon core. *Astrophys. Space Sci.* 31:497–514. <https://doi.org/10.1007/BF00644102>
- Ivanova N, Heinke CO, Rasio FA, Belczynski K, Fregeau JM (2008) Formation and evolution of compact binaries in globular clusters - II. Binaries with neutron stars. *MNRAS* 386:553–576. <https://doi.org/10.1111/j.1365-2966.2008.13064.x> [arXiv:0706.4096](https://arxiv.org/abs/0706.4096)
- Ivezić Ž, Kahn SM, Tyson JA, et al. (2019) LSST: From Science Drivers to Reference Design and Anticipated Data Products. *ApJ* 873(2):111. <https://doi.org/10.3847/1538-4357/ab042c> [arXiv:0805.2366](https://arxiv.org/abs/0805.2366) [astro-ph]
- Iwamoto K, Brachwitz F, Nomoto K, et al. (1999) Nucleosynthesis in chan-

- drasekhar mass models for type Ia supernovae and constraints on progenitor systems and burning-front propagation. *ApJS* 125:439–462. <https://doi.org/10.1086/313278>. [arXiv:astro-ph/0002337](https://arxiv.org/abs/astro-ph/0002337)
- Janish R, Narayan V, Riggins P (2019) Type Ia supernovae from dark matter core collapse. *Phys. Rev. D* 100(3):035008. <https://doi.org/10.1103/PhysRevD.100.035008>. [arXiv:1905.00395](https://arxiv.org/abs/1905.00395) [hep-ph]
- Jha SW (2017) Type Iax Supernovae. In: Alsabti AW, Murdin P (eds) *Handbook of Supernovae*. Springer, Cham, p 375. https://doi.org/10.1007/978-3-319-21846-5_42
- Jha SW, Maguire K, Sullivan M (2019) Observational properties of thermonuclear supernovae. *Nature Astronomy* 3:706–716. <https://doi.org/10.1038/s41550-019-0858-0>. [arXiv:1908.02303](https://arxiv.org/abs/1908.02303) [astro-ph.HE]
- Ji S, Fisher RT, García-Berro E, et al. (2013) The Post-merger Magnetized Evolution of White Dwarf Binaries: The Double-degenerate Channel of Sub-Chandrasekhar Type Ia Supernovae and the Formation of Magnetized White Dwarfs. *ApJ* 773(2):136. <https://doi.org/10.1088/0004-637X/773/2/136>. [arXiv:1302.5700](https://arxiv.org/abs/1302.5700) [astro-ph.SR]
- Jiang JA, Doi M, Maeda K, et al. (2017) A hybrid type Ia supernova with an early flash triggered by helium-shell detonation. *Nature* 550(7674):80–83. <https://doi.org/10.1038/nature23908>. [arXiv:1710.01824](https://arxiv.org/abs/1710.01824) [astro-ph.HE]
- Jiang Ja, Doi M, Maeda K, Shigeyama T (2018) Surface Radioactivity or Interactions? Multiple Origins of Early-excess Type Ia Supernovae and Associated Subclasses. *ApJ* 865(2):149. <https://doi.org/10.3847/1538-4357/aadb9a>. [arXiv:1808.06343](https://arxiv.org/abs/1808.06343) [astro-ph.HE]
- Jiang Ja, Maeda K, Kawabata M, et al. (2021) Discovery of the Fastest Early Optical Emission from Overluminous SN Ia 2020hvf: A Thermonuclear Explosion within a Dense Circumstellar Environment. *ApJ Lett.* 923(1):L8. <https://doi.org/10.3847/2041-8213/ac375f>. [arXiv:2111.09470](https://arxiv.org/abs/2111.09470) [astro-ph.HE]
- Jones DO, Foley RJ, Narayan G, et al. (2021) The Young Supernova Experiment: Survey Goals, Overview, and Operations. *ApJ* 908(2):143. <https://doi.org/10.3847/1538-4357/abd7f5>. [arXiv:2010.09724](https://arxiv.org/abs/2010.09724) [astro-ph.HE]
- Jones S, Röpke FK, Pakmor R, et al. (2016) Do electron-capture supernovae make neutron stars?. First multidimensional hydrodynamic simulations of the oxygen deflagration. *A&A* 593:A72. <https://doi.org/10.1051/0004-6361/201628321>. [arXiv:1602.05771](https://arxiv.org/abs/1602.05771) [astro-ph.SR]
- Jones S, Röpke FK, Fryer C, et al. (2019) Remnants and ejecta of thermonuclear electron-capture supernovae. Constraining oxygen-neon deflagrations in high-density white dwarfs. *A&A* 622:A74. <https://doi.org/10.1051/0004-6361/201834381>
- Jordan I G C, Graziani C, Fisher RT, et al. (2012a) The Detonation Mechanism of the Pulsationally Assisted Gravitationally Confined Detonation Model of Type Ia Supernovae. *ApJ* 759(1):53. <https://doi.org/10.1088/0004-637X/759/1/53>. [arXiv:1202.3997](https://arxiv.org/abs/1202.3997) [astro-ph.HE]
- Jordan I George C, Perets HB, Fisher RT, van Rossum DR (2012b) Failed-detonation Supernovae: Subluminous Low-velocity Ia Supernovae and their Kicked Remnant White Dwarfs with Iron-rich

- Cores. *ApJ Lett.* 761(2):L23. <https://doi.org/10.1088/2041-8205/761/2/L23>. [arXiv:1208.5069](https://arxiv.org/abs/1208.5069) [astro-ph.HE]
- José J, Shore SN, Casanova J (2020) 123-321 models of classical novae. *A&A* 634:A5. <https://doi.org/10.1051/0004-6361/201936893>. [arXiv:1912.08443](https://arxiv.org/abs/1912.08443) [astro-ph.SR]
- Kahabka P, van den Heuvel EPJ (1997) Luminous supersoft X-ray sources. *ARA&A* 35:69–100. <https://doi.org/10.1146/annurev.astro.35.1.69>
- Kang Y, Lee YW, Kim YL, Chung C, Ree CH (2020) Early-type Host Galaxies of Type Ia Supernovae. II. Evidence for Luminosity Evolution in Supernova Cosmology. *ApJ* 889(1):8. <https://doi.org/10.3847/1538-4357/ab5afc10.48550/arXiv.1912.04903>. [arXiv:1912.04903](https://arxiv.org/abs/1912.04903) [astro-ph.GA]
- Karakas AI (2010) Updated stellar yields from asymptotic giant branch models. *MNRAS* 403(3):1413–1425. <https://doi.org/10.1111/j.1365-2966.2009.16198.x>. [arXiv:0912.2142](https://arxiv.org/abs/0912.2142) [astro-ph.SR]
- Karakas AI (2014) Helium enrichment and carbon-star production in metal-rich populations. *MNRAS* 445(1):347–358. <https://doi.org/10.1093/mnras/stu1727>. [arXiv:1408.5936](https://arxiv.org/abs/1408.5936) [astro-ph.SR]
- Kasen D (2010) Seeing the Collision of a Supernova with Its Companion Star. *ApJ* 708:1025–1031. <https://doi.org/10.1088/0004-637X/708/2/1025>. [arXiv:0909.0275](https://arxiv.org/abs/0909.0275) [astro-ph.HE]
- Kasen D, Nugent P, Thomas RC, Wang L (2004) Could there be a hole in Type Ia supernovae? *ApJ* 610:876–887. <https://doi.org/10.1086/421699>. [arXiv:astro-ph/0311009](https://arxiv.org/abs/astro-ph/0311009)
- Kasen D, Röpke FK, Woosley SE (2009) The diversity of type Ia supernovae from broken symmetries. *Nature* 460:869–872. <https://doi.org/10.1038/nature08256>. [arXiv:0907.0708](https://arxiv.org/abs/0907.0708)
- Kashi A, Soker N (2011) A circumbinary disc in the final stages of common envelope and the core-degenerate scenario for Type Ia supernovae. *MNRAS* 417:1466–1479. <https://doi.org/10.1111/j.1365-2966.2011.19361.x>. [arXiv:1105.5698](https://arxiv.org/abs/1105.5698) [astro-ph.SR]
- Kashyap R, Fisher R, García-Berro E, et al. (2015) Spiral Instability Can Drive Thermonuclear Explosions in Binary White Dwarf Mergers. *ApJ Lett.* 800(1):L7. <https://doi.org/10.1088/2041-8205/800/1/L7>. [arXiv:1501.05645](https://arxiv.org/abs/1501.05645) [astro-ph.SR]
- Kashyap R, Haque T, Lorén-Aguilar P, García-Berro E, Fisher R (2018) Double-degenerate Carbon-Oxygen and Oxygen-Neon White Dwarf Mergers: A New Mechanism for Faint and Rapid Type Ia Supernovae. *ApJ* 869(2):140. <https://doi.org/10.3847/1538-4357/aaedb7>. [arXiv:1811.00013](https://arxiv.org/abs/1811.00013) [astro-ph.SR]
- Kasliwal MM, Kulkarni SR, Gal-Yam A, et al. (2012) Calcium-rich Gap Transients in the Remote Outskirts of Galaxies. *ApJ* 755:161. <https://doi.org/10.1088/0004-637X/755/2/161>. [arXiv:1111.6109](https://arxiv.org/abs/1111.6109) [astro-ph.HE]
- Kato M, Hachisu I (2003) V445 puppis: Helium nova on a massive white dwarf. *ApJ Lett.* 598:L107–L110. <https://doi.org/10.1086/380597>. [arXiv:astro-ph/0310351](https://arxiv.org/abs/astro-ph/0310351)
- Kato M, Hachisu I (2004) Mass accumulation efficiency in helium shell flashes

- for various white dwarf masses. *ApJ Lett.* 613:L129–L132 (KH04). <https://doi.org/10.1086/425249>. [arXiv:astro-ph/0407632](https://arxiv.org/abs/astro-ph/0407632)
- Kelly PL, Hicken M, Burke DL, Mandel KS, Kirshner RP (2010) Hubble Residuals of Nearby Type Ia Supernovae are Correlated with Host Galaxy Masses. *ApJ* 715:743–756. <https://doi.org/10.1088/0004-637X/715/2/743>. [arXiv:0912.0929](https://arxiv.org/abs/0912.0929) [astro-ph.CO]
- Kelly PL, Fox OD, Filippenko AV, et al. (2014) Constraints on the Progenitor System of the Type Ia Supernova 2014J from Pre-explosion Hubble Space Telescope Imaging. *ApJ* 790(1):3. <https://doi.org/10.1088/0004-637X/790/1/3>. [arXiv:1403.4250](https://arxiv.org/abs/1403.4250) [astro-ph.GA]
- Kemp AJ, Karakas AI, Casey AR, et al. (2021) Population synthesis of accreting white dwarfs: rates and evolutionary pathways of H and He novae. *MNRAS* 504(4):6117–6143. <https://doi.org/10.1093/mnras/stab1160>. [arXiv:2104.10870](https://arxiv.org/abs/2104.10870) [astro-ph.SR]
- Kenyon SJ, Livio M, Mikolajewska J, Tout CA (1993) On Symbiotic Stars and Type IA Supernovae. *ApJ Lett.* 407:L81. <https://doi.org/10.1086/186811>
- Kerzendorf WE, Sim SA (2014) A spectral synthesis code for rapid modelling of supernovae. *MNRAS* 440(1):387–404. <https://doi.org/10.1093/mnras/stu055>. [arXiv:1401.5469](https://arxiv.org/abs/1401.5469) [astro-ph.SR]
- Kerzendorf WE, Schmidt BP, Asplund M, et al. (2009) Subaru High-Resolution Spectroscopy of Star G in the Tycho Supernova Remnant. *ApJ* 701:1665–1672. <https://doi.org/10.1088/0004-637X/701/2/1665>. [arXiv:0906.0982](https://arxiv.org/abs/0906.0982)
- Khokhlov AM (1991a) Delayed detonation model for type Ia supernovae. *A&A* 245:114–128
- Khokhlov AM (1991b) Mechanisms for the initiation of detonations in the degenerate matter of supernovae. *A&A* 246:383–396
- Khokhlov AM (1991c) Nucleosynthesis in delayed detonation models of Type Ia supernovae. *A&A* 245:L25–L28
- Kirby EN, Xie JL, Guo R, et al. (2019) Evidence for Sub-Chandrasekhar Type Ia Supernovae from Stellar Abundances in Dwarf Galaxies. *ApJ* 881(1):45. <https://doi.org/10.3847/1538-4357/ab2c02>. [arXiv:1906.10126](https://arxiv.org/abs/1906.10126) [astro-ph.SR]
- Kirsebom OS, Jones S, Strömberg DF, et al. (2019) Discovery of an Exceptionally Strong β -Decay Transition of ^{20}F and Implications for the Fate of Intermediate-Mass Stars. *Phys. Rev. Lett.* 123(26):262701. <https://doi.org/10.1103/PhysRevLett.123.262701>. [arXiv:1905.09407](https://arxiv.org/abs/1905.09407) [astro-ph.SR]
- Kirshner RP (2010) Foundations of supernova cosmology. In: Ruiz-Lapuente P (ed) *Dark Energy: Observational and Theoretical Approaches*. Cambridge University Press, p 151. [arXiv:0910.0257](https://arxiv.org/abs/0910.0257)
- Kobayashi C, Umeda H, Nomoto K, Tominaga N, Ohkubo T (2006) Galactic Chemical Evolution: Carbon through Zinc. *ApJ* 653:1145–1171. <https://doi.org/10.1086/508914>. [astro-ph/0608688](https://arxiv.org/abs/astro-ph/0608688)
- Kobayashi C, Nomoto K, Hachisu I (2015) Subclasses of Type Ia Supernovae as the Origin of $[\alpha/\text{Fe}]$ Ratios in Dwarf Spheroidal Galaxies. *ApJ Lett.* 804:L24. <https://doi.org/10.1088/2041-8205/804/1/L24>. [arXiv:1503.06739](https://arxiv.org/abs/1503.06739)
- Kollmeier JA, Chen P, Dong S, et al. (2019) $\text{H}\alpha$ emission in the nebular spec-

- trum of the Type Ia supernova ASASSN-18tb. *MNRAS* 486(3):3041–3046. <https://doi.org/10.1093/mnras/stz953>. [arXiv:1902.02251](https://arxiv.org/abs/1902.02251) [astro-ph.HE]
- Korol V, Koop O, Rossi EM (2018) Detectability of Double White Dwarfs in the Local Group with LISA. *ApJ Lett.* 866(2):L20. <https://doi.org/10.3847/2041-8213/aae587>. [arXiv:1808.05959](https://arxiv.org/abs/1808.05959) [astro-ph.HE]
- Korol V, Hallakoun N, Toonen S, Karnesis N (2022) Observationally driven Galactic double white dwarf population for LISA. *MNRAS* 511(4):5936–5947. <https://doi.org/10.1093/mnras/stac415>. [arXiv:2109.10972](https://arxiv.org/abs/2109.10972) [astro-ph.HE]
- Krisciunas K, Contreras C, Burns CR, et al. (2017) The Carnegie Supernova Project. I. Third Photometry Data Release of Low-redshift Type Ia Supernovae and Other White Dwarf Explosions. *AJ* 154(5):211. <https://doi.org/10.3847/1538-3881/aa8df0>. [arXiv:1709.05146](https://arxiv.org/abs/1709.05146) [astro-ph.IM]
- Kromer M, Sim SA, Fink M, et al. (2010) Double-detonation Sub-Chandrasekhar Supernovae: Synthetic Observables for Minimum Helium Shell Mass Models. *ApJ* 719:1067–1082. <https://doi.org/10.1088/0004-637X/719/2/1067>. [arXiv:1006.4489](https://arxiv.org/abs/1006.4489) [astro-ph.HE]
- Kromer M, Fink M, Stanishev V, et al. (2013) 3d deflagration simulations leaving bound remnants: a model for 2002cx-like type ia supernovae. *MNRAS* 429:2287–2297. <https://doi.org/10.1093/mnras/sts498>. [arXiv:1210.5243](https://arxiv.org/abs/1210.5243) [astro-ph.HE]
- Kromer M, Ohlmann ST, Pakmor R, et al. (2015) Deflagrations in hybrid CONE white dwarfs: a route to explain the faint Type Iax supernova 2008ha. *MNRAS* 450:3045–3053. <https://doi.org/10.1093/mnras/stv886>. [arXiv:1503.04292](https://arxiv.org/abs/1503.04292) [astro-ph.HE]
- Kuhlen M, Woosley SE, Glatzmaier GA (2006) Carbon ignition in Type Ia supernovae. II. A three-dimensional numerical model. *ApJ* 640:407–416. <https://doi.org/10.1086/500105>. [arXiv:astro-ph/0509367](https://arxiv.org/abs/astro-ph/0509367)
- Kupfer T, Korol V, Shah S, et al. (2018) LISA verification binaries with updated distances from Gaia Data Release 2. *MNRAS* 480(1):302–309. <https://doi.org/10.1093/mnras/sty1545>. [arXiv:1805.00482](https://arxiv.org/abs/1805.00482) [astro-ph.SR]
- Kushnir D, Waxman E (2020) Constraints on the density distribution of type Ia supernovae ejecta inferred from late-time light-curve flattening. *MNRAS* 493(4):5617–5624. <https://doi.org/10.1093/mnras/staa690>. [arXiv:2001.10005](https://arxiv.org/abs/2001.10005) [astro-ph.HE]
- Kushnir D, Katz B, Dong S, Livne E, Fernández R (2013) Head-on Collisions of White Dwarfs in Triple Systems Could Explain Type Ia Supernovae. *ApJ Lett.* 778(2):L37. <https://doi.org/10.1088/2041-8205/778/2/L37>. [arXiv:1303.1180](https://arxiv.org/abs/1303.1180) [astro-ph.HE]
- Kuuttila J, Gilfanov M, Seitenzahl IR, Woods TE, Vogt FPA (2019) Excluding supersoft X-ray sources as progenitors for four Type Ia supernovae in the Large Magellanic Cloud. *MNRAS* 484(1):1317–1324. <https://doi.org/10.1093/mnras/stz065>. [arXiv:1812.08799](https://arxiv.org/abs/1812.08799) [astro-ph.HE]
- Kwok LA, Jha SW, Temim T, et al. (2023) A JWST Near- and Mid-infrared Nebular Spectrum of the Type Ia Supernova 2021aefx. *ApJ Lett.* 944(1):L3. <https://doi.org/10.3847/2041-8213/acb4ec>. [arXiv:2211.00038](https://arxiv.org/abs/2211.00038) [astro-ph.HE]

- Lach F, Röpke FK, Seitenzahl IR, et al. (2020) Nucleosynthesis imprints from different Type Ia supernova explosion scenarios and implications for galactic chemical evolution. *A&A* 644:A118. <https://doi.org/10.1051/0004-6361/202038721>. [arXiv:2010.14084](https://arxiv.org/abs/2010.14084) [astro-ph.SR]
- Lach F, Callan FP, Sim SA, Röpke FK (2022) Models of pulsationally assisted gravitationally confined detonations with different ignition conditions. *A&A* 659:A27. <https://doi.org/10.1051/0004-6361/202142194>. [arXiv:2111.14394](https://arxiv.org/abs/2111.14394) [astro-ph.SR]
- Lamers HJGLM, Levesque EM (2017) *Understanding Stellar Evolution*. IOP Publishing, Bristol. <https://doi.org/10.1088/978-0-7503-1278-3>
- Langanke K, Martinez-Pinedo G (2000) Shell-model calculations of stellar weak interaction rates. II. Weak rates for nuclei in the mass range $A = 45 - 65$ in supernovae environments. *Nucl Phys A* 673:481–508. [arXiv:nuc-th/0001018](https://arxiv.org/abs/nuc-th/0001018)
- Leavitt HS, Pickering EC (1912) Periods of 25 Variable Stars in the Small Magellanic Cloud. *Harvard College Observatory Circular* 173:1–3
- Lee JHS, Knystautas R, Yoshikawa N (1978) Photochemical initiation of gaseous detonations. *Acta Astronautica* 5:971–982
- Leibundgut B (2000) Type Ia supernovae. *A&A Rev.* 10:179–209. <https://doi.org/10.1007/s001590000009>. [arXiv:astro-ph/0003326](https://arxiv.org/abs/astro-ph/0003326)
- Leibundgut B, Kirshner RP, Phillips MM, et al. (1993) SN 1991bg – A type Ia supernova with a difference. *AJ* 105:301–313. <https://doi.org/10.1086/116427>
- Lemaître G (1927) Un Univers homogène de masse constante et de rayon croissant rendant compte de la vitesse radiale des nébuleuses extra-galactiques. *Ann Soc Sci Bruxelles* 47:49–59
- Leonard DC (2007) Constraining the type Ia supernova progenitor: The search for hydrogen in nebular spectra. *ApJ* 670:1275–1282. <https://doi.org/10.1086/522367>. [arXiv:0710.3166](https://arxiv.org/abs/0710.3166)
- Leoni M, Ishida EEO, Peloton J, Möller A (2022) Fink: Early supernovae Ia classification using active learning. *A&A* 663:A13. <https://doi.org/10.1051/0004-6361/202142715>. [arXiv:2111.11438](https://arxiv.org/abs/2111.11438) [astro-ph.IM]
- Lesaffre P, Han Z, Tout CA, Podsiadlowski P, Martin RG (2006) The c flash and the ignition conditions of Type Ia supernovae. *MNRAS* 368:187–195. <https://doi.org/10.1111/j.1365-2966.2006.10068.x>. [arXiv:astro-ph/0601443](https://arxiv.org/abs/astro-ph/0601443)
- Leung SC, Chu MC, Lin LM (2015) Dark Matter Admixed Type Ia Supernovae. *ApJ* 812(2):110. <https://doi.org/10.1088/0004-637X/812/2/110>. [arXiv:1509.01871](https://arxiv.org/abs/1509.01871) [astro-ph.CO]
- Li W, Filippenko AV, Chornock R, et al. (2003) SN 2002cx: The Most Peculiar Known Type Ia Supernova. *PASP* 115:453–473. <https://doi.org/10.1086/374200>. [arXiv:astro-ph/0301428](https://arxiv.org/abs/astro-ph/0301428)
- Li W, Bloom JS, Podsiadlowski P, et al. (2011a) Exclusion of a luminous red giant as a companion star to the progenitor of supernova SN 2011fe. *Nature* 480:348–350. <https://doi.org/10.1038/nature10646>. [arXiv:1109.1593](https://arxiv.org/abs/1109.1593) [astro-ph.CO]
- Li W, Chornock R, Leaman J, et al. (2011b) Nearby supernova rates

- from the Lick Observatory Supernova Search – III. The rate-size relation, and the rates as a function of galaxy Hubble type and colour. *MNRAS* 412:1473–1507. <https://doi.org/10.1111/j.1365-2966.2011.18162.x>. [arXiv:1006.4613](https://arxiv.org/abs/1006.4613) [astro-ph.SR]
- Li W, Leaman J, Chornock R, et al. (2011c) Nearby supernova rates from the Lick Observatory Supernova Search – II. the observed luminosity functions and fractions of supernovae in a complete sample. *MNRAS* 412:1441–1472. <https://doi.org/10.1111/j.1365-2966.2011.18160.x>. [arXiv:1006.4612](https://arxiv.org/abs/1006.4612) [astro-ph.SR]
- Lisewski AM, Hillebrandt W, Woosley SE, Niemeyer JC, Kerstein AR (2000) Distributed burning in Type Ia supernovae: A statistical approach. *ApJ* 537:405–413. <https://doi.org/10.1086/309015>. [arXiv:astro-ph/9909508](https://arxiv.org/abs/astro-ph/9909508)
- Liu ZW, Pakmor R, Seitenzahl IR, et al. (2013) The Impact of Type Ia Supernova Explosions on Helium Companions in the Chandrasekhar-mass Explosion Scenario. *ApJ* 774(1):37. <https://doi.org/10.1088/0004-637X/774/1/37>. [arXiv:1307.5579](https://arxiv.org/abs/1307.5579) [astro-ph.SR]
- Liu ZW, Stancliffe RJ, Abate C, Wang B (2015) Pre-explosion Companion Stars in Type Ia Supernovae. *ApJ* 808:138. <https://doi.org/10.1088/0004-637X/808/2/138>. [arXiv:1506.04903](https://arxiv.org/abs/1506.04903) [astro-ph.SR]
- Liu ZW, Röpke FK, Zeng Y, Heger A (2021) Observational signatures of the surviving donor star in the double-detonation model of Type Ia supernovae. *A&A* 654:A103. <https://doi.org/10.1051/0004-6361/202141518>. [arXiv:2109.09980](https://arxiv.org/abs/2109.09980) [astro-ph.SR]
- Liu ZW, Röpke FK, Han Z (2023) Type Ia Supernova Explosions in Binary Systems: A Review. *Res Astron Astrophys* 23(8):082001. <https://doi.org/10.1088/1674-4527/acd89e>. [arXiv:2305.13305](https://arxiv.org/abs/2305.13305) [astro-ph.HE]
- Livio M, Riess AG (2003) Have the elusive progenitors of type Ia supernovae been discovered? *ApJ Lett.* 594:L93–L94. <https://doi.org/10.1086/378765>. [arXiv:astro-ph/0308018](https://arxiv.org/abs/astro-ph/0308018)
- Livne E (1990) Successive detonations in accreting white dwarfs as an alternative mechanism for type I supernovae. *ApJ Lett.* 354:L53–L55. <https://doi.org/10.1086/185721>
- Livne E, Arnett D (1995) Explosions of sub-Chandrasekhar mass white dwarfs in two dimensions. *ApJ* 452:62–74. <https://doi.org/10.1086/176279>
- Livne E, Glasner AS (1990) Geometrical effects in off-center detonation of helium shells. *ApJ* 361:244–250. <https://doi.org/10.1086/169189>
- Livne E, Glasner AS (1991) Numerical simulations of off-center detonations in helium shells. *ApJ* 370:272–281. <https://doi.org/10.1086/169813>
- Lundmark K (1932) The pre-Tychonic Novae. *Lund Observatory Circular* 8:216–218
- Lundmark K (1935) On the novae and their classification among the variable stars. *Meddel Lunds Astron Obs Ser II* 74:1–20
- Maeda K, Benetti S, Stritzinger M, et al. (2010) An asymmetric explosion as the origin of spectral evolution diversity in type Ia supernovae. *Nature* 466:82–85. <https://doi.org/10.1038/nature09122>. [arXiv:1006.5888](https://arxiv.org/abs/1006.5888)
- Magee MR, Cuddy C, Maguire K, et al. (2022) The detection efficiency of Type Ia supernovae from the Zwicky Transient Facility: limits on the intrinsic rate

- of early flux excesses. *MNRAS* 513(2):3035–3049. <https://doi.org/10.1093/mnras/stac1045>. [arXiv:2204.09705](https://arxiv.org/abs/2204.09705) [astro-ph.HE]
- Maguire K (2017) Type Ia Supernovae. In: Alsabti AW, Murdin P (eds) *Handbook of Supernovae*. Springer, Cham, p 293. https://doi.org/10.1007/978-3-319-21846-5_36
- Maguire K, Kotak R, Smartt SJ, et al. (2010) Type II-P supernovae as standardized candles: improvements using near-infrared data. *MNRAS* 403(1):L11–L15. <https://doi.org/10.1111/j.1745-3933.2009.00804.x>. [arXiv:0912.3107](https://arxiv.org/abs/0912.3107) [astro-ph.CO]
- Maguire K, Taubenberger S, Sullivan M, Mazzali PA (2016) Searching for swept-up hydrogen and helium in the late-time spectra of 11 nearby Type Ia supernovae. *MNRAS* 457(3):3254–3265. <https://doi.org/10.1093/mnras/stv2991>. [arXiv:1512.07107](https://arxiv.org/abs/1512.07107) [astro-ph.SR]
- Maguire K, Magee MR, Leloudas G, et al. (2023) SN 2020udy: an SN Iax with strict limits on interaction consistent with a helium-star companion. *MNRAS* 525(1):1210–1228. <https://doi.org/10.1093/mnras/stad2316>. [arXiv:2304.12361](https://arxiv.org/abs/2304.12361) [astro-ph.HE]
- Mannucci F, Della Valle M, Panagia N, et al. (2005) The supernova rate per unit mass. *A&A* 433:807–814. <https://doi.org/10.1051/0004-6361:20041411>. [arXiv:astro-ph/0411450](https://arxiv.org/abs/astro-ph/0411450)
- Mannucci F, Della Valle M, Panagia N (2006) Two populations of progenitors for Type Ia supernovae? *MNRAS* 370:773–783. <https://doi.org/10.1111/j.1365-2966.2006.10501.x>. [arXiv:astro-ph/0510315](https://arxiv.org/abs/astro-ph/0510315)
- Maoz D, Badenes C (2010) The supernova rate and delay time distribution in the magellanic clouds. *MNRAS* 407:1314–1327. <https://doi.org/10.1111/j.1365-2966.2010.16988.x>. [arXiv:1003.3031](https://arxiv.org/abs/1003.3031) [astro-ph.GA]
- Maoz D, Graur O (2017) Star Formation, Supernovae, Iron, and α : Consistent Cosmic and Galactic Histories. *ApJ* 848(1):25. <https://doi.org/10.3847/1538-4357/aa8b6e>. [arXiv:1703.04540](https://arxiv.org/abs/1703.04540) [astro-ph.HE]
- Maoz D, Mannucci F (2012) Type-ia supernova rates and the progenitor problem: A review. *PASA* 29:447–465. <https://doi.org/10.1071/AS11052>. [arXiv:1111.4492](https://arxiv.org/abs/1111.4492) [astro-ph.CO]
- Maoz D, Sharon K, Gal-Yam A (2010) The Supernova Delay Time Distribution in Galaxy Clusters and Implications for Type-Ia Progenitors and Metal Enrichment. *ApJ* 722:1879–1894. <https://doi.org/10.1088/0004-637X/722/2/1879>. [arXiv:1006.3576](https://arxiv.org/abs/1006.3576) [astro-ph.CO]
- Maoz D, Mannucci F, Li W, et al. (2011) Nearby supernova rates from the Lick Observatory Supernova Search - IV. A recovery method for the delay-time distribution. *MNRAS* 412(3):1508–1521. <https://doi.org/10.1111/j.1365-2966.2010.16808.x>. [arXiv:1002.3056](https://arxiv.org/abs/1002.3056) [astro-ph.CO]
- Maoz D, Mannucci F, Brandt TD (2012) The delay-time distribution of Type Ia supernovae from Sloan II. *MNRAS* 426:3282–3294. <https://doi.org/10.1111/j.1365-2966.2012.21871.x>. [arXiv:1206.0465](https://arxiv.org/abs/1206.0465) [astro-ph.CO]
- Maoz D, Mannucci F, Nelemans G (2014) Observational Clues to the Progenitors of Type Ia Supernovae. *ARA&A* 52:107–170. <https://doi.org/10.1146/annurev-astro-082812-141031>. [arXiv:1312.0628](https://arxiv.org/abs/1312.0628)

- Maoz D, Hallakoun N, Badenes C (2018) The separation distribution and merger rate of double white dwarfs: improved constraints. *MNRAS* 476(2):2584–2590. <https://doi.org/10.1093/mnras/sty339>. [arXiv:1801.04275](https://arxiv.org/abs/1801.04275) [astro-ph.SR]
- Margutti R, Parrent J, Kamble A, et al. (2014) No X-Rays from the Very Nearby Type Ia SN 2014J: Constraints on Its Environment. *ApJ* 790(1):52. <https://doi.org/10.1088/0004-637X/790/1/52>. [arXiv:1405.1488](https://arxiv.org/abs/1405.1488) [astro-ph.HE]
- Marietta E, Burrows A, Fryxell B (2000) Type Ia supernova explosions in binary systems: The impact on the secondary star and its consequences. *ApJS* 128:615–650. <https://doi.org/10.1086/313392>. [arXiv:astro-ph/9908116](https://arxiv.org/abs/astro-ph/9908116)
- Marquardt KS, Sim SA, Ruiter AJ, et al. (2015) Type Ia supernovae from exploding oxygen-neon white dwarfs. *A&A* 580:A118. <https://doi.org/10.1051/0004-6361/201525761>. [arXiv:1506.05809](https://arxiv.org/abs/1506.05809) [astro-ph.SR]
- Marsh TR, Nelemans G, Steeghs D (2004) Mass transfer between double white dwarfs. *MNRAS* 350:113–128. <https://doi.org/10.1111/j.1365-2966.2004.07564.x>. [arXiv:astro-ph/0312577](https://arxiv.org/abs/astro-ph/0312577)
- Matteucci F (2021) Modelling the chemical evolution of the Milky Way. *A&A Rev.* 29(1):5. <https://doi.org/10.1007/s00159-021-00133-8>. [arXiv:2106.13145](https://arxiv.org/abs/2106.13145) [astro-ph.GA]
- Matteucci F, Greggio L (1986) Relative roles of type I and II supernovae in the chemical enrichment of the interstellar gas. *A&A* 154:279–287
- Mazzali PA, Chugai N, Turatto M, et al. (1997) The properties of the peculiar type IA supernova 1991bg – II. The amount of ^{56}Ni and the total ejecta mass determined from spectrum synthesis and energetics considerations. *MNRAS* 284:151–171
- Mazzali PA, Benetti S, Altavilla G, et al. (2005) High-velocity features: A ubiquitous property of Type Ia supernovae. *ApJ Lett.* 623:L37–L40. <https://doi.org/10.1086/429874>. [arXiv:astro-ph/0502531](https://arxiv.org/abs/astro-ph/0502531)
- Mazzali PA, Röpke FK, Benetti S, Hillebrandt W (2007) A common explosion mechanism for Type Ia supernovae. *Science* 315:825–828. <https://doi.org/10.1126/science.1136259>. [arXiv:astro-ph/0702351](https://arxiv.org/abs/astro-ph/0702351)
- Mazzali PA, Sauer DN, Pastorello A, Benetti S, Hillebrandt W (2008) Abundance stratification in Type Ia supernovae – II. the rapidly declining, spectroscopically normal SN2004eo. *MNRAS* 386:1897–1906. <https://doi.org/10.1111/j.1365-2966.2008.13199.x>. [arXiv:0803.1383](https://arxiv.org/abs/0803.1383)
- Mazzali PA, Sullivan M, Filippenko AV, et al. (2015) Nebular spectra and abundance tomography of the Type Ia supernova SN 2011fe: a normal SN Ia with a stable Fe core. *MNRAS* 450(3):2631–2643. <https://doi.org/10.1093/mnras/stv761>. [arXiv:1504.04857](https://arxiv.org/abs/1504.04857) [astro-ph.HE]
- McCully C, Jha SW, Foley RJ, et al. (2014) A luminous, blue progenitor system for the type Iax supernova 2012Z. *Nature* 512:54–56. <https://doi.org/10.1038/nature13615>. [arXiv:1408.1089](https://arxiv.org/abs/1408.1089) [astro-ph.SR]
- McCully C, Jha SW, Scalzo RA, et al. (2022) Still Brighter than Pre-explosion, SN 2012Z Did Not Disappear: Comparing Hubble Space Telescope Observations a Decade Apart. *ApJ* 925(2):138. <https://doi.org/10.3847/1538-4357/>

- ac3bbd. [arXiv:2106.04602](https://arxiv.org/abs/2106.04602) [astro-ph.HE]
- McWilliam A, Rich RM, Smecker-Hane TA (2003) Constraints on the Origin of Manganese from the Composition of the Sagittarius Dwarf Spheroidal Galaxy and the Galactic Bulge. *ApJ Lett.* 592(1):L21–L24. <https://doi.org/10.1086/377441>
- McWilliam A, Piro AL, Badenes C, Bravo E (2018) Evidence for a Sub-Chandrasekhar-mass Type Ia Supernova in the Ursa Minor Dwarf Galaxy. *ApJ* 857(2):97. <https://doi.org/10.3847/1538-4357/aab772>. [arXiv:1710.05030](https://arxiv.org/abs/1710.05030) [astro-ph.HE]
- Meakin CA, Seitzzahl I, Townsley D, et al. (2009) Study of the detonation phase in the gravitationally confined detonation model of Type Ia supernovae. *ApJ* 693:1188–1208. <https://doi.org/10.1088/0004-637X/693/2/1188>. [arXiv:0806.4972](https://arxiv.org/abs/0806.4972)
- Meldorf C, Palmese A, Brout D, et al. (2023) The Dark Energy Survey Supernova Program results: type Ia supernova brightness correlates with host galaxy dust. *MNRAS* 518(2):1985–2004. <https://doi.org/10.1093/mnras/stac3056>. [arXiv:2206.06928](https://arxiv.org/abs/2206.06928) [astro-ph.CO]
- Meng X, Chen X, Han Z (2007) The impact of Type Ia supernova explosions on the companions in a binary system. *PASJ* 59:835–840
- Mennekens N, Vanbeveren D, De Greve JP, De Donder E (2010) The delay-time distribution of type Ia supernovae: a comparison between theory and observation. *A&A* 515:A89. <https://doi.org/10.1051/0004-6361/201014115>. [arXiv:1003.2491](https://arxiv.org/abs/1003.2491) [astro-ph.SR]
- Mernier F, de Plaa J, Pinto C, et al. (2016) Origin of central abundances in the hot intra-cluster medium. II. Chemical enrichment and supernova yield models. *A&A* 595:A126. <https://doi.org/10.1051/0004-6361/201628765>. [arXiv:1608.03888](https://arxiv.org/abs/1608.03888) [astro-ph.GA]
- Mernier F, Biffi V, Yamaguchi H, et al. (2018) Enrichment of the Hot Intra-cluster Medium: Observations. *Space Sci. Rev.* 214(8):129. <https://doi.org/10.1007/s11214-018-0565-7>. [arXiv:1811.01967](https://arxiv.org/abs/1811.01967) [astro-ph.HE]
- Meyers J, Aldering G, Barbary K, et al. (2012) The Hubble Space Telescope Cluster Supernova Survey. III. Correlated Properties of Type Ia Supernovae and Their Hosts at $0.9 < Z < 1.46$. *ApJ* 750(1):1. <https://doi.org/10.1088/0004-637X/750/1/1>. [arXiv:1201.3989](https://arxiv.org/abs/1201.3989) [astro-ph.CO]
- Miller AA, Magee MR, Polin A, et al. (2020) The Spectacular Ultraviolet Flash from the Peculiar Type Ia Supernova 2019yvq. *ApJ* 898(1):56. <https://doi.org/10.3847/1538-4357/ab9e05>. [arXiv:2005.05972](https://arxiv.org/abs/2005.05972) [astro-ph.HE]
- Minkowski R (1939) The spectra of the supernovae in IC 4182 and in NGC 1003. *ApJ* 89:156–217
- Miyaji S, Nomoto K, Yokoi K, Sugimoto D (1980) Supernova triggered by electron captures. *PASJ* 32:303
- Moll R, Woosley SE (2013) Multi-dimensional models for double detonation in sub-chandrasekhar mass white dwarfs. *ApJ* 774:137. <https://doi.org/10.1088/0004-637X/774/2/137>. [arXiv:1303.0324](https://arxiv.org/abs/1303.0324) [astro-ph.HE]
- Moll R, Raskin C, Kasen D, Woosley SE (2014) Type Ia Supernovae from Merging White Dwarfs. I. Prompt Detonations. *ApJ* 785:105. <https://doi.org/10.1088/0004-637X/785/1/105>

- [org/10.1088/0004-637X/785/2/105](https://doi.org/10.1088/0004-637X/785/2/105). [arXiv:1311.5008](https://arxiv.org/abs/1311.5008) [astro-ph.HE]
- Möller A, de Boissière T (2020) SuperNNova: an open-source framework for Bayesian, neural network-based supernova classification. *MNRAS* 491(3):4277–4293. <https://doi.org/10.1093/mnras/stz3312>. [arXiv:1901.06384](https://arxiv.org/abs/1901.06384) [astro-ph.IM]
- Möller A, Ruhlmann-Kleider V, Leloup C, et al. (2016) Photometric classification of type Ia supernovae in the SuperNova Legacy Survey with supervised learning. *JACP* 2016(12):008. <https://doi.org/10.1088/1475-7516/2016/12/008>. [arXiv:1608.05423](https://arxiv.org/abs/1608.05423) [astro-ph.IM]
- Möller A, Peloton J, Ishida EEO, et al. (2021) FINK, a new generation of broker for the LSST community. *MNRAS* 501(3):3272–3288. <https://doi.org/10.1093/mnras/staa3602>. [arXiv:2009.10185](https://arxiv.org/abs/2009.10185) [astro-ph.IM]
- Moon DS, Ni YQ, Drout MR, et al. (2021) Rapidly Declining Hostless Type Ia Supernova KSP-OT-201509b from the KMTNet Supernova Program: Transitional Nature and Constraint on ^{56}Ni Distribution and Progenitor Type. *ApJ* 910(2):151. <https://doi.org/10.3847/1538-4357/abe466>. [arXiv:2103.16663](https://arxiv.org/abs/2103.16663) [astro-ph.HE]
- Moore K, Townsley DM, Bildsten L (2013) The effects of curvature and expansion on helium detonations on white dwarf surfaces. *ApJ* 776:97. <https://doi.org/10.1088/0004-637X/776/2/97>. [arXiv:1308.4193](https://arxiv.org/abs/1308.4193) [astro-ph.SR]
- Morán-Fraile J, Holas A, Röpke FK, Pakmor R, Schneider FRN (2024) Faint calcium-rich transient from a double detonation of a $0.6 M_{\odot}$ carbon-oxygen white dwarf star. *A&A* 683:A44. <https://doi.org/10.1051/0004-6361/202347769>. [arXiv:2310.19669](https://arxiv.org/abs/2310.19669) [astro-ph.SR]
- Morgan R, Nord B, Bechtol K, et al. (2022) DeepZipper: A Novel Deep-learning Architecture for Lensed Supernovae Identification. *ApJ* 927(1):109. <https://doi.org/10.3847/1538-4357/ac5178>. [arXiv:2112.01541](https://arxiv.org/abs/2112.01541) [astro-ph.CO]
- Müller B, Melson T, Heger A, Janka HT (2017) Supernova simulations from a 3D progenitor model - Impact of perturbations and evolution of explosion properties. *MNRAS* 472(1):491–513. <https://doi.org/10.1093/mnras/stx1962>. [arXiv:1705.00620](https://arxiv.org/abs/1705.00620) [astro-ph.SR]
- Müller E, Arnett WD (1986) Carbon combustion supernovae – numerical studies of the final evolution of degenerate carbon-oxygen cores. *ApJ* 307:619–643. <https://doi.org/10.1086/164448>
- Munari U, Renzini A (1992) Are Symbiotic Stars the Precursors of Type IA Supernovae? *ApJ Lett.* 397:L87. <https://doi.org/10.1086/186551>
- Napiwotzki R, Karl CA, Lisker T, et al. (2020) The ESO supernovae type Ia progenitor survey (SPY). The radial velocities of 643 DA white dwarfs. *A&A* 638:A131. <https://doi.org/10.1051/0004-6361/201629648>. [arXiv:1906.10977](https://arxiv.org/abs/1906.10977) [astro-ph.SR]
- Nelemans G, Portegies Zwart SF, Verbunt F, Yungelson LR (2001) Population synthesis for double white dwarfs. II. Semi-detached systems: AM CVn stars. *A&A* 368:939–949. <https://doi.org/10.1051/0004-6361:20010049>. [arXiv:astro-ph/0101123](https://arxiv.org/abs/astro-ph/0101123) [astro-ph]
- Nelemans G, Toonen S, Bours M (2013) Theoretical Delay Time Distribu-

- tions. In: Di Stefano R, Orio M, Moe M (eds) *Binary Paths to Type Ia Supernovae Explosions*. vol 281. pp 225–231. <https://doi.org/10.1017/S1743921312015098>. arXiv:1204.2960 [astro-ph.HE]
- Neopane S, Bhargava K, Fisher R, et al. (2022) Near-Chandrasekhar-mass Type Ia Supernovae from the Double-degenerate Channel. *ApJ* 925(1):92. <https://doi.org/10.3847/1538-4357/ac3b52>. arXiv:2111.09890 [astro-ph.HE]
- Neunteufel P, Yoon SC, Langer N (2016) Models for the evolution of close binaries with He-star and white dwarf components towards Type Ia supernova explosions. *A&A* 589:A43. <https://doi.org/10.1051/0004-6361/201527845>. arXiv:1603.00768 [astro-ph.SR]
- Neunteufel P, Preece H, Kruckow M, et al. (2022) Properties and applications of a predicted population of runaway He-sdO/B stars ejected from single degenerate He-donor SNe. *A&A* 663:A91. <https://doi.org/10.1051/0004-6361/202142864>. arXiv:2112.07469 [astro-ph.SR]
- Niemeyer JC (1999) Can deflagration-detonation transitions occur in type Ia supernovae? *ApJ Lett.* 523:L57–L60. <https://doi.org/10.1086/312253>. arXiv:astro-ph/9906142
- Niemeyer JC, Woosley SE (1997) The thermonuclear explosion of Chandrasekhar mass white dwarfs. *ApJ* 475:740–753. <https://doi.org/10.1086/303544>. arXiv:astro-ph/9607032
- Niemeyer JC, Hillebrandt W, Woosley SE (1996) Off-center deflagrations in Chandrasekhar mass Type Ia supernova models. *ApJ* 471:903–914. <https://doi.org/10.1086/178017>. arXiv:astro-ph/9605169
- Noebauer UM, Kromer M, Taubenberger S, et al. (2017) Early light curves for Type Ia supernova explosion models. *MNRAS* 472(3):2787–2799. <https://doi.org/10.1093/mnras/stx2093>. arXiv:1706.03613 [astro-ph.HE]
- Nomoto K (1982a) Accreting white dwarf models for type I supernovae. I. presupernova evolution and triggering mechanisms. *ApJ* 253:798–810. <https://doi.org/10.1086/159682>
- Nomoto K (1982b) Accreting white dwarf models for type I supernovae. II. Off-center detonation supernovae. *ApJ* 257:780–792. <https://doi.org/10.1086/160031>
- Nomoto K (1984) Evolution of 8-10 solar mass stars toward electron capture supernovae. I - Formation of electron-degenerate O + NE + MG cores. *ApJ* 277:791–805. <https://doi.org/10.1086/161749>
- Nomoto K, Iben I Jr (1985) Carbon ignition in a rapidly accreting degenerate dwarf—A clue to the nature of the merging process in close binaries. *ApJ* 297:531–537. <https://doi.org/10.1086/163547>
- Nomoto K, Leung SC (2018) Single Degenerate Models for Type Ia Supernovae: Progenitor’s Evolution and Nucleosynthesis Yields. *Space Sci. Rev.* 214(4):67. <https://doi.org/10.1007/s11214-018-0499-0>. arXiv:1805.10811 [astro-ph.HE]
- Nomoto K, Sugimoto D (1977) Rejuvenation of Helium White Dwarfs by Mass Accretion. *PASJ* 29:765–780
- Nomoto K, Sugimoto D, Neo S (1976) Carbon deflagration supernova, an

- alternative to carbon detonation. *Astrophys. Space Sci.* 39:L37–L42. <https://doi.org/10.1007/BF00648354>
- Nomoto K, Thielemann FK, Wheeler JC (1984a) Explosive nucleosynthesis and Type I supernovae. *ApJ Lett.* 279:L23–L26. <https://doi.org/10.1086/184247>
- Nomoto K, Thielemann FK, Yokoi K (1984b) Accreting white dwarf models of Type I supernovae. III. carbon deflagration supernovae. *ApJ* 286:644–658. <https://doi.org/10.1086/162639>
- Nomoto K, Saio H, Kato M, Hachisu I (2007) Thermal stability of white dwarfs accreting hydrogen-rich matter and progenitors of type ia supernovae. *ApJ* 663:1269–1276. <https://doi.org/10.1086/518465>. [arXiv:astro-ph/0603351](https://arxiv.org/abs/astro-ph/0603351)
- Nonaka A, Aspden AJ, Zingale M, et al. (2012) High-resolution simulations of convection preceding ignition in Type Ia supernovae using adaptive mesh refinement. *ApJ* 745:73. <https://doi.org/10.1088/0004-637X/745/1/73>. [arXiv:1111.3086](https://arxiv.org/abs/1111.3086) [astro-ph.HE]
- North P, Cescutti G, Jablonka P, et al. (2012) Manganese in dwarf spheroidal galaxies. *A&A* 541:A45. <https://doi.org/10.1051/0004-6361/201118636>. [arXiv:1203.4491](https://arxiv.org/abs/1203.4491) [astro-ph.GA]
- Nugent P, Phillips M, Baron E, Branch D, Hauschildt P (1995) Evidence for a Spectroscopic Sequence among Type 1a Supernovae. *ApJ Lett.* 455:L147. <https://doi.org/10.1086/309846>. [arXiv:astro-ph/9510004](https://arxiv.org/abs/astro-ph/9510004) [astro-ph]
- O’Brien JT, Kerzendorf WE, Fullard A, et al. (2021) Probabilistic Reconstruction of Type Ia Supernova SN 2002bo. *ApJ Lett.* 916(2):L14. <https://doi.org/10.3847/2041-8213/ac1173>. [arXiv:2105.07910](https://arxiv.org/abs/2105.07910) [astro-ph.SR]
- Oguri M, Marshall PJ (2010) Gravitationally lensed quasars and supernovae in future wide-field optical imaging surveys. *MNRAS* 405(4):2579–2593. <https://doi.org/10.1111/j.1365-2966.2010.16639.x>. [arXiv:1001.2037](https://arxiv.org/abs/1001.2037) [astro-ph.CO]
- Ohlmann ST, Kromer M, Fink M, et al. (2014) The white dwarf’s carbon fraction as a secondary parameter of Type Ia supernovae. *A&A* 572:A57. <https://doi.org/10.1051/0004-6361/201423924>. [arXiv:1409.2866](https://arxiv.org/abs/1409.2866) [astro-ph.SR]
- Oke JB, Searle L (1974) The spectra of supernovae. *ARA&A* 12:315–329. <https://doi.org/10.1146/annurev.aa.12.090174.001531>
- Paczynski B (1967) Gravitational Waves and the Evolution of Close Binaries. *Acta Astronomica* 17:287–296
- Paczynski B (1970) Evolution of Single Stars. I. Stellar Evolution from Main Sequence to White Dwarf or Carbon Ignition. *Acta Astron.* 20:47
- Paczynski B (1971) Evolutionary processes in close binary systems. *ARA&A* 9:183. <https://doi.org/10.1146/annurev.aa.09.090171.001151>
- Pagnotta A, Hamacher DW, Tanabe K, Trimble V, Vogt N (2020) Historical Novæ and Supernovæ. In: *IAU General Assembly*. pp 171–175. <https://doi.org/10.1017/S1743921319004009>
- Pakmor R, Röpke FK, Weiss A, Hillebrandt W (2008) The impact of type Ia supernovae on main sequence binary companions. *A&A* 489:943–951. <https://doi.org/10.1051/0004-6361/200810456>. [arXiv:0807.3331](https://arxiv.org/abs/0807.3331)
- Pakmor R, Kromer M, Röpke FK, et al. (2010) Sub-luminous type ia supernovae from the mergers of equal-mass white dwarfs with mass $\sim 0.9m_{\odot}$.

- Nature 463:61–64. <https://doi.org/10.1038/nature08642>. arXiv:0911.0926
- Pakmor R, Edelmann P, Roepke FK, Hillebrandt W (2011) Stellar gadget, in preparation
- Pakmor R, Kromer M, Taubenberger S, et al. (2012) Normal Type Ia supernovae from violent mergers of white dwarf binaries. *ApJ Lett.* 747:L10. <https://doi.org/10.1088/2041-8205/747/1/L10>. arXiv:1201.5123 [astro-ph.HE]
- Pakmor R, Kromer M, Taubenberger S, Springel V (2013) Helium-ignited violent mergers as a unified model for normal and rapidly declining type Ia supernovae. *ApJ Lett.* 770:L8. <https://doi.org/10.1088/2041-8205/770/1/L8>. arXiv:1302.2913 [astro-ph.HE]
- Pakmor R, Springel V, Bauer A, et al. (2016) Improving the convergence properties of the moving-mesh code AREPO. *MNRAS* 455(1):1134–1143. <https://doi.org/10.1093/mnras/stv2380>. arXiv:1503.00562 [astro-ph.GA]
- Pakmor R, Zenati Y, Perets HB, Toonen S (2021) Thermonuclear explosion of a massive hybrid HeCO white dwarf triggered by a He detonation on a companion. *MNRAS* 503(4):4734–4747. <https://doi.org/10.1093/mnras/stab686>. arXiv:2103.06277 [astro-ph.SR]
- Pakmor R, Callan FP, Collins CE, et al. (2022) On the fate of the secondary white dwarf in double-degenerate double-detonation Type Ia supernovae. *MNRAS* 517(4):5260–5271. <https://doi.org/10.1093/mnras/stac3107>. arXiv:2203.14990 [astro-ph.SR]
- Pakmor R, Seitzzahl IR, Ruiter AJ, et al. (2024) Type Ia supernova explosion models are inherently multidimensional. arXiv e-prints arXiv:2402.11010. <https://doi.org/10.48550/arXiv.2402.11010>. arXiv:2402.11010 [astro-ph.HE]
- Palicio PA, Matteucci F, Della Valle M, Spitoni E (2024) Cosmic Type Ia supernova rate and constraints on supernova Ia progenitors. *A&A* 689:A203. <https://doi.org/10.1051/0004-6361/202449740>
- Pan KC, Ricker PM, Taam RE (2013) Evolution of Post-impact Remnant Helium Stars in Type Ia Supernova Remnants within the Single-degenerate Scenario. *ApJ* 773(1):49. <https://doi.org/10.1088/0004-637X/773/1/49>. arXiv:1303.1228 [astro-ph.HE]
- Pan YC (2020) High-velocity Type Ia Supernova Has a Unique Host Environment. *ApJ Lett.* 895(1):L5. <https://doi.org/10.3847/2041-8213/ab8e47>. arXiv:2004.14544 [astro-ph.HE]
- Pankey TJ (1962) Possible thermonuclear activities in natural terrestrial minerals. PhD thesis, Howard University
- Panther FH, Seitzzahl IR, Ruiter AJ, et al. (2019) SN1991bg-like supernovae are associated with old stellar populations. *PASA* 36:e031. <https://doi.org/10.1017/pasa.2019.24>. arXiv:1904.10139 [astro-ph.GA]
- Pascale M, Frye BL, Pierel JDR, et al. (2024) SN H0pe: The First Measurement of H_0 from a Multiply-Imaged Type Ia Supernova, Discovered by JWST. arXiv e-prints arXiv:2403.18902 [astro-ph.CO]
- Patat F (2017) Introduction to Supernova Polarimetry. In: Alsabti AW, Murdin P (eds) *Handbook of Supernovae*. Springer, Cham, p 1017. https://doi.org/10.1007/978-3-319-21846-5_110

- Patat F, Benetti S, Cappellaro E, Turatto M (2006) Reflections on reflexions – II. Effects of light echoes on the luminosity and spectra of Type Ia supernovae. *MNRAS* 369(4):1949–1960. <https://doi.org/10.1111/j.1365-2966.2006.10451.x>. [arXiv:astro-ph/0512574](https://arxiv.org/abs/astro-ph/0512574) [astro-ph]
- Patat F, Chandra P, Chevalier R, et al. (2007) Detection of circumstellar material in a normal Type Ia supernova. *Science* 317:924–926. <https://doi.org/10.1126/science.1143005>. [arXiv:0707.2793](https://arxiv.org/abs/0707.2793)
- Patel B, McCully C, Jha SW, et al. (2014) Three Gravitationally Lensed Supernovae behind CLASH Galaxy Clusters. *ApJ* 786(1):9. <https://doi.org/10.1088/0004-637X/786/1/9>. [arXiv:1312.0943](https://arxiv.org/abs/1312.0943) [astro-ph.CO]
- Patterson J, Oksanen A, Kemp J, et al. (2017) T Pyxidis: death by a thousand novae. *MNRAS* 466(1):581–592. <https://doi.org/10.1093/mnras/stw2970>. [arXiv:1603.00291](https://arxiv.org/abs/1603.00291) [astro-ph.SR]
- Patterson MT, Bellm EC, Rusholme B, et al. (2019) The Zwicky Transient Facility Alert Distribution System. *PASP* 131(995):018001. <https://doi.org/10.1088/1538-3873/aae904>. [arXiv:1902.02227](https://arxiv.org/abs/1902.02227) [astro-ph.IM]
- Pearson J, Sand DJ, Lundqvist P, et al. (2024) Strong Carbon Features and a Red Early Color in the Underluminous Type Ia SN 2022xkq. *ApJ* 960(1):29. <https://doi.org/10.3847/1538-4357/ad0153>. [arXiv:2309.10054](https://arxiv.org/abs/2309.10054) [astro-ph.HE]
- Pelisoli I, Neunteufel P, Geier S, et al. (2021) A hot subdwarf-white dwarf super-Chandrasekhar candidate supernova Ia progenitor. *Nature Astronomy* 5:1052–1061. <https://doi.org/10.1038/s41550-021-01413-0>. [arXiv:2107.09074](https://arxiv.org/abs/2107.09074) [astro-ph.SR]
- Penney R, Hoefflich P (2014) Thermonuclear Supernovae: Probing Magnetic Fields by Positrons and Late-time IR Line Profiles. *ApJ* 795(1):84. <https://doi.org/10.1088/0004-637X/795/1/84>. [arXiv:1409.2159](https://arxiv.org/abs/1409.2159) [astro-ph.HE]
- Perets HB, Gal-Yam A, Mazzali PA, et al. (2010) A faint type of supernova from a white dwarf with a helium-rich companion. *Nature* 465:322–325. <https://doi.org/10.1038/nature09056>. [arXiv:0906.2003](https://arxiv.org/abs/0906.2003)
- Perlmutter S, Aldering G, Goldhaber G, et al. (1999) Measurements of Omega and Lambda from 42 high-redshift supernovae. *ApJ* 517:565–586. <https://doi.org/10.1086/307221>. [arXiv:astro-ph/9812133](https://arxiv.org/abs/astro-ph/9812133)
- Peters PC (1964) Gravitational radiation and the motion of two point masses. *Phys Rev* 136:B1224–B1232. <https://doi.org/10.1103/PhysRev.136.B1224>
- Phillips MM (1993) The absolute magnitudes of Type Ia supernovae. *ApJ Lett.* 413:L105–L108. <https://doi.org/10.1086/186970>
- Phillips MM, Burns CR (2017) The Peak Luminosity - Decline Rate Relationship for Type Ia Supernovae. In: Alsabti AW, Murdin P (eds) *Handbook of Supernovae*. Springer, Cham, p 2543. https://doi.org/10.1007/978-3-319-21846-5_100
- Phillips MM, Wells LA, Suntzeff NB, et al. (1992) SN 1991T – Further evidence of the heterogeneous nature of type Ia supernovae. *AJ* 103:1632–1637. <https://doi.org/10.1086/116177>
- Phillips MM, Lira P, Suntzeff NB, et al. (1999) The reddening-free decline rate versus luminosity relationship for Type Ia supernovae. *AJ* 118:1766–1776.

- <https://doi.org/10.1086/301032>. [arXiv:astro-ph/9907052](https://arxiv.org/abs/astro-ph/9907052)
- Pierel JDR, Rodney S, Vernardos G, et al. (2021) Projected Cosmological Constraints from Strongly Lensed Supernovae with the Roman Space Telescope. *ApJ* 908(2):190. <https://doi.org/10.3847/1538-4357/abd8d3>. [arXiv:2010.12399](https://arxiv.org/abs/2010.12399) [astro-ph.CO]
- Pierel JDR, Newman AB, Dhawan S, et al. (2024) Lensed Type Ia Supernova “Encore” at $z = 2$: The First Instance of Two Multiply Imaged Supernovae in the Same Host Galaxy. *ApJ Lett.* 967(2):L37. <https://doi.org/10.3847/2041-8213/ad4648>. [arXiv:2404.02139](https://arxiv.org/abs/2404.02139) [astro-ph.CO]
- Piersanti L, Gagliardi S, Iben J Icko, Tornambé A (2003) Carbon-Oxygen White Dwarf Accreting CO-Rich Matter. II. Self-Regulating Accretion Process up to the Explosive Stage. *ApJ* 598(2):1229–1238. <https://doi.org/10.1086/378952>
- Piersanti L, Tornambé A, Yungelson LR (2014) He-accreting white dwarfs: accretion regimes and final outcomes. *MNRAS* 445(3):3239–3262. <https://doi.org/10.1093/mnras/stu1885>. [arXiv:1409.3589](https://arxiv.org/abs/1409.3589) [astro-ph.SR]
- Piro AL, Bildsten L (2008) Neutronization during type Ia supernova simmering. *ApJ* 673:1009–1013. <https://doi.org/10.1086/524189>. [arXiv:0710.1600](https://arxiv.org/abs/0710.1600)
- Piro AL, Chang P (2008) Convection during the late stages of simmering in Type Ia supernovae. *ApJ* 678:1158–1164. <https://doi.org/10.1086/529368>. [arXiv:0801.1321](https://arxiv.org/abs/0801.1321)
- Piro AL, Morozova VS (2016) Exploring the Potential Diversity of Early Type Ia Supernova Light Curves. *ApJ* 826(1):96. <https://doi.org/10.3847/0004-637X/826/1/96>. [arXiv:1512.03442](https://arxiv.org/abs/1512.03442) [astro-ph.HE]
- Piro AL, Thompson TA, Kochanek CS (2014) Reconciling ^{56}Ni production in Type Ia supernovae with double degenerate scenarios. *MNRAS* 438:3456–3464. <https://doi.org/10.1093/mnras/stt2451>. [arXiv:1308.0334](https://arxiv.org/abs/1308.0334) [astro-ph.HE]
- Plewa T, Calder AC, Lamb DQ (2004) Type Ia supernova explosion: Gravitationally confined detonation. *ApJ Lett.* 612:L37–L40. <https://doi.org/10.1086/424036>. [arXiv:astro-ph/0405163](https://arxiv.org/abs/astro-ph/0405163)
- Polin A, Nugent P, Kasen D (2019) Observational Predictions for Sub-Chandrasekhar Mass Explosions: Further Evidence for Multiple Progenitor Systems for Type Ia Supernovae. *ApJ* 873(1):84. <https://doi.org/10.3847/1538-4357/aafb6a>. [arXiv:1811.07127](https://arxiv.org/abs/1811.07127) [astro-ph.HE]
- Polin A, Nugent P, Kasen D (2021) Nebular Models of Sub-Chandrasekhar Mass Type Ia Supernovae: Clues to the Origin of Ca-rich Transients. *ApJ* 906(1):65. <https://doi.org/10.3847/1538-4357/abcccc>. [arXiv:1910.12434](https://arxiv.org/abs/1910.12434) [astro-ph.HE]
- Poludnenko AY, Chambers J, Ahmed K, Gamezo VN, Taylor BD (2019) A unified mechanism for unconfined deflagration-to-detonation transition in terrestrial chemical systems and type Ia supernovae. *Science* 366(6465):aau7365. <https://doi.org/10.1126/science.aau7365>. [arXiv:1911.00050](https://arxiv.org/abs/1911.00050) [astro-ph.HE]
- Postnov KA, Yungelson LR (2014) The Evolution of Compact Binary Star Systems. *Living Rev Relativ* 17:3. <https://doi.org/10.12942/lrr-2014-3>.

- [arXiv:1403.4754](#) [astro-ph.HE]
- Poznanski D, Butler N, Filippenko AV, et al. (2009) Improved Standardization of Type II-P Supernovae: Application to an Expanded Sample. *ApJ* 694(2):1067–1079. <https://doi.org/10.1088/0004-637X/694/2/1067>. [arXiv:0810.4923](#) [astro-ph]
- Poznanski D, Chornock R, Nugent PE, et al. (2010) An Unusually Fast-Evolving Supernova. *Science* 327(5961):58. <https://doi.org/10.1126/science.1181709>. [arXiv:0911.2699](#) [astro-ph.SR]
- Prajs S, Sullivan M, Smith M, et al. (2017) The volumetric rate of superluminous supernovae at $z \sim 1$. *MNRAS* 464(3):3568–3579. <https://doi.org/10.1093/mnras/stw1942>. [arXiv:1605.05250](#) [astro-ph.HE]
- Prialnik D, Kovetz A (1995) An extended grid of multicycle nova evolution models. *ApJ* 445:789–810. <https://doi.org/10.1086/175741>
- Pruzhinskaya MV, Novinskaya AK, Pauna N, Rosnet P (2020) The dependence of Type Ia Supernovae SALT2 light-curve parameters on host galaxy morphology. *MNRAS* 499(4):5121–5135. <https://doi.org/10.1093/mnras/staa3173>. [arXiv:2006.09433](#) [astro-ph.CO]
- Pskovskii IP (1977) Light curves, color curves, and expansion velocity of type I supernovae as functions of the rate of brightness decline. *Soviet Astronomy* 21:675–682
- Qin YJ, Zabludoff A, Arcavi I, et al. (2024) The statistics and environments of hostless supernovae. *MNRAS* 530(4):4695–4711. <https://doi.org/10.1093/mnras/stae887>. [arXiv:2409.13804](#) [astro-ph.SR]
- Raddi R, Hollands MA, Gänsicke BT, et al. (2018) Anatomy of the hyper-runaway star LP 40-365 with Gaia. *MNRAS* 479(1):L96–L101. <https://doi.org/10.1093/mnrasl/sly103>. [arXiv:1804.09677](#) [astro-ph.SR]
- Raddi R, Hollands MA, Koester D, et al. (2019) Partly burnt runaway stellar remnants from peculiar thermonuclear supernovae. *MNRAS* 489(2):1489–1508. <https://doi.org/10.1093/mnras/stz1618>. [arXiv:1902.05061](#) [astro-ph.SR]
- Rahman N, Janka HT, Stockinger G, Woosley SE (2022) Pulsational pair-instability supernovae: gravitational collapse, black hole formation, and beyond. *MNRAS* 512(3):4503–4540. <https://doi.org/10.1093/mnras/stac758>. [arXiv:2112.09707](#) [astro-ph.HE]
- Rajamuthukumar AS, Hamers AS, Neunteufel P, Pakmor R, de Mink SE (2023) Triple Evolution: An Important Channel in the Formation of Type Ia Supernovae. *ApJ* 950(1):9. <https://doi.org/10.3847/1538-4357/acc86c>. [arXiv:2211.04463](#) [astro-ph.SR]
- Ramsay G, Green MJ, Marsh TR, et al. (2018) Physical properties of AM CVn stars: New insights from Gaia DR2. *A&A* 620:A141. <https://doi.org/10.1051/0004-6361/201834261>. [arXiv:1810.06548](#) [astro-ph.SR]
- Raskin C, Kasen D (2013) Tidal Tail Ejection as a Signature of Type Ia Supernovae from White Dwarf Mergers. *ApJ* 772(1):1. <https://doi.org/10.1088/0004-637X/772/1/1>. [arXiv:1304.4957](#) [astro-ph.HE]
- Raskin C, Timmes FX, Scannapieco E, Diehl S, Fryer C (2009) On Type Ia supernovae from the collisions of two white dwarfs. *MNRAS* 399:L156–L159.

- <https://doi.org/10.1111/j.1745-3933.2009.00743.x>. arXiv:0907.3915 [astro-ph.SR]
- Raskin C, Kasen D, Moll R, Schwab J, Woosley S (2014) Type Ia Supernovae from Merging White Dwarfs. II. Post-merger Detonations. *ApJ* 788:75. <https://doi.org/10.1088/0004-637X/788/1/75>. arXiv:1312.3649 [astro-ph.HE]
- Rebassa-Mansergas A, Toonen S, Korol V, Torres S (2019) Where are the double-degenerate progenitors of Type Ia supernovae? *MNRAS* 482(3):3656–3668. <https://doi.org/10.1093/mnras/sty2965>. arXiv:1809.07158 [astro-ph.SR]
- Reinecke M, Hillebrandt W, Niemeyer JC (1999) Thermonuclear explosions of Chandrasekhar-mass C+O white dwarfs. *A&A* 347:739–747. arXiv:astro-ph/9812120
- Rest A, Suntzeff NB, Olsen K, et al. (2005) Light echoes from ancient supernovae in the Large Magellanic Cloud. *Nature* 438(7071):1132–1134. <https://doi.org/10.1038/nature04365>. arXiv:astro-ph/0510738 [astro-ph]
- Riess AG, Filippenko AV, Challis P, et al. (1998) Observational evidence from supernovae for an accelerating universe and a cosmological constant. *AJ* 116:1009–1038. <https://doi.org/10.1086/300499>. arXiv:astro-ph/9805201
- Rigault M, Brinnel V, Aldering G, et al. (2020) Strong dependence of Type Ia supernova standardization on the local specific star formation rate. *A&A* 644:A176. <https://doi.org/10.1051/0004-6361/201730404>. arXiv:1806.03849 [astro-ph.CO]
- Riley J, Agrawal P, Barrett JW, et al. (2022) Rapid Stellar and Binary Population Synthesis with COMPAS. *ApJS* 258(2):34. <https://doi.org/10.3847/1538-4365/ac416c>. arXiv:2109.10352 [astro-ph.IM]
- Rodney SA, Riess AG, Strolger LG, et al. (2014) Type Ia Supernova Rate Measurements to Redshift 2.5 from CANDELS: Searching for Prompt Explosions in the Early Universe. *AJ* 148(1):13. <https://doi.org/10.1088/0004-6256/148/1/13>. arXiv:1401.7978 [astro-ph.CO]
- Rodney SA, Brammer GB, Pierel JDR, et al. (2021) A gravitationally lensed supernova with an observable two-decade time delay. *Nature Astronomy* 5:1118–1125. <https://doi.org/10.1038/s41550-021-01450-9>. arXiv:2106.08935 [astro-ph.CO]
- Rodríguez Ó, Meza N, Pineda-García J, Ramirez M (2021) The iron yield of normal Type II supernovae. *MNRAS* 505(2):1742–1774. <https://doi.org/10.1093/mnras/stab1335>. arXiv:2105.03268 [astro-ph.SR]
- Rodríguez Ó, Maoz D, Nakar E (2023) The Iron Yield of Core-collapse Supernovae. *ApJ* 955(1):71. <https://doi.org/10.3847/1538-4357/ace2bd>. arXiv:2209.05552 [astro-ph.HE]
- Roelofs GHA, Nelemans G, Groot PJ (2007) The population of AM CVn stars from the Sloan Digital Sky Survey. *MNRAS* 382(2):685–692. <https://doi.org/10.1111/j.1365-2966.2007.12451.x>. arXiv:0709.2951 [astro-ph]
- Röpke FK (2017) Combustion in Thermonuclear Supernova Explosions. In: Alsabti AW, Murdin P (eds) *Handbook of Supernovae*. Springer, Cham, p 1185. https://doi.org/10.1007/978-3-319-21846-5_58

- Röpke FK, De Marco O (2023) Simulations of common-envelope evolution in binary stellar systems: physical models and numerical techniques. *Living Rev Comput Astrophys* 9:2. <https://doi.org/10.1007/s41115-023-00017-x>. [arXiv:2212.07308](https://arxiv.org/abs/2212.07308) [astro-ph.SR]
- Röpke FK, Hillebrandt W (2005) Full-star type Ia supernova explosion models. *A&A* 431:635–645. <https://doi.org/10.1051/0004-6361:20041859>. [arXiv:astro-ph/0409286](https://arxiv.org/abs/astro-ph/0409286)
- Röpke FK, Sim SA (2018) Models for type ia supernovae and related astrophysical transients. *Space Sci. Rev.* 214:1–17
- Röpke FK, Hillebrandt W, Niemeyer JC, Woosley SE (2006) Multi-spot ignition in type Ia supernova models. *A&A* 448:1–14. <https://doi.org/10.1051/0004-6361:20053926>. [arXiv:astro-ph/0510474](https://arxiv.org/abs/astro-ph/0510474)
- Röpke FK, Hillebrandt W, Schmidt W, et al. (2007) A three-dimensional deflagration model for Type Ia supernovae compared with observations. *ApJ* 668:1132–1139. <https://doi.org/10.1086/521347>. [arXiv:0707.1024](https://arxiv.org/abs/0707.1024)
- Röpke FK, Kromer M, Seitenzahl IR, et al. (2012) Constraining Type Ia Supernova Models: SN 2011fe as a Test Case. *ApJ Lett.* 750:L19. <https://doi.org/10.1088/2041-8205/750/1/L19>. [arXiv:1203.4839](https://arxiv.org/abs/1203.4839) [astro-ph.SR]
- Rosswoog S, Kasen D, Guillochon J, Ramirez-Ruiz E (2009) Collisions of white dwarfs as a new progenitor channel for Type Ia supernovae. *ApJ Lett.* 705:L128–L132. <https://doi.org/10.1088/0004-637X/705/2/L128>. [arXiv:0907.3196](https://arxiv.org/abs/0907.3196) [astro-ph.HE]
- Roy NC, Tiwari V, Bobrick A, et al. (2022) 3D Hydrodynamical Simulations of Helium-ignited Double-degenerate White Dwarf Mergers. *ApJ Lett.* 932(2):L24. <https://doi.org/10.3847/2041-8213/ac75e7>. [arXiv:2204.09683](https://arxiv.org/abs/2204.09683) [astro-ph.SR]
- Rubin D, Hayden B, Huang X, et al. (2018) The Discovery of a Gravitationally Lensed Supernova Ia at Redshift 2.22. *ApJ* 866(1):65. <https://doi.org/10.3847/1538-4357/aad565>. [arXiv:1707.04606](https://arxiv.org/abs/1707.04606) [astro-ph.GA]
- Ruiter AJ (2020) Type Ia supernova sub-classes and progenitor origin. *IAU Symposium* 357:1–15. <https://doi.org/10.1017/S1743921320000587>. [arXiv:2001.02947](https://arxiv.org/abs/2001.02947) [astro-ph.SR]
- Ruiter AJ, Belczynski K, Fryer C (2009) Rates and delay times of type ia supernovae. *ApJ* 699:2026–2036. <https://doi.org/10.1088/0004-637X/699/2/2026>. [arXiv:0904.3108](https://arxiv.org/abs/0904.3108)
- Ruiter AJ, Belczynski K, Sim SA, et al. (2011) Delay times and rates for type ia supernovae and thermonuclear explosions from double-detonation sub-chandrasekhar mass models. *MNRAS* 417:408–419. <https://doi.org/10.1111/j.1365-2966.2011.19276.x>. [arXiv:1011.1407](https://arxiv.org/abs/1011.1407) [astro-ph.SR]
- Ruiter AJ, Sim SA, Pakmor R, et al. (2013) On the brightness distribution of type ia supernovae from violent white dwarf mergers. *MNRAS* 429:1425–1436. <https://doi.org/10.1093/mnras/sts423>. [arXiv:1209.0645](https://arxiv.org/abs/1209.0645) [astro-ph.SR]
- Ruiter AJ, Belczynski K, Sim SA, Seitenzahl IR, Kwiatkowski D (2014) The effect of helium accretion efficiency on rates of Type Ia supernovae: double detonations in accreting binaries. *MNRAS* 440:L101–L105. <https://doi.org/10.1093/mnras/flu030>. [arXiv:1401.0341](https://arxiv.org/abs/1401.0341) [astro-ph.SR]

- Ruiter AJ, Ferrario L, Belczynski K, et al. (2019) On the formation of neutron stars via accretion-induced collapse in binaries. *MNRAS* <https://doi.org/10.1093/mnras/stz001>. [arXiv:1802.02437](https://arxiv.org/abs/1802.02437) [astro-ph.SR]
- Ruiz-Lapuente P (2019) Surviving companions of Type Ia supernovae: theory and observations. *New Astron. Rev.* 85:101523. <https://doi.org/10.1016/j.newar.2019.101523>. [arXiv:1812.04977](https://arxiv.org/abs/1812.04977) [astro-ph.SR]
- Ruiz-Lapuente P, Comeron F, Méndez J, et al. (2004) The binary progenitor of Tycho Brahe's 1572 supernova. *Nature* 431:1069–1072. <https://doi.org/10.1038/nature03006>. [arXiv:astro-ph/0410673](https://arxiv.org/abs/astro-ph/0410673)
- Rust BW (1974) The use of supernovae light curves for testing the expansion hypothesis and other cosmological relations. PhD thesis, University of Illinois, Urbana-Champaign
- Saio H, Nomoto K (1985) Evolution of a merging pair of C+O white dwarfs to form a single neutron star. *A&A* 150:L21–L23
- Samland M, Hensler G, Theis C (1997) Modeling the Evolution of Disk Galaxies. I. The Chemodynamical Method and the Galaxy Model. *ApJ* 476(2):544–559. <https://doi.org/10.1086/303627>
- Sand DJ, Graham ML, Bildfell C, et al. (2012) The multi-epoch nearby cluster survey: Type Ia supernova rate measurement in $z \sim 0.1$ clusters and the late-time delay time distribution. *ApJ* 746:163. <https://doi.org/10.1088/0004-637X/746/2/163>. [arXiv:1110.1632](https://arxiv.org/abs/1110.1632) [astro-ph.CO]
- Sanders JL, Belokurov V, Man KTF (2021) Evidence for sub-Chandrasekhar Type Ia supernovae from the last major merger. *MNRAS* 506(3):4321–4343. <https://doi.org/10.1093/mnras/stab1951>. [arXiv:2106.11324](https://arxiv.org/abs/2106.11324) [astro-ph.GA]
- Saselli M, Mazzali PA, Pian E, et al. (2014) Abundance stratification in Type Ia supernovae - IV. The luminous, peculiar SN 1991T. *MNRAS* 445(1):711–725. <https://doi.org/10.1093/mnras/stu1777>. [arXiv:1409.0116](https://arxiv.org/abs/1409.0116) [astro-ph.SR]
- Sato Y, Nakasato N, Tanikawa A, et al. (2015) A Systematic Study of Carbon-Oxygen White Dwarf Mergers: Mass Combinations for Type Ia Supernovae. *ApJ* 807:105. <https://doi.org/10.1088/0004-637X/807/1/105>. [arXiv:1505.01646](https://arxiv.org/abs/1505.01646) [astro-ph.HE]
- Sato Y, Nakasato N, Tanikawa A, et al. (2016) The Critical Mass Ratio of Double White Dwarf Binaries for Violent Merger-induced Type Ia Supernova Explosions. *ApJ* 821(1):67. <https://doi.org/10.3847/0004-637X/821/1/67>. [arXiv:1603.01088](https://arxiv.org/abs/1603.01088) [astro-ph.HE]
- Savonije GJ, de Kool M, van den Heuvel EPJ (1986) The minimum orbital period for ultra-compact binaries with the helium burning secondaries. *A&A* 155:51–57
- Scalzo RA, Ruiter AJ, Sim SA (2014) The ejected mass distribution of Type Ia supernovae: a significant rate of non-Chandrasekhar-mass progenitors. *MNRAS* 445:2535–2544. <https://doi.org/10.1093/mnras/stu1808>. [arXiv:1408.6601](https://arxiv.org/abs/1408.6601) [astro-ph.HE]
- Scalzo RA, Yuan F, Childress MJ, et al. (2017) The SkyMapper Transient Survey. *PASA* 34:e030. <https://doi.org/10.1017/pasa.2017.24>. [arXiv:1702.05585](https://arxiv.org/abs/1702.05585) [astro-ph.IM]

- Scalzo RA, Parent E, Burns C, et al. (2019) Probing Type Ia supernova properties using bolometric light curves from the Carnegie Supernova Project and the CfA Supernova Group. *MNRAS* 483(1):628–647. <https://doi.org/10.1093/mnras/sty3178>. [arXiv:1811.08969](https://arxiv.org/abs/1811.08969) [astro-ph.HE]
- Scannapieco E, Bildsten L (2005) The Type Ia Supernova Rate. *ApJ Lett.* 629:L85–L88. <https://doi.org/10.1086/452632>. [arXiv:astro-ph/0507456](https://arxiv.org/abs/astro-ph/0507456)
- Schaefer BE (2023) The path from the Chinese and Japanese observations of supernova 1181 AD, to a Type Iax supernova, to the merger of CO and ONe white dwarfs. *MNRAS* 523(3):3885–3904. <https://doi.org/10.1093/mnras/stad717>. [arXiv:2301.04807](https://arxiv.org/abs/2301.04807) [astro-ph.SR]
- Schaefer BE, Pagnotta A (2012) An absence of ex-companion stars in the Type Ia supernova remnant SNR 0509-67.5. *Nature* 481:164–166. <https://doi.org/10.1038/nature10692>
- Schmidt BP, Kirshner RP, Leibundgut B, et al. (1994) SN 1991T: Reflections of Past Glory. *ApJ Lett.* 434:L19. <https://doi.org/10.1086/187562>. [arXiv:astro-ph/9407097](https://arxiv.org/abs/astro-ph/9407097) [astro-ph]
- Schmidt BP, Suntzeff NB, Phillips MM, et al. (1998) The High-Z Supernova Search: Measuring Cosmic Deceleration and Global Curvature of the Universe Using Type Ia Supernovae. *ApJ* 507:46–63. <https://doi.org/10.1086/306308>. [arXiv:astro-ph/9805200](https://arxiv.org/abs/astro-ph/9805200)
- Schmidt W, Ciaraldi-Schoolmann F, Niemeyer JC, Röpke FK, Hillebrandt W (2010) Turbulence in a three-dimensional deflagration model for Type Ia supernovae. II. Intermittency and the deflagration-to-detonation transition probability. *ApJ* 710:1683–1693. <https://doi.org/10.1088/0004-637X/710/2/1683>. [arXiv:0911.4345](https://arxiv.org/abs/0911.4345)
- Schwab J (2021) Evolutionary Models for the Remnant of the Merger of Two Carbon-Oxygen Core White Dwarfs. *ApJ* 906(1):53. <https://doi.org/10.3847/1538-4357/abc87e>. [arXiv:2011.03546](https://arxiv.org/abs/2011.03546) [astro-ph.SR]
- Schwab J, Shen KJ, Quataert E, Dan M, Rosswog S (2012) The viscous evolution of white dwarf merger remnants. *MNRAS* 427(1):190–203. <https://doi.org/10.1111/j.1365-2966.2012.21993.x>. [arXiv:1207.0512](https://arxiv.org/abs/1207.0512) [astro-ph.HE]
- Scolnic D, Brout D, Carr A, et al. (2022) The Pantheon+ Analysis: The Full Data Set and Light-curve Release. *ApJ* 938(2):113. <https://doi.org/10.3847/1538-4357/ac8b7a>. [arXiv:2112.03863](https://arxiv.org/abs/2112.03863) [astro-ph.CO]
- Scolnic DM, Jones DO, Rest A, et al. (2018) The Complete Light-curve Sample of Spectroscopically Confirmed SNe Ia from Pan-STARRS1 and Cosmological Constraints from the Combined Pantheon Sample. *ApJ* 859(2):101. <https://doi.org/10.3847/1538-4357/aab9bb>. [arXiv:1710.00845](https://arxiv.org/abs/1710.00845) [astro-ph.CO]
- Seitenzahl IR, Pakmor R (2023) Nucleosynthesis and tracer methods in Type Ia supernovae. *Handbook of Nuclear Physics* pp 3809–3842
- Seitenzahl IR, Townsley DM (2017) Nucleosynthesis in Thermonuclear Supernovae. In: Alsabti AW, Murdin P (eds) *Handbook of Supernovae*. Springer, Cham, p 1955. https://doi.org/10.1007/978-3-319-21846-5_87
- Seitenzahl IR, Meakin CA, Lamb DQ, Truran JW (2009a) Initiation of the detonation in the gravitationally confined detonation model of Type Ia

- supernovae. *ApJ* 700:642–653. <https://doi.org/10.1088/0004-637X/700/1/642>. [arXiv:0905.3104](https://arxiv.org/abs/0905.3104)
- Seitenzahl IR, Meakin CA, Townsley DM, Lamb DQ, Truran JW (2009b) Spontaneous initiation of detonations in white dwarf environments: Determination of critical sizes. *ApJ* 696:515–527. <https://doi.org/10.1088/0004-637X/696/1/515>. [arXiv:0901.3677](https://arxiv.org/abs/0901.3677)
- Seitenzahl IR, Taubenberger S, Sim SA (2009c) Late-time supernova light curves: the effect of internal conversion and Auger electrons. *MNRAS* 400:531–535. <https://doi.org/10.1111/j.1365-2966.2009.15478.x>. [arXiv:0908.0247](https://arxiv.org/abs/0908.0247) [astro-ph.SR]
- Seitenzahl IR, Townsley DM, Peng F, Truran JW (2009d) Nuclear statistical equilibrium for Type Ia supernova simulations. *Atomic Data and Nuclear Data Tables* 95:96–114. <https://doi.org/10.1016/j.adt.2008.08.001>
- Seitenzahl IR, Cescutti G, Röpke FK, Ruiter AJ, Pakmor R (2013a) Solar abundance of manganese: a case for near chandrasekhar-mass Type Ia supernova progenitors. *A&A* 559:L5. <https://doi.org/10.1051/0004-6361/201322599>. [arXiv:1309.2397](https://arxiv.org/abs/1309.2397) [astro-ph.SR]
- Seitenzahl IR, Ciaraldi-Schoolmann F, Röpke FK, et al. (2013b) Three-dimensional delayed-detonation models with nucleosynthesis for Type Ia supernovae. *MNRAS* 429:1156–1172. <https://doi.org/10.1093/mnras/sts402>. [arXiv:1211.3015](https://arxiv.org/abs/1211.3015) [astro-ph.SR]
- Seitenzahl IR, Kromer M, Ohlmann ST, et al. (2016) Three-dimensional simulations of gravitationally confined detonations compared to observations of SN 1991T. *A&A* 592:A57. <https://doi.org/10.1051/0004-6361/201527251>. [arXiv:1606.00089](https://arxiv.org/abs/1606.00089) [astro-ph.SR]
- Seitenzahl IR, Ghavamian P, Laming JM, Vogt FPA (2019) Optical Tomography of the Chemical Elements Synthesized in Type Ia Supernovae. *Phys. Rev. Lett.* 123(4):041101. <https://doi.org/10.1103/PhysRevLett.123.041101>. [arXiv:1906.05972](https://arxiv.org/abs/1906.05972) [astro-ph.SR]
- Shahaf S, Hallakoun N, Mazeh T, et al. (2024) Triage of the Gaia DR3 astrometric orbits. II. A census of white dwarfs. *MNRAS* 529(4):3729–3743. <https://doi.org/10.1093/mnras/stae773>. [arXiv:2309.15143](https://arxiv.org/abs/2309.15143) [astro-ph.SR]
- Shappee BJ, Kochanek CS, Stanek KZ (2013) Type Ia Single Degenerate Survivors must be Overluminous. *ApJ* 765(2):150. <https://doi.org/10.1088/0004-637X/765/2/150>. [arXiv:1205.5028](https://arxiv.org/abs/1205.5028) [astro-ph.SR]
- Sharma S, Hayden MR, Bland-Hawthorn J, et al. (2022) The GALAH Survey: dependence of elemental abundances on age and metallicity for stars in the Galactic disc. *MNRAS* 510(1):734–752. <https://doi.org/10.1093/mnras/stab3341>. [arXiv:2011.13818](https://arxiv.org/abs/2011.13818) [astro-ph.GA]
- Sharma Y, Sollerman J, Fremling C, et al. (2023) A Systematic Study of Ia-CSM Supernovae from the ZTF Bright Transient Survey. *ApJ* 948(1):52. <https://doi.org/10.3847/1538-4357/acbc16>. [arXiv:2301.04637](https://arxiv.org/abs/2301.04637) [astro-ph.HE]
- Shen KJ, Bildsten L (2009) Unstable helium shell burning on accreting white dwarfs. *ApJ* 699:1365–1373. <https://doi.org/10.1088/0004-637X/699/2/1365>. [arXiv:0903.0654](https://arxiv.org/abs/0903.0654)

- Shen KJ, Moore K (2014) The Initiation and Propagation of Helium Detonations in White Dwarf Envelopes. *ApJ* 797:46. <https://doi.org/10.1088/0004-637X/797/1/46>. [arXiv:1409.3568](https://arxiv.org/abs/1409.3568) [astro-ph.HE]
- Shen KJ, Bildsten L, Kasen D, Quataert E (2012) The Long-term Evolution of Double White Dwarf Mergers. *ApJ* 748(1):35. <https://doi.org/10.1088/0004-637X/748/1/35>. [arXiv:1108.4036](https://arxiv.org/abs/1108.4036) [astro-ph.HE]
- Shen KJ, Toonen S, Graur O (2017) The Evolution of the Type Ia Supernova Luminosity Function. *ApJ Lett.* 851(2):L50. <https://doi.org/10.3847/2041-8213/aaa015>. [arXiv:1710.09384](https://arxiv.org/abs/1710.09384) [astro-ph.HE]
- Shen KJ, Kasen D, Miles BJ, Townsley DM (2018) Sub-Chandrasekhar-mass White Dwarf Detonations Revisited. *ApJ* 854:52. <https://doi.org/10.3847/1538-4357/aaa8de>. [arXiv:1706.01898](https://arxiv.org/abs/1706.01898) [astro-ph.HE]
- Shen KJ, Boos SJ, Townsley DM, Kasen D (2021) Multidimensional Radiative Transfer Calculations of Double Detonations of Sub-Chandrasekhar-mass White Dwarfs. *ApJ* 922(1):68. <https://doi.org/10.3847/1538-4357/ac2304>. [arXiv:2108.12435](https://arxiv.org/abs/2108.12435) [astro-ph.SR]
- Shingles LJ, Sim SA, Kromer M, et al. (2020) Monte Carlo radiative transfer for the nebular phase of Type Ia supernovae. *MNRAS* 492(2):2029–2043. <https://doi.org/10.1093/mnras/stz3412>. [arXiv:1912.02214](https://arxiv.org/abs/1912.02214) [astro-ph.HE]
- Shingles LJ, Flörs A, Sim SA, et al. (2022) Modelling the ionization state of Type Ia supernovae in the nebular phase. *MNRAS* 512(4):6150–6163. <https://doi.org/10.1093/mnras/stac902>. [arXiv:2203.16561](https://arxiv.org/abs/2203.16561) [astro-ph.HE]
- Siebert MR, Dimitriadis G, Polin A, Foley RJ (2020) Strong Calcium Emission Indicates that the Ultraviolet-flashing SN Ia 2019yvy Was the Result of a Sub-Chandrasekhar-mass Double-detonation Explosion. *ApJ Lett.* 900(2):L27. <https://doi.org/10.3847/2041-8213/abae6e>. [arXiv:2007.13793](https://arxiv.org/abs/2007.13793) [astro-ph.HE]
- Silverman JM, Ganeshalingam M, Li W, et al. (2011) Fourteen months of observations of the possible super-Chandrasekhar mass Type Ia Supernova 2009dc. *MNRAS* 410:585–611. <https://doi.org/10.1111/j.1365-2966.2010.17474.x>. [arXiv:1003.2417](https://arxiv.org/abs/1003.2417) [astro-ph.HE]
- Silverman JM, Nugent PE, Gal-Yam A, et al. (2013) Type Ia Supernovae Strongly Interacting with Their Circumstellar Medium. *ApJS* 207(1):3. <https://doi.org/10.1088/0067-0049/207/1/3>. [arXiv:1304.0763](https://arxiv.org/abs/1304.0763) [astro-ph.CO]
- Silverman JM, Vinkó J, Marion GH, et al. (2015) High-velocity features of calcium and silicon in the spectra of Type Ia supernovae. *MNRAS* 451(2):1973–2014. <https://doi.org/10.1093/mnras/stv1011>. [arXiv:1502.07278](https://arxiv.org/abs/1502.07278) [astro-ph.HE]
- Sim SA, Röpke FK, Hillebrandt W, et al. (2010) Detonations in sub-chandrasekhar-mass c+o white dwarfs. *ApJ Lett.* 714:L52–L57. <https://doi.org/10.1088/2041-8205/714/1/L52>. [arXiv:1003.2917](https://arxiv.org/abs/1003.2917)
- Sim SA, Fink M, Kromer M, et al. (2012) 2D simulations of the double-detonation model for thermonuclear transients from low-mass carbon-oxygen white dwarfs. *MNRAS* 420:3003–3016. <https://doi.org/10.1111/j.1365-2966.2011.20162.x>. [arXiv:1111.2117](https://arxiv.org/abs/1111.2117) [astro-ph.HE]

- Sim SA, Seitzzahl IR, Kromer M, et al. (2013) Synthetic light curves and spectra for three-dimensional delayed-detonation models of Type Ia supernovae. *MNRAS* 436:333–347. <https://doi.org/10.1093/mnras/stt1574>. [arXiv:1308.4833](https://arxiv.org/abs/1308.4833) [astro-ph.HE]
- Simionescu A, Nakashima S, Yamaguchi H, et al. (2019) Constraints on the chemical enrichment history of the Perseus Cluster of galaxies from high-resolution X-ray spectroscopy. *MNRAS* 483(2):1701–1721. <https://doi.org/10.1093/mnras/sty3220>. [arXiv:1806.00932](https://arxiv.org/abs/1806.00932) [astro-ph.HE]
- Skúladóttir Á, Puls AA, Amarsi AM, et al. (2023) The 4MOST Survey of Dwarf Galaxies and their Stellar Streams (4DWARFS). *The Messenger* 190:19–21. <https://doi.org/10.18727/0722-6691/5304>
- Soker N, Bear E (2023) The core degenerate scenario for the Type Ia supernova SN 2020eyj. *MNRAS* 521(3):4561–4567. <https://doi.org/10.1093/mnras/stad798>. [arXiv:2211.04353](https://arxiv.org/abs/2211.04353) [astro-ph.SR]
- Solheim JE, Yungelson LR (2005) The white dwarfs in am cvn systems – candidates for SN Ia? In: Koester D, Moehler S (eds) 14th European Workshop on White Dwarfs. *Astronomical Society of the Pacific Conference Series*, vol 334. p 387. [arXiv:astro-ph/0411053](https://arxiv.org/abs/astro-ph/0411053)
- Souropanis D, Chiotellis A, Boumis P, et al. (2022) Linking the properties of accreting white dwarfs with the ionization state of their ambient medium. *MNRAS* 513(2):2369–2384. <https://doi.org/10.1093/mnras/stac89010.48550>. [arXiv:2203.16647](https://arxiv.org/abs/2203.16647) [astro-ph.SR]
- Sparks WM, Stecher TP (1974) Supernova: The result of the death spiral of a white dwarf into a red giant. *ApJ* 188:149. <https://doi.org/10.1086/152697>
- Spyromilio J, Meikle WPS, Allen DA, Graham JR (1992) A large mass of iron in supernova 1991T. *MNRAS* 258:53P–56P
- Srivastav S, Moore T, Nicholl M, et al. (2023) Unprecedented Early Flux Excess in the Hybrid 02es-like Type Ia Supernova 2022ywc Indicates Interaction with Circumstellar Material. *ApJ Lett.* 956(2):L34. <https://doi.org/10.3847/2041-8213/acffaf>. [arXiv:2308.06019](https://arxiv.org/abs/2308.06019) [astro-ph.HE]
- Starrfield S, Sparks WM, Truran JW (1985) Recurrent novae as a consequence of the accretion of solar material onto a 1.38 M white dwarf. *ApJ* 291:136–146. <https://doi.org/10.1086/163048>
- Stehle M, Mazzali PA, Benetti S, Hillebrandt W (2005a) Abundance stratification in Type Ia supernovae – i. the case of SN 2002bo. *MNRAS* 360:1231–1243. <https://doi.org/10.1111/j.1365-2966.2005.09116.x>. [arXiv:astro-ph/0409342](https://arxiv.org/abs/astro-ph/0409342)
- Stehle M, Mazzali PA, Hillebrandt W (2005b) Abundance Tomography of Type Ia Supernovae. *Nucl. Phys. A* 758:470–473. <https://doi.org/10.1016/j.nuclphysa.2005.05.087>
- Sternberg A, Gal-Yam A, Simon JD, et al. (2011) Circumstellar material in Type Ia supernovae via sodium absorption features. *Science* 333:856–. <https://doi.org/10.1126/science.1203836>. [arXiv:1108.3664](https://arxiv.org/abs/1108.3664) [astro-ph.HE]
- Stritzinger M, Leibundgut B, Walch S, Contardo G (2006a) Constraints on the progenitor systems of type Ia supernovae. *A&A* 450:241–251. <https://doi.org/10.1051/0004-6361:20053652>. [arXiv:astro-ph/0506415](https://arxiv.org/abs/astro-ph/0506415)

- Stritzinger M, Mazzali PA, Sollerman J, Benetti S (2006b) Consistent estimates of ^{56}Ni yields for Type Ia supernovae. *A&A* 460:793–798. <https://doi.org/10.1051/0004-6361:20065514>. [arXiv:astro-ph/0609232](https://arxiv.org/abs/astro-ph/0609232)
- Strolger LG, Rodney SA, Pacifici C, Narayan G, Graur O (2020) Delay Time Distributions of Type Ia Supernovae from Galaxy and Cosmic Star Formation Histories. *ApJ* 890(2):140. <https://doi.org/10.3847/1538-4357/ab6a97>. [arXiv:2001.05967](https://arxiv.org/abs/2001.05967) [astro-ph.GA]
- Sullivan M (2009) SN Ia Properties from the Supernova Legacy Survey. In: Giobbi G, Tornambe A, Raimondo G, et al. (eds) *Probing Stellar Populations Out to the Distant Universe: Cefalu 2008*, Proceedings of the International Conference. American Institute of Physics Conference Series, vol 1111. pp 539–546. <https://doi.org/10.1063/1.3141606>
- Sullivan M, Ellis RS, Aldering G, et al. (2003) The Hubble diagram of type Ia supernovae as a function of host galaxy morphology. *MNRAS* 340:1057–1075. <https://doi.org/10.1046/j.1365-8711.2003.06312.x>. [arXiv:astro-ph/0211444](https://arxiv.org/abs/astro-ph/0211444)
- Sullivan M, Le Borgne D, Pritchett CJ, et al. (2006) Rates and properties of Type Ia supernovae as a function of mass and star formation in their host galaxies. *ApJ* 648:868–883. <https://doi.org/10.1086/506137>. [arXiv:astro-ph/0605455](https://arxiv.org/abs/astro-ph/0605455)
- Sullivan M, Conley A, Howell DA, et al. (2010) The dependence of Type Ia Supernovae luminosities on their host galaxies. *MNRAS* 406:782–802. <https://doi.org/10.1111/j.1365-2966.2010.16731.x>. [arXiv:1003.5119](https://arxiv.org/abs/1003.5119) [astro-ph.CO]
- Sutherland PG, Wheeler JC (1984) Models for Type I supernovae - partially incinerated white dwarfs. *ApJ* 280:282–297. <https://doi.org/10.1086/161995>
- Taam RE (1980) The long-term evolution of accreting carbon white dwarfs. *ApJ* 242:749–755. <https://doi.org/10.1086/158509>
- Takaro T, Foley RJ, McCully C, et al. (2020) Constraining Type Iax supernova progenitor systems with stellar population age dating. *MNRAS* 493(1):986–1002. <https://doi.org/10.1093/mnras/staa294>. [arXiv:1901.05461](https://arxiv.org/abs/1901.05461) [astro-ph.HE]
- Tanaka M, Mazzali PA, Stanishev V, et al. (2011) Abundance stratification in Type Ia supernovae - III. The normal SN 2003du. *MNRAS* 410(3):1725–1738. <https://doi.org/10.1111/j.1365-2966.2010.17556.x>. [arXiv:1008.3140](https://arxiv.org/abs/1008.3140) [astro-ph.SR]
- Tanikawa A (2018) High-resolution Hydrodynamic Simulation of Tidal Detonation of a Helium White Dwarf by an Intermediate Mass Black Hole. *ApJ* 858(1):26. <https://doi.org/10.3847/1538-4357/aaba79>. [arXiv:1711.05451](https://arxiv.org/abs/1711.05451) [astro-ph.HE]
- Tanikawa A, Nomoto K, Nakasato N (2018) Three-dimensional Simulation of Double Detonations in the Double-degenerate Model for Type Ia Supernovae and Interaction of Ejecta with a Surviving White Dwarf Companion. *ApJ* 868(2):90. <https://doi.org/10.3847/1538-4357/aae9ee>. [arXiv:1808.01545](https://arxiv.org/abs/1808.01545) [astro-ph.HE]
- Tanikawa A, Nomoto K, Nakasato N, Maeda K (2019) Double-detonation Models for Type Ia Supernovae: Trigger of Detonation in Companion

- White Dwarfs and Signatures of Companions' Stripped-off Materials. *ApJ* 885(2):103. <https://doi.org/10.3847/1538-4357/ab46b6>. arXiv:1909.09770 [astro-ph.HE]
- Taubenberger S (2017) The Extremes of Thermonuclear Supernovae. In: Alsabti AW, Murdin P (eds) *Handbook of Supernovae*. Springer, Cham, p 317. https://doi.org/10.1007/978-3-319-21846-5_37
- Taubenberger S, Benetti S, Childress M, et al. (2011) High luminosity, slow ejecta and persistent carbon lines: SN 2009dc challenges thermonuclear explosion scenarios. *MNRAS* 412:2735–2762. <https://doi.org/10.1111/j.1365-2966.2010.18107.x>. arXiv:1011.5665 [astro-ph.SR]
- Thielemann FK, Nomoto K, Yokoi K (1986) Explosive nucleosynthesis in carbon deflagration models of Type I supernovae. *A&A* 158:17–33
- Thielemann FK, Brachwitz F, Höflich P, Martinez-Pinedo G, Nomoto K (2004) The physics of type Ia supernovae. *New Astron. Rev.* 48(7-8):605–610. <https://doi.org/10.1016/j.newar.2003.12.038>
- Thompson TA (2011) Accelerating compact object mergers in triple systems with the kozai resonance: A mechanism for "prompt" type ia supernovae, gamma-ray bursts, and other exotica. *ApJ* 741:82. <https://doi.org/10.1088/0004-637X/741/2/82>. arXiv:1011.4322 [astro-ph.HE]
- Timmes FX, Niemeyer JC (2000) Regimes of helium burning. *ApJ* 537:993–997. <https://doi.org/10.1086/309043>. arXiv:astro-ph/0005339
- Timmes FX, Woosley SE, Weaver TA (1995) Galactic chemical evolution: Hydrogen through zinc. *ApJS* 98:617–658. <https://doi.org/10.1086/192172>. astro-ph/9411003
- Timmes FX, Brown EF, Truran JW (2003) On variations in the peak luminosity of Type Ia supernovae. *ApJ Lett.* 590:L83–L86. <https://doi.org/10.1086/376721>. arXiv:astro-ph/0305114
- Tinsley BM (1977) Masses of Supernova Progenitors. In: Schramm DN (ed) *Supernovae*. Astrophysics and Space Science Library, vol 66. D. Reidel, Dordrecht, p 117. https://doi.org/10.1007/978-94-010-1229-4_11
- Tisserand P, Crawford CL, Clayton GC, et al. (2022) The dawn of a new era for dustless HdC stars with Gaia eDR3. *A&A* 667:A83. <https://doi.org/10.1051/0004-6361/202142916>. arXiv:2112.07693 [astro-ph.SR]
- Tiwari V, Graur O, Fisher R, et al. (2022) The late-time light curves of Type Ia supernovae: confronting models with observations. *MNRAS* 515(3):3703–3715. <https://doi.org/10.1093/mnras/stac1618>. arXiv:2206.02812 [astro-ph.HE]
- Tolstoy E, Hill V, Tosi M (2009) Star-Formation Histories, Abundances, and Kinematics of Dwarf Galaxies in the Local Group. *ARA&A* 47(1):371–425. <https://doi.org/10.1146/annurev-astro-082708-101650>. arXiv:0904.4505 [astro-ph.CO]
- Tonry JL, Schmidt BP, Barris B, et al. (2003) Cosmological results from high-z supernovae. *ApJ* 594:1–24. <https://doi.org/10.1086/376865>. arXiv:astro-ph/0305008
- Toonen S, Nelemans G, Portegies Zwart S (2012) Supernova type ia progenitors from merging double white dwarfs. using a new population synthe-

- sis model. *A&A* 546:A70. <https://doi.org/10.1051/0004-6361/201218966>. [arXiv:1208.6446](https://arxiv.org/abs/1208.6446) [astro-ph.HE]
- Toonen S, Nelemans G, Bours M, et al. (2013) Progenitors of Supernovae Type Ia. In: Krziesiński J, Stachowski G, Moskalik P, Bajan K (eds) 18th European White Dwarf Workshop. *Astronomical Society of the Pacific Conference Series*, vol 469. p 329. <https://doi.org/10.48550/arXiv.1302.0495>. [arXiv:1302.0495](https://arxiv.org/abs/1302.0495) [astro-ph.HE]
- Toonen S, Claeys JSW, Mennekens N, Ruiter AJ (2014) PopCORN: Hunting down the differences between binary population synthesis codes. *A&A* 562:A14. <https://doi.org/10.1051/0004-6361/201321576>. [arXiv:1311.6503](https://arxiv.org/abs/1311.6503) [astro-ph.SR]
- Toonen S, Perets HB, Igoshev AP, Michaely E, Zenati Y (2018) The demographics of neutron star - white dwarf mergers. Rates, delay-time distributions, and progenitors. *A&A* 619:A53. <https://doi.org/10.1051/0004-6361/201833164>. [arXiv:1804.01538](https://arxiv.org/abs/1804.01538) [astro-ph.HE]
- Torres S, Rebassa-Mansergas A, Camisassa ME, Raddi R (2021) The Gaia DR2 halo white dwarf population: the luminosity function, mass distribution, and its star formation history. *MNRAS* 502(2):1753–1767. <https://doi.org/10.1093/mnras/stab079>. [arXiv:2101.03341](https://arxiv.org/abs/2101.03341) [astro-ph.GA]
- Totani T, Morokuma T, Oda T, Doi M, Yasuda N (2008) Delay time distribution measurement of type ia supernovae by the subaru/xmm-newton deep survey and implications for the progenitor. *PASJ* 60:1327–. [arXiv:0804.0909](https://arxiv.org/abs/0804.0909)
- Townsley DM, Moore K, Bildsten L (2012) Laterally Propagating Detonations in Thin Helium Layers on Accreting White Dwarfs. *ApJ* 755:4. <https://doi.org/10.1088/0004-637X/755/1/4>. [arXiv:1205.6517](https://arxiv.org/abs/1205.6517) [astro-ph.SR]
- Townsley DM, Miles BJ, Shen KJ, Kasen D (2019) Double Detonations with Thin, Modestly Enriched Helium Layers can Make Normal Type Ia Supernovae. *ApJ Lett.* 878(2):L38. <https://doi.org/10.3847/2041-8213/ab27cd>. [arXiv:1903.10960](https://arxiv.org/abs/1903.10960) [astro-ph.SR]
- Toy M, Wiseman P, Sullivan M, et al. (2023) Rates and properties of Type Ia supernovae in galaxy clusters within the dark energy survey. *MNRAS* 526(4):5292–5305. <https://doi.org/10.1093/mnras/stad2982>. [arXiv:2302.05184](https://arxiv.org/abs/2302.05184) [astro-ph.HE]
- Truran JW, Arnett WD, Cameron AGW (1967) Nucleosynthesis in supernova shock waves. *Canadian Journal of Physics* 45:2315–2332
- Tucker MA, Shappee BJ, Vallely PJ, et al. (2020) Nebular spectra of 111 Type Ia supernovae disfavour single-degenerate progenitors. *MNRAS* 493(1):1044–1062. <https://doi.org/10.1093/mnras/stz3390>. [arXiv:1903.05115](https://arxiv.org/abs/1903.05115) [astro-ph.HE]
- Tucker MA, Ashall C, Shappee BJ, et al. (2021) SN 2019yvq Does Not Conform to SN Ia Explosion Models. *ApJ* 914(1):50. <https://doi.org/10.3847/1538-4357/abf93b>. [arXiv:2009.07856](https://arxiv.org/abs/2009.07856) [astro-ph.HE]
- Tucker MA, Shappee BJ, Kochanek CS, et al. (2022) The whisper of a whisper of a bang: 2400 d of the Type Ia SN 2011fe reveals the decay of ^{55}Fe . *MNRAS* 517(3):4119–4131. <https://doi.org/10.1093/mnras/stac2873>. [arXiv:2111.01144](https://arxiv.org/abs/2111.01144) [astro-ph.HE]

- Tutukov A, Yungelson L (1996) Double-degenerate semidetached binaries with helium secondaries: cataclysmic variables, supersoft x-ray sources, supernovae and accretion-induced collapses. *MNRAS* 280:1035–1045
- Uddin SA, Mould J, Lidman C, Ruhlmann-Kleider V, Zhang BR (2017) The Influence of Host Galaxies in Type Ia Supernova Cosmology. *ApJ* 848(1):56. <https://doi.org/10.3847/1538-4357/aa8df7>. arXiv:1709.05830 [astro-ph.CO]
- Uddin SA, Burns CR, Phillips MM, et al. (2020) The Carnegie Supernova Project-I: Correlation between Type Ia Supernovae and Their Host Galaxies from Optical to Near-infrared Bands. *ApJ* 901(2):143. <https://doi.org/10.3847/1538-4357/abafb7>. arXiv:2006.15164 [astro-ph.CO]
- Umeda H, Nomoto K, Kobayashi C, Hachisu I, Kato M (1999) The origin of the diversity of Type Ia supernovae and the environmental effects. *ApJ Lett.* 522:L43–L47. <https://doi.org/10.1086/312213>. arXiv:astro-ph/9906192
- Valley PJ, Tucker MA, Shappee BJ, et al. (2020) Signatures of bimodality in nebular phase Type Ia supernova spectra. *MNRAS* 492(3):3553–3565. <https://doi.org/10.1093/mnras/staa003>. arXiv:1902.00037 [astro-ph.HE]
- van Kerkwijk MH, Chang P, Justham S (2010) Sub-chandrasekhar white dwarf mergers as the progenitors of type ia supernovae. *ApJ Lett.* 722:L157–L161. <https://doi.org/10.1088/2041-8205/722/2/L157>. arXiv:1006.4391 [astro-ph.SR]
- Vennes S, Nemeth P, Kawka A, et al. (2017) An unusual white dwarf star may be a surviving remnant of a subluminous Type Ia supernova. *Science* 357:680–683. <https://doi.org/10.1126/science.aam8378>. arXiv:1708.05568 [astro-ph.SR]
- Vink J (2017) Supernova 1604, Kepler’s Supernova, and its Remnant. In: Alsabti AW, Murdin P (eds) *Handbook of Supernovae*. Springer, p 139. https://doi.org/10.1007/978-3-319-21846-5_49
- Walsh D, Carswell RF, Weymann RJ (1979) 0957+561 A, B: twin quasistellar objects or gravitational lens? *Nature* 279:381–384. <https://doi.org/10.1038/279381a0>
- Wang B, Han Z (2010) The helium star donor channel for the progenitors of type Ia supernovae with different metallicities. *A&A* 515:A88. <https://doi.org/10.1051/0004-6361/200913976>. arXiv:1003.4050 [astro-ph.SR]
- Wang B, Han Z (2012) Progenitors of type ia supernovae. *New Astron Rev* 56:122–141. <https://doi.org/10.1016/j.newar.2012.04.001>. arXiv:1204.1155 [astro-ph.SR]
- Wang B, Meng X, Chen X, Han Z (2009a) The helium star donor channel for the progenitors of Type Ia supernovae. *MNRAS* 395(2):847–854. <https://doi.org/10.1111/j.1365-2966.2009.14545.x>. arXiv:0901.3496 [astro-ph.SR]
- Wang B, Justham S, Han Z (2013) Producing Type Iax supernovae from a specific class of helium-ignited WD explosions. *A&A* 559:A94. <https://doi.org/10.1051/0004-6361/201322298>. arXiv:1310.2297 [astro-ph.SR]
- Wang L, Wheeler JC (2008) Spectropolarimetry of Supernovae. *ARA&A* 46:433–474. <https://doi.org/10.1146/annurev.astro.46.060407.145139>. arXiv:0811.1054

- Wang L, Wheeler JC, Li Z, Clocchiatti A (1996) Broadband Polarimetry of Supernovae: SN 1994D, SN 1994Y, SN 1994ae, SN 1995D, and SN 1995H. *ApJ* 467:435. <https://doi.org/10.1086/177617>. [arXiv:astro-ph/9602155](https://arxiv.org/abs/astro-ph/9602155) [astro-ph]
- Wang L, Baade D, Patat F (2007) Spectropolarimetric diagnostics of thermonuclear supernova explosions. *Science* 315:212–214. <https://doi.org/10.1126/science.1121656>. [arXiv:astro-ph/0611902](https://arxiv.org/abs/astro-ph/0611902)
- Wang Q, Rest A, Dimitriadis G, et al. (2024) Flight of the Bumblebee: the Early Excess Flux of Type Ia Supernova 2023bee Revealed by TESS, Swift, and Young Supernova Experiment Observations. *ApJ* 962(1):17. <https://doi.org/10.3847/1538-4357/ad0edb>. [arXiv:2305.03779](https://arxiv.org/abs/2305.03779) [astro-ph.HE]
- Wang X, Filippenko AV, Ganeshalingam M, et al. (2009b) Improved Distances to Type Ia Supernovae with Two Spectroscopic Subclasses. *ApJ Lett.* 699(2):L139–L143. <https://doi.org/10.1088/0004-637X/699/2/L139>. [arXiv:0906.1616](https://arxiv.org/abs/0906.1616) [astro-ph.CO]
- Wang X, Wang L, Filippenko AV, et al. (2012) Evidence for Type Ia Supernova Diversity from Ultraviolet Observations with the Hubble Space Telescope. *ApJ* 749(2):126. <https://doi.org/10.1088/0004-637X/749/2/126>. [arXiv:1110.5809](https://arxiv.org/abs/1110.5809) [astro-ph.HE]
- Warner B (1995) The AM Canum Venaticorum Stars. *Astrophys. Space Sci.* 225(2):249–270. <https://doi.org/10.1007/BF00613240>
- Warner B, Robinson EL (1972) Observations of rapid variables - IX. AM CVn (HZ 29). *MNRAS* 159:101–111. <https://doi.org/10.1093/mnras/159.1.101>
- Webbink RF (1984) Double white dwarfs as progenitors of R Coronae Borealis stars and Type I supernovae. *ApJ* 277:355–360. <https://doi.org/10.1086/161701>
- Wheeler JC, Harkness RP (1990) Type I supernovae. *Rep Prog Phys* 53:1467–1557
- Whelan J, Iben IJ (1973) Binaries and supernovae of type I. *ApJ* 186:1007–1014
- Wickramasinghe DT, Ferrario L (2000) Magnetism in Isolated and Binary White Dwarfs. *PASP* 112(773):873–924. <https://doi.org/10.1086/316593>
- Wiseman P, Sullivan M, Smith M, et al. (2021) Rates and delay times of Type Ia supernovae in the Dark Energy Survey. *MNRAS* 506(3):3330–3348. <https://doi.org/10.1093/mnras/stab1943>. [arXiv:2105.11954](https://arxiv.org/abs/2105.11954) [astro-ph.GA]
- Wiseman P, Sullivan M, Smith M, Popovic B (2023) Further evidence that galaxy age drives observed Type Ia supernova luminosity differences. *MNRAS* 520(4):6214–6222. <https://doi.org/10.1093/mnras/stad488>. [arXiv:2302.05341](https://arxiv.org/abs/2302.05341) [astro-ph.GA]
- Woods TE, Ghavamian P, Badenes C, Gilfanov M (2017) No hot and luminous progenitor for Tycho’s supernova. *Nature Astronomy* 1:800–804. <https://doi.org/10.1038/s41550-017-0263-5>. [arXiv:1709.09190](https://arxiv.org/abs/1709.09190) [astro-ph.SR]
- Woods TE, Ghavamian P, Badenes C, Gilfanov M (2018) Balmer-dominated Shocks Exclude Hot Progenitors for Many Type Ia Supernovae. *ApJ* 863(2):120. <https://doi.org/10.3847/1538-4357/aad1ee>. [arXiv:1807.03798](https://arxiv.org/abs/1807.03798) [astro-ph.HE]

- Woosley SE (2007) Type Ia supernovae: Burning and detonation in the distributed regime. *ApJ* 668:1109–1117. <https://doi.org/10.1086/520835>. [arXiv:0709.4237](https://arxiv.org/abs/0709.4237)
- Woosley SE, Kasen D (2011) Sub-Chandrasekhar Mass Models for Supernovae. *ApJ* 734:38. <https://doi.org/10.1088/0004-637X/734/1/38>. [arXiv:1010.5292](https://arxiv.org/abs/1010.5292) [astro-ph.HE]
- Woosley SE, Weaver TA (1994a) Massive stars, supernovae, and nucleosynthesis. In: Bludman SA, Mochkovitch R, Zinn-Justin J (eds) *Les Houches Session LIV: Supernovae*. North-Holland, Amsterdam, pp 63–154
- Woosley SE, Weaver TA (1994b) Sub-Chandrasekhar mass models for Type Ia supernovae. *ApJ* 423:371–379. <https://doi.org/10.1086/173813>
- Woosley SE, Weaver TA (1995) The Evolution and Explosion of Massive Stars. II. Explosive Hydrodynamics and Nucleosynthesis. *ApJS* 101:181. <https://doi.org/10.1086/192237>
- Woosley SE, Arnett WD, Clayton DD (1973) The Explosive Burning of Oxygen and Silicon. *ApJS* 26:231. <https://doi.org/10.1086/190282>
- Woosley SE, Weaver TA, Taam RE (1980) Models for Type I supernovae. In: Wheeler JC (ed) *Texas Workshop on Type I Supernovae*. pp 96–112
- Woosley SE, Taam RE, Weaver TA (1986) Models for Type I supernova. I – Detonations in white dwarfs. *ApJ* 301:601–623. <https://doi.org/10.1086/163926>
- Woosley SE, Kerstein AR, Aspden AJ (2011) Flames in type Ia supernova: Deflagration-detonation transition in the oxygen-burning flame. *ApJ* 734:37. <https://doi.org/10.1088/0004-637X/734/1/37>
- Yang J, Wang L, Suntzeff N, et al. (2022) Using 1991T/1999aa-like Type Ia Supernovae as Standardizable Candles. *ApJ* 938(1):83. <https://doi.org/10.3847/1538-4357/ac8c97>. [arXiv:2209.06301](https://arxiv.org/abs/2209.06301) [astro-ph.HE]
- Yoon SC, Podsiadlowski P, Rosswog S (2007) Remnant evolution after a carbon-oxygen white dwarf merger. *MNRAS* 380:933–948. <https://doi.org/10.1111/j.1365-2966.2007.12161.x>. [arXiv:0704.0297](https://arxiv.org/abs/0704.0297)
- Yoshida S (2021) Decihertz Gravitational Waves from Double White Dwarf Merger Remnants. *ApJ* 906(1):29. <https://doi.org/10.3847/1538-4357/abc7bd>. [arXiv:2009.13017](https://arxiv.org/abs/2009.13017) [astro-ph.HE]
- Yungelson L, Livio M (1998) Type IA Supernovae: an Examination of Potential Progenitors and the Redshift Distribution. *ApJ* 497:168–177. <https://doi.org/10.1086/305455>. [astro-ph/9711201](https://arxiv.org/abs/astro-ph/9711201)
- Yungelson LR, Kuranov AG (2017) Merging white dwarfs and Type Ia supernovae. *MNRAS* 464:1607–1632. <https://doi.org/10.1093/mnras/stw2432>
- Yungelson LR, Livio M (2000) Supernova rates: A cosmic history. *ApJ* 528:108–117. <https://doi.org/10.1086/308174>. [arXiv:astro-ph/9907359](https://arxiv.org/abs/astro-ph/9907359)
- Zel’dovich YB, Barenblatt GI, Librovich VB, Makhviladze G (1980) *The Mathematical Theory of Combustion and Explosions*. Nauka, Moscow. English translation 1985 Consultants Bureau (Plenum), New York.
- Zenati Y, Perets HB, Dessart L, et al. (2023) The Origins of Calcium-rich Supernovae From Disruptions of CO White Dwarfs by Hybrid He-CO White Dwarfs. *ApJ* 944(1):22. <https://doi.org/10.3847/1538-4357/acaf65>.

- [arXiv:2207.13110](https://arxiv.org/abs/2207.13110) [astro-ph.HE]
- Zheng W, Kelly PL, Filippenko AV (2018) An Empirical Fitting Method to Type Ia Supernova Light Curves. III. A Three-parameter Relationship: Peak Magnitude, Rise Time, and Photospheric Velocity. *ApJ* 858(2):104. <https://doi.org/10.3847/1538-4357/aabaeb>. [arXiv:1712.01495](https://arxiv.org/abs/1712.01495) [astro-ph.HE]
- Zhou P, Leung SC, Li Z, et al. (2021) Chemical Abundances in Sgr A East: Evidence for a Type Iax Supernova Remnant. *ApJ* 908(1):31. <https://doi.org/10.3847/1538-4357/abbd45>. [arXiv:2006.15049](https://arxiv.org/abs/2006.15049) [astro-ph.HE]
- Zhou WH, Wang B, Zhao G (2014) Double-detonation model of type Ia supernovae with a variable helium layer ignition mass. *Res Astron Astrophys* 14(9):1146-1156. <https://doi.org/10.1088/1674-4527/14/9/005>
- Zhu C, Pakmor R, van Kerkwijk MH, Chang P (2015) Magnetized Moving Mesh Merger of a Carbon-Oxygen White Dwarf Binary. *ApJ Lett.* 806(1):L1. <https://doi.org/10.1088/2041-8205/806/1/L1>. [arXiv:1504.01732](https://arxiv.org/abs/1504.01732) [astro-ph.SR]
- Zingale M, Almgren AS, Bell JB, Nonaka A, Woosley SE (2009) Low Mach Number Modeling of Type IA Supernovae. IV. White Dwarf Convection. *ApJ* 704:196-210. <https://doi.org/10.1088/0004-637X/704/1/196>. [arXiv:0908.2668](https://arxiv.org/abs/0908.2668)
- Zingale M, Nonaka A, Almgren AS, et al. (2013) Low Mach Number Modeling of Convection in Helium Shells on Sub-Chandrasekhar White Dwarfs. I. Methodology. *ApJ* 764(1):97. <https://doi.org/10.1088/0004-637X/764/1/97>. [arXiv:1212.4380](https://arxiv.org/abs/1212.4380) [astro-ph.SR]
- Zwicky F (1942) On the Frequency of Supernovae. II. *ApJ* 96:28. <https://doi.org/10.1086/144430>